Ecophysiology of mixotrophic flagellates

Dissertation zur Erlangung des
akademischen Grades eines Doktors der Naturwissenschaften

vorgelegt von
Rottberger, Julia

an der

Universität Konstanz

Mathematisch-Naturwissenschaftliche Sektion

Fachbereich Biologie

Tag der mündlichen Prüfung: 21.10.2013

1. **Referent: Professor Dr. Kroth**
2. **Referent: Professor Dr. Rothhaupt**
3. **Referent: Professor Dr. Boenigk**

Contents

List of figures and tables

Zusammenfassung

Mixotrophe Algen kombinieren Photoautotropie mit Chemoheterotrophie, also den photosynthetischen Biomasseaufbau aus Kohlenstoffdioxid mit dem Biomasseaufbau aus aufgenommenen organischen Substanzen. Mixotrophe Chrysophyten sind Flagellaten, die im Bodensee im Zuge der Reoligotrophierung besonders gut gedeihen, jedoch ist wenig über ihre Stoffwechselwege bekannt. Ziel dieser Arbeit war, die Regulation des Kohlenstoffmetabolismus mixotropher Chrysophyten auf physiologischer und molekularbiologischer Ebene zu untersuchen.

Es wurden Chrysophyten unterschiedlicher Ernährungsweise miteinander verglichen. Dabei wurde gezeigt, dass ein Partikelzähler geeignet ist, um bakterielle Kontaminationen in allen untersuchten Chrysophytenkulturen zu detektieren, Zellzählungen durchzuführen und Veränderungen in der Durchschnittszellgröße, dem Gesamtzellvolumen und der Größenverteilung der einzelligen Protisten zu untersuchen. In Wachstumsexperimenten unter verschiedenen Lichtbedingungen und mit unterschiedlichen Kohlenstoffquellen wurde demonstriert, dass die heterotrophe Chrysophyte *Poteriospumella lacustris* und der mixotrophe Stamm *Poterioochromonas malhamensis* unter chemoheterotrophen Bedingungen gedeihen. Beide Chrysophyten wuchsen nicht photoautotroph, dennoch zeigte *Poterioochromonas malhamensis* photosynthetische Aktivität und überlebte mit Licht länger als im Dunklen. Die photoautotrophe Chrysophyte *Mallomonas annulata* und der mixotrophe Stamm *Dinobryon divergens* waren beim Wachstum in anorganischem Medium lichtlimitiert. In dieser Eigenschaft waren sie vergleichbar mit der photoautotrophen Diatomee *Phaeodactylum tricornutum*, die als Referenzstamm diente. *Dinobryon divergens* wuchs in der Gegenwart von Bakterien im Licht aber nicht im Dunklen. Aufgrund der deutlichen Unterschiede in der Ernährungspräferenz der zwei mixotrophen Chrysophyten *Poterioochromonas malhamensis* und *Dinobryon divergens* konkurriert *Dinobryon divergens* wahrscheinlich hauptsächlich mit photoautotrophen und *Poteriospumella lacustris* mit heterotrophen Einzellern. Folglich würden diese beiden mixotrophen Stämme vermutlich unterschiedliche vertikale Schichten der Wassersäule besiedeln.

Basierend auf den vergleichenden physiologischen Studien wurden die vier unterschiedlichen Chrysophytenstämme unter geeigneten Wachstumsbedingungen kultiviert und Transkriptomanalysen mit Hilfe eines 454-Sequenzierungsansatzes durchgeführt. Insgesamt wurden 213.361 contigs mit einer Durchschnittslänge von 611 Nukleotiden mit BLAST2GO annotiert und funktionell sortiert. Transkripte aus Glykolyse, Gluconeogenese, Calvin Zyklus, Photorespiration und Harnstoffzyklus wurden sowohl von der photoautotrophen als auch von beiden mixotrophen Chrysophyten exprimiert. Es wurden viele metabolische Parallelen zwischen *Mallomonas annulata* und *Phaeodactylum tricornutum* gefunden. Die beiden mixotrophen Stämme unterschieden sich von *Mallomonas annulata* durch die Abwesenheit wichtiger Transkripte für die photoautotrophe Lebensweise wie etwa die der Schlüsselenzyme des oxidativen Pentosephosphatweges und der carboxylierenden Enzyme im Plastiden. Einige plastidäre glykolytische Transkripte wurden für *Poteriospumella lacustris* gefunden und stellen den ersten Hinweis auf metabolische Aktivität in dem farblosen, nicht photosynthetischen Plastiden dieses Protisten dar. Insgesamt wurde eine breite Basis für Expressionsanalysen der Stoffwechselwege von Chrysophyten und für weitere vergleichende molekulare und physiologische Studien gebildet.

Summary

Mixotrophy in algae is a type of nutrition situated between the metabolic modes of photoautotrophy (building biomass from inorganic molecules via photosynthesis) and chemoheterotrophy (building biomass from organic substances via uptake of food). Mixotrophic chrysophytes are a group of flagellate protists prospering during re-oligotrophication of Lake Constance. However, little is known about metabolic pathways of chrysophytes. The aim of this thesis was to investigate the physiological and molecular regulation of carbon metabolism in mixotrophic chrysophytes.

As a first step comparative physiological analyses of nutritionally diverse chrysophytes were conducted. A particle analyser was shown to be a helpful tool to monitor chrysophyte cultures for bacterial contaminations, to perform cell counts and to detect changes in mean cell size, total cell biovolume and size distribution of the unicellular protists. Growth experiments under different light regimes and with different carbon sources demonstrated that *Poteriospumella lacustris* and the mixotrophic *Poterioochromonas malhamensis* could strive under chemoheterotrophic conditions. Both strains were not growing photoautotrophically, however, *Poterioochromonas malhamensis* showed some photosynthetic activity and was able to survive longer when kept in the light. Similar to the photoautotrophic diatom *Phaeodactylum tricornutum*, which served as a reference strain, the photoautotototrophic strain *Mallomonas annulata* and the mixotrophic chrysophyte *Dinobryon divergens* showed light limited growth when kept in inorganic media. Even though *Dinobryon divergens* consumed living bacteria, it did not grow in the dark in the presence of bacteria. Due to the relevant differences in general nutritional preferences between the two mixotrophic strains *Poterioochromonas malhamensis* and *Dinobryon divergens*, we propose that during re-oligotrophication, *Dinobryon divergens* might primarily compete with photoautotrophic algae while *Poterioochromonas malhamensis* presumably mainly competes with chemoheterotrophic organisms and that they, thus, may colonize different vertical layers of the water column.

In a second step *Mallomonas annulata*, *Dinobryon divergens*, *Poterioochromonas malhamensis* and *Poteriospumella lacustris* were grown under suitable culturing conditions according to the comparative physiological studies and transcriptomic analyses and comparisons were performed applying a 454-sequencing approach. A total of 213,361 contigs with an average length of 611 nucleotides were annotated and functionally sorted using BLAST2GO. The transcripts of the pathways of glycolysis, gluconeogenesis, Calvin Cycle, photorespiration and urea cycle were expressed in the photoautotrophic and both mixotrophic chrysophytes. Many metabolic parallels regarding primary carbon metabolism were found between *Mallomonas annulata* and the diatom *Phaeodactylum tricornutum*. However, the two mixotrophic strains differed from *Mallomonas annulata* by the absence of transcripts for putative key enzymes involved in the oxidative pentose phosphate pathway and carboxylating reactions localized in the plastid. These enzymes are important for photoautotrophic performance. A set of glycolytic transcripts of the heterotrophic chrysophyte was found to be targeted to the plastid targeted. This represents a first hint for metabolic activity in the colourless, non-photosynthetic plastid of *Poteriospumella lacustris*. Altogether this study lays a profound base for expression analyses of metabolic pathways of chrysophytes and further molecular studies.

Chapter 1

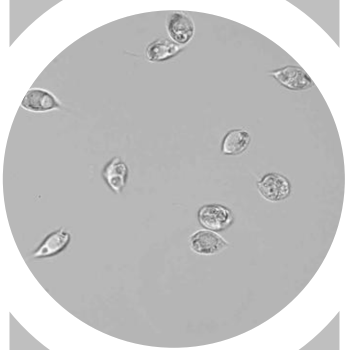

General Introduction

by Julia Rottberger

1. General Introduction

Organisms require energy to produce biomass and to sustain life. The utilization of adenosine triphosphate (ATP) as an energy equivalent and carbon for biomass formation are universal features found among all known organisms. Yet, the ways of accomplishing energy production (catabolism) and biomass production (anabolism) are manifold which may be a consequence of adapting to the differing nutritional limitations of the habitats organisms live in.

The observation that the nutritional mode is connected to the characteristics of a habitat has led to the introduction of a trophical classification concept to differentiate between bacteria. According to this scheme, bacteria can be distinguished regarding the energy source, the electron donor or the carbon source utilized to perform the biochemical reactions that are needed for the generation of ATP and for biomass formation (Fuchs and Schlegel, 2007). Chemotrophic bacteria use the energy available from exergonic chemical reactions and phototrophic bacteria utilize light as an energy source. If the electron donor is an organic compound, like for example glucose, a bacterium is referred to as organotrophic whereas it is called lithotrophic in case of inorganic electron donors like water, iron or nitrate. Autotrophs are able to sequester inorganic carbon in form of carbon dioxide (CO_2) while heterotrophs rely on organic carbon compounds produced by other organism. According to these classifications cyanobacteria are photolithoautotrophs because they perform photosynthesis, i.e. the fixation of CO_2 with the help of light energy and use of H_2O as the electron donor (Fuchs and Schlegel, 2007).

The trophical classification concept was developed for bacteria but may also apply to other, multicellular organisms like e.g. humans which are chemoorganoheterotrophs (Meyer, 1993). However, classification is not always easy. Plants for example are generally considered as photolithoautotrophs because the nutritional concept is correlating to that of cyanobacteria. Yet, chlorophyll-lacking organs of plants like roots, seeds or sprouts do not perform photosynthesis and may still grow and develop heterotrophically in the dark. If the nutrition of an organism switches between the different trophic categories, the nutritional mode is called mixotrophic. In the case of plants, the common agreement is that photolithoautotrophy remains applicable because chlorophyll-free organs are composed from organic storage compounds which were built up photolithoautotrophically by the green tissues of the plant. Nevertheless, there are some mixotrophic green plants which do not only perform photosynthesis but also obtain additional carbon from their symbiotic fungi and even heterotrophic plants exist which are non-photosynthetic and totally rely on carbon provided by a fungus (Selosse and Roy, 2009).

The term “mixotrophy” is applied differently to eukaryotes and bacteria. Among eukaryotes, mixotrophs are organisms that are capable of autotrophic and heterotrophic nutrition. For reasons of simplification, autotrophy is often reduced to photoautotrophy because other forms of autotrophic nutrition are rare in eukaryotes. Except for land plants and some symbiotic relationships, photoautotrophic organisms are called algae independent of whether they are eukaryotes or prokaryotes. The biochemical processes leading to photoautotrophic carbon fixation are termed photosynthesis. All eukaryotes conducting photosynthesis utilize a special cell compartment called chloroplast or plastid. Hence, all unicellular eukaryotes containing a plastid and being capable of ingesting organic carbon either by phagotrophy (up-take of particles or organisms) or osmotrophy (up-take of dissolved compounds) are also classified as mixotrophic algae (e.g. Jones, 2000). In spite of being a persuasive concept for algae, the latter classification also includes primarily photoautotrophic algae that employ phagotrophy to obtain other essential substances apart from carbon for growth (e.g. N, P). Within the bacterial trophical classification concept such organisms would not be called mixotrophic organisms.

The origin of the plastid may explain the phylogenetic diversity among mixotrophic algae. Plastids evolved from endosymbiosis, an evolutionary event in the cause of which a most likely heterotrophic, unicellular eukaryote engulfed a cyanobacteria-like prokaryote and instead of totally digesting it, the eukaryotic host maintained the prokaryote as an endosymbiont and profited from its photosynthetic capability (Figure 1.1). The organisms evolving from primary endocytobiosis are the Archeaplastida consisting of red algae, green algae and glaucophytes (Moreira et al., 2000). Additionally, in independent secondary endocytobiotic events a eukaryotic unicellular flagellate engulfed and intracellularly maintained a green alga or a red alga (e.g. Keeling, 2004). Flagellates are eukaryotes which are motile due to agile filamentous structures. Finally, there is evidence for tertiary and possibly quaternary endcytobiotic events. Many algae inherit at least one flagellum handed on by the endocytobiotic host cell (Cavalier-Smith, 2002) which makes them belong to the flagellates independent from whether they derived by primary, secondary, tertiary or quaternary endosymbiosis. Evidence for the different endocytobiotic events comes from the presence of more than two plastidic envelope membranes in complex algae (Archibald,

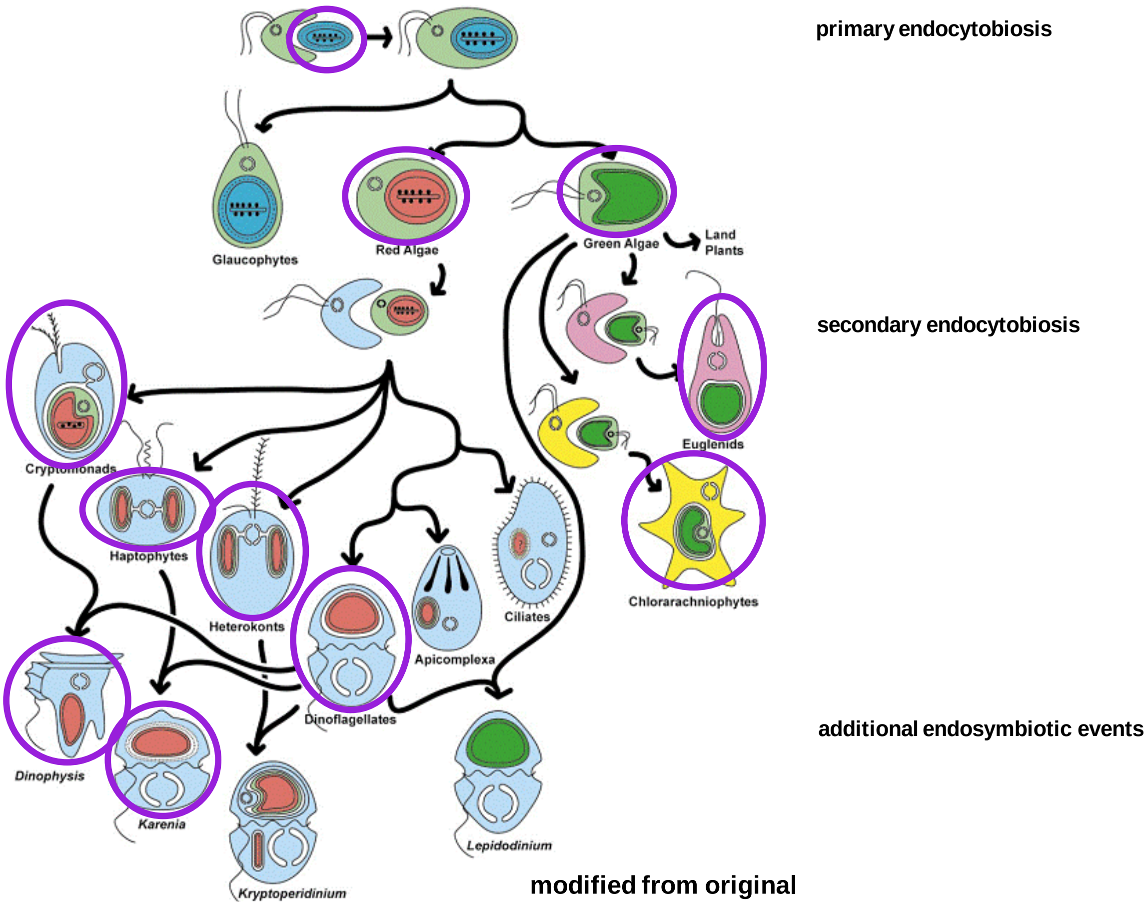

Figure 1.1: Schematic overview demonstrating the occurrence of mixotrophic nutrition in the different endosymbiotic lineages. Taxonomic classes with mixotrophic representatives are marked by purple circles. The original figure demonstrating endsymbiotic evolution was extracted from Keeling (2004). Literature references for mixotrophy: Cyanobacteria: (Kang et al., 2004); Cryptophyta, Haptophyta, Heterokonts, Chlorarachniophytes, Euglenophyta, Dinoflagellates: (Raven, 1997); Green Algae: (Laliberte and Delanoue, 1993); Red algae: (Oesterhelt et al., 1999); Dinophysis: (Stöcker et al., 2006); Karenia: (Glibert et al., 2009)

2009), the chemical composition of the plastid membranes (Jarvis et al., 2000; Gould et al., 2008) and from phylogenetic analysis of genes (e.g. Douglas and Turner, 1991). The analysis of nuclear and organellar genomes revealed that during endocytobiosis the genome(s) of the engulfed prokaryote or alga were not only reduced but horizontal gene transfer to the host genome or in the reciprocal direction took place. For example there are genes in the nuclear genome that are homologous to eukaryotic sequences whereas others are more closely related to bacteria (Timmis et al., 2004).
Due to the heterotrophic features of the different host cells and the photoautotrophic features of the endosymbionts, a combination of heterotrophic and autotrophic nutrition is found in many flagellate and non-motile algae. Theoretically, the reduction of an endosymbiont to an organelle must have required re-arrangements of biochemical pathways and the establishment of suitable protein transport and exchange machinery between the cell compartments enabling the passage of several membranes (Gould et al., 2008). In line with this, nuclear encoded chloroplast proteins from rhodophytes, glaucophytes and the viridiplantae possess cleavable N-terminal transit peptides (TP), which direct them to the chloroplast (Soll and Schleiff, 2004; Jarvis, 2008). Nuclear encoded plastid proteins of secondary endocytobionts are first directed into the lumen of the ER by a signal peptide (SP) (Bhaya and Grossman, 1991) which is cleaved-off after import. Thereby, a TP is exposed and mediates further transport over the remaining membranes into the plastid (Gould, 2008; Lang, 1998). A characteristic cleavage site motif has been identified for plastid stroma proteins of diatoms which are secondary endosymbionts (Gruber et al., 2007; Archibald, 2009). Moreover, biochemical and molecular analysis of the model diatom *Phaeodactylum tricornutum*, has shown that metabolism and intracellular distribution of pathways is different from green alga or higher plants (e.g. Gruber et al., 2009).

In the past ten years, it has been acknowledged that mixotrophy is a common trait among algae. In oligotrophic aqueous environments particularly mixotrophic chrysophytes (Figure 1.2) have been shown to thrive well (Gaedke, 1998; Anneville and Pelletier, 2000; Dokulil and Teubner, 2005). However, details on the physiology of chrysophytes still need to be puzzled out and studies on molecular metabolic aspects are almost completely missing. The first physiological studies on carbon exploitation of a chrysophyte species were performed in the 1950s (Pringsheim, 1952). Since then, various factors besides carbon and phosphorous availability (Rothhaupt, 1996a) like e.g. vitamin requirements (Heinrich, 1955), light (de Castro et al., 2009), pH (Moser and Weisse, 2011a) and temperature (Moser and Weisse, 2011b; Wilken et al., 2013) have been shown to affect the competitive strength of mixotrophic chrysophytes. Still, each of the mentioned parameters may affect single chrysophytes in a different way (Watson and McCauley, 2010; Moser and Weisse, 2011a). Thus, it is difficult to explain the success of certain mixotrophic species without extensive investigations because the physiological costs and benefits of mixotrophic nutrition have not been described yet. Recently 400 putative proteins derived from cDNA of *Ochromonas danica* were identified (Terauchi et al., 2010) and single genes or proteins of interest have been analyzed (e.g. Lacoste-Royal and Gibbs, 1985; Harper and Keeling, 2003; Boenigk et al., 2005; Cavalier-Smith and Chao, 2006). However, no comprehensive genomic data sets, gene or protein expression profiles of chrysophyte species are publicly accessible.

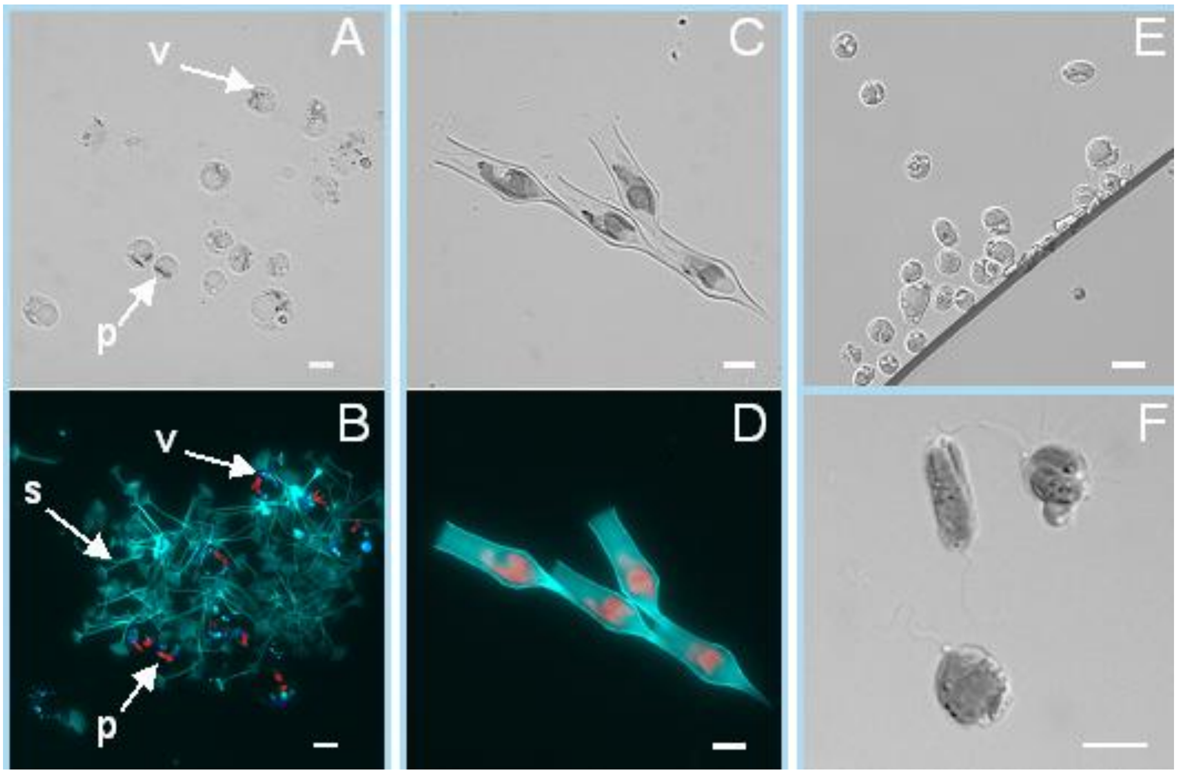

Figure 1.2: Chrysophytes isolated from oligotrophic lakes: the mixotrophic strain *Poterioochromonas malhamensis* (A+B), the mixotrophic strain *Dinobryon divergens* (C+D), the heterotrophic strain *Poteriospumella lacustris* (E) and the photoautotrophic strain *Mallomonas annulata* (F). A) Bright field image of *Poterioochromonas malhamensis*, v: vesicles, p: plastid. **B)** Merged fluorescence images showing the plastids in red, the vesicles in dark blue and the chitin stalks in light blue. v: vesicles, p: plastid, s: stalk. **C)** Bright field image of a colony of *Dinobryon divergens*. **D)** Merged fluorescence image showing the plastids in red and the cellulose envelopes (loricas) in light blue. **E)** Bright field image of cells of *Poteriospumella lacustris* cells gathered at the air-water interface. **F)** Bright field image of *Mallomonas annulata* cells. The scale bars represent 10 µm.

As long as more indicative measures are not available, the trophic state of a lake is one of the indicators to consider when predicting the presence of mixotrophic chrysophytes. In Lake Constance, the input of anthropogenic phosphorus beginning in the 1960s led to eutrophication which peaked in the 1970s with phosphorus concentrations of ~80 µg l^{-1} (Landesanstalt für Umwelt, Messungen und Naturschutz Baden-Württemberg, http://www.lubw.baden-wuerttemberg.de/servlet/is/4879/). Since then, improvements in municipal wastewater treatment and agricultural fertilization techniques have resulted in decreasing phosphorus concentrations and finally, in a return of the lake to its oligotrophic status with phosphorus concentrations of ~8 µg l^{-1} (http://www.lubw.baden-wuerttemberg.de/servlet/is/4879/).

The transformation of CO_2 into organic carbon by algae and cyanobacteria provides the nutritional fundament for multifaceted heterotrophic life in a lake. During the re-oligotrophication process of Lake Constance phytoplankton regulation has shifted from a top-down control by grazing organism to a bottom-up control by phosphorus concentrations (Kerimoglu et al., 2013). This also implies that the most successful phytoplankton species are no longer the least edible ones but those who cope best with limited phosphorus conditions.

As a consequence of re-oligotrophication, the contribution of mixotrophic chrysophyte species like *Dinobryon spp.* to total phytoplankton biovolume increased (Gaedke, 1998). A popular explanation for the success of mixotrophic chrysophytes is the exploitation of bacteria as carbon and phosphorus source (Thingstad et al., 1996; Kamjunke et al., 2007; Unrein et al., 2007). Thereby, mixotrophs achieve a competitive advantage under oligotrophic conditions compared to photoautotrophs which obligatorily depend on the typically limited deposits of dissolved phosphorus.

The main purpose of the research initiative implementing this thesis is to improve our knowledge on ecology, physiology and molecular biology of organismic interactions in Lake Constance as a case study to evaluate the impact of re-oligotrophication. Judged by their increased abundances over the last decades and their ability to act as primary producers and consumers, mixotrophic flagellates are of great importance in the food-web of Lake Constance. This thesis was designed to describe the molecular regulation of mixotrophic physiology with a special focus on the carbohydrate metabolism in chrysophytes. Thereby new insights that complement the existing knowledge and theories about mixotrophic flagellates and their ecophysiologic role during re-oligotrophication were to be attained.
Basically, this thesis compromises a two step experimental design. Previous studies showed that mixotrophic chrysophytes very sensitively react to changes in the experimental settings, but the responses to changes differ between species and even between strains. Hence, as the different studies were not performed under identical conditions, it is difficult to relate them to each other. Thus, as a first step, broadly based comparative physiological studies were designed. Autotrophic, mixotrophic and heterotrophic chrysophyte strains were chosen and their cultures newly established in the laboratory. Chapter 2 deals with the suitability of detecting bacterial contaminations in chrysophyte cultures with an automatic particle counter flow (Coulter counter). Morphological characteristics of the chrysophyte strains in the light and in the dark were analyzed and the results are presented in chapter 3. Chapter 4 addresses the effect of changes in nutritional parameters like e.g. light or carbon availability regarding physiological features (e.g. growth rates, oxygen evolution rates). As a second step, the newly gained physiological insights were utilized to choose suitable culturing conditions to perform a comparative EST-based transcriptomics approach. DNA and protein sequences of expressed genes were annotated, sorted and compared among the strains regarding major metabolic carbon pathways. These studies and the results are summarized in chapter 5.

Chapter 2

Detection of bacterial contaminations in algal cultures from the size distribution

by Julia Rottberger, Peter G. Kroth and Ansgar Gruber
contents of this chapter were accepted as an application note by the company Beckman Coulter

2. Detection of bacterial contaminations in algal cultures from the size distribution

2.1. Introduction

Some species of the golden algae (*Chrysophyceae*) grow photosynthetically with light as energy source and CO_2 as inorganic carbon source (autotrophic growth). Other chrysophyceans compulsorily depend on organic carbon sources and do not perform photosynthesis (heterotrophic growth) (Raven et al., 1995). Moreover, there are golden algae which utilize inorganic as well as organic carbon sources (Porter, 1988). This nutritional mode is called mixotrophy. Currently, the metabolic regulation of carbon exploitation in mixotrophic chrysophyceans is only partially understood and is probably dependent on the environmental conditions (Rothhaupt, 1996b; de Castro et al., 2009; Moser and Weisse, 2011a, b; Wilken et al., 2013). Growth experiments under conditions favoring the different nutritional modes are important tools to clarify the regulation of mixotrophic growth. In such experiments, total cell counts are an accurate parameter to determine growth.

The culture media used for such growth experiments usually contain organic carbon sources that can also be used by possible bacterial contaminants, which of course has an impact on the outcome of the experiments. It is therefore necessary to detect the presence of bacterial contaminants as early as possible. Common methods to monitor cultures for bacterial contamination are the platting of culture aliquots on solidified media or fluorescence and light microscopic assays. All these methods have to be performed in addition to the algal cell counts. The Multisizer III (Beckman Coulter) provides the possibility to perform total cell counts in a fast and reliable manner and, at the same time, to detect bacterial contaminations by the size distribution of cells.

2.2. Experiments

2.2.1. Culturing conditions

The mixotrophic Chrysophyceans *Ochromonas danica* and *Poterioochromonas malhamensis* were grown in a culturing medium with organic carbon sources in Erlenmayer-flasks without agitation at a temperature of 20 °C and a light intensity of 30 µmol photons m^{-2} s^{-1} (Figure 2.1).

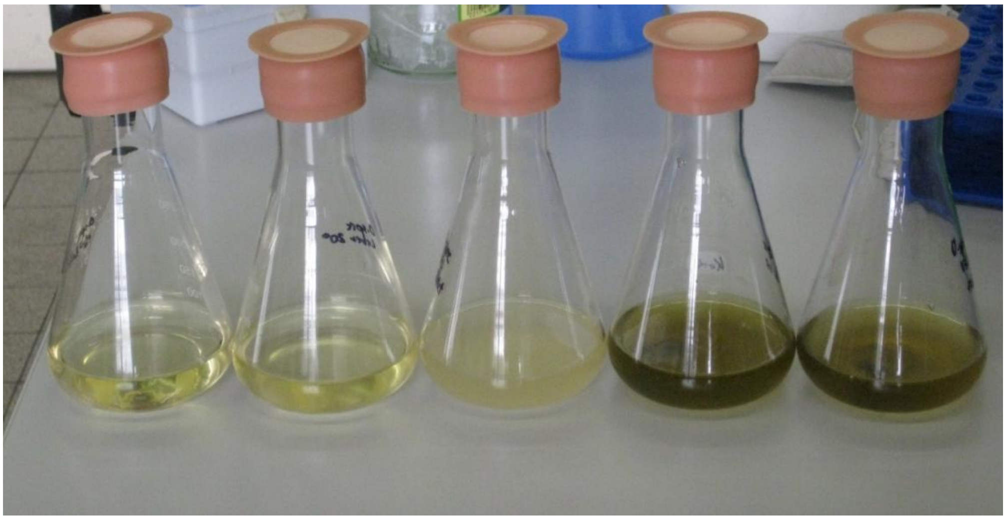

Figure 2.1: Different growth states of *Ochromonas danica* in a medium supplemented with organic carbon sources.

2.2.2. Determination of total cell numbers

All cell suspensions were analyzed with the Multisizer III to determine total cell numbers. A capillary with an aperture of 100 µm was chosen for measurements as cell size of the algae was expected to be between 3 µm and 15 µm (Figure 2.2) which corresponds to a volume of 20 -1000 µm³. 50-500 µl of cell suspension were suspended in 12 ml Isoton II-Diluent. The volume of utilized cell suspension was specifically adjusted to avoid that the concentration index in the "Extended operator mode" of the Multisizer III software exceeded the 10 % value during measurements. Three measurements with 500 µl of the cell/ Isoton-Diluent mixture were performed per sample. The average of the three measurements was saved as a file of the type "#AV". One sample containing the corresponding volume of culture medium instead

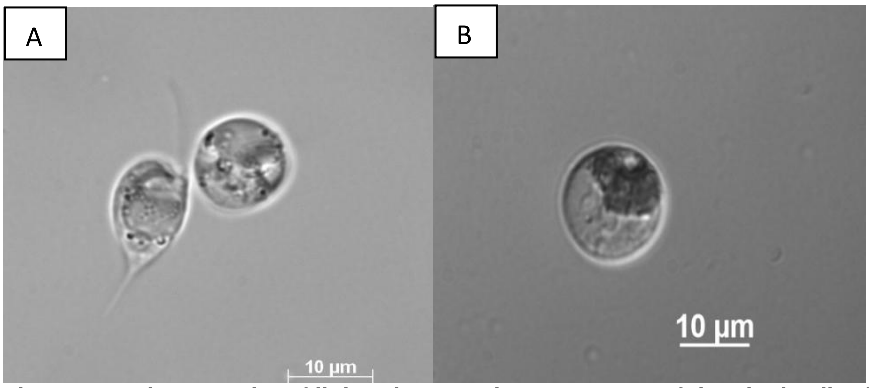

Figure 2.2: Photographs of light microscopic appearance of the algal cells. (A) Two cells of *Ochromonas danica*. (B) A cell of *Poterioochromonas malhamensis*.

of cell suspension was analyzed to eliminate the background caused by particles in the medium like fibers, crystals and dust. This background measurement was subtracted from the average file using the Multisizer III software.

2.2.3. Sensitivity of the Multisizer III for particles in the range of bacterial sizes using a 100 µm capillary and detection of bacteria

All algal cultures were examined concerning bacterial contaminations using the Multisizer III (aperture of 100 µm). Usage of the 30 µm aperture turned out not to be feasible as it often got blocked by algal cells during the measurements.

Aliquots of *P. malhamensis* cultures were mixed with different concentrations of heat inactivated bacteria to investigate the sensitivity of the Multisizer III for particles in the size range of the bacterial peak (<20 μm^3). The concentration of added bacteria was determined by optical density (OD) measurements at a wavelength of 600 nm. The optical density of bacterial cells in the mixed suspensions with algal cells was gained by measuring reference samples which contained bacterial suspension and a corresponding volume of pure medium instead of the algal cell suspension. In case the OD_{600} measured was >1, the cell suspension was diluted to get values <1. The bacterial cell suspension investigated had an initial calculated OD_{600}=10. The particle size distribution was recorded by the Multisizer III. For verification of the results, the samples were analyzed by microscopy. Aliquots of the cell suspensions were treated with a fluorescent dye (SYBR-Green) to facilitate visibility of the bacteria, and fluorescence microscopy was performed subsequently (400x magnification).

2.3. Results

2.3.1. Size distribution patterns of the two algal species

The spherical or drop shaped algae *Ochromonas danica* and *Poterioochromonas malhamensis* are of similar cell size (Figure 2.2). Accordingly, size distribution patterns of those two algae recorded by the Multisizer III software during measurements were very similar (Figure 2.3).

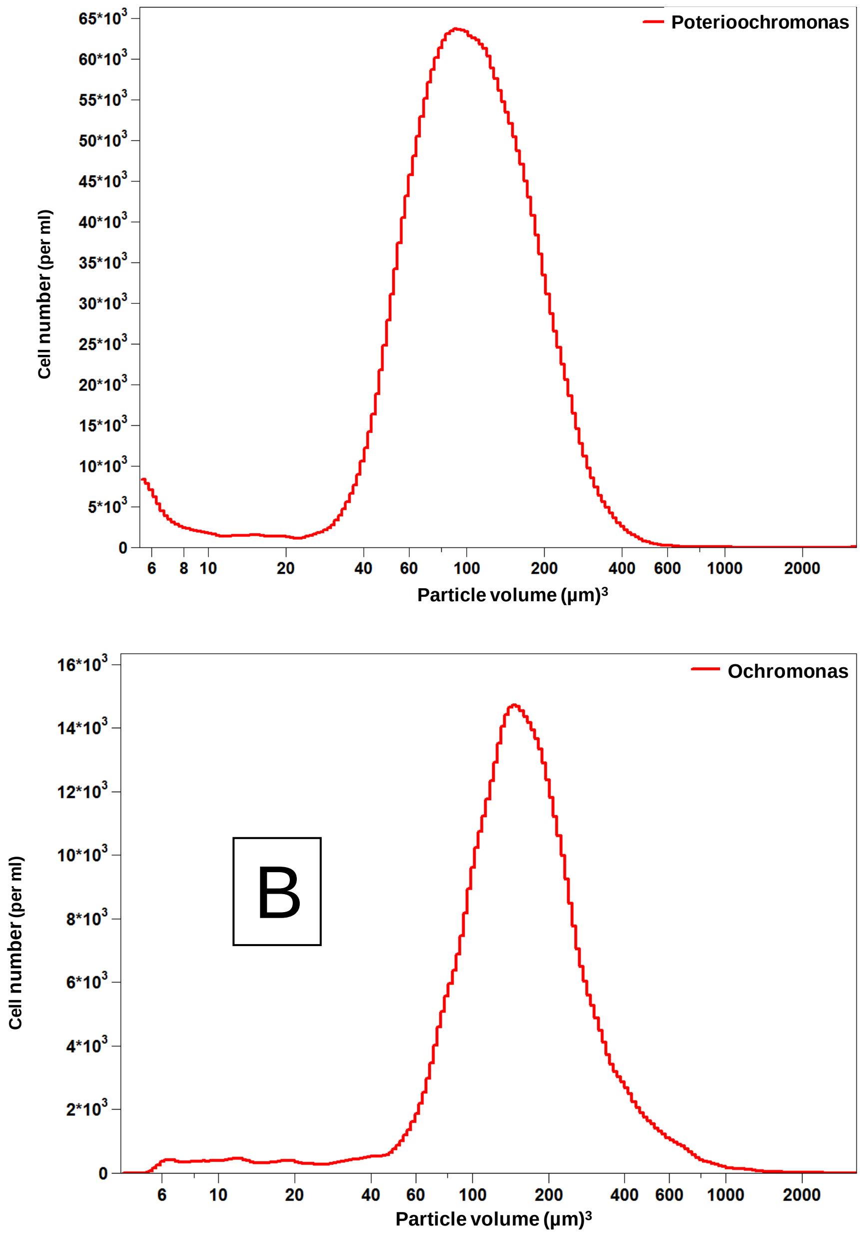

Figure 2.3: Characteristic cell volume distribution of the investigated algal species. (A) *Poterioochromonas malhamensis* (B) *Ochromonas danica*.

2.3.2. Detectability of bacterial contaminations

Cultures of *Poterioochromonas malhamensis* and *Ochromonas danica* generally were axenic, which means that only the algae but no bacteria were present. The capillary with the 100 µm aperture was successfully applied in all approaches to detect the presence of bacteria during measurements with the Multisizer III. High particle density in the region <20 µm³ (a particle diameter <3 µm, respectively) during exponential growth phase were characteristic for bacterial contaminations. This was especially true if the particle densities in this size range were higher than those of the algal population (20-2000 µm³ or 3.5-20 µm particle diameter) (Figure 2.4).

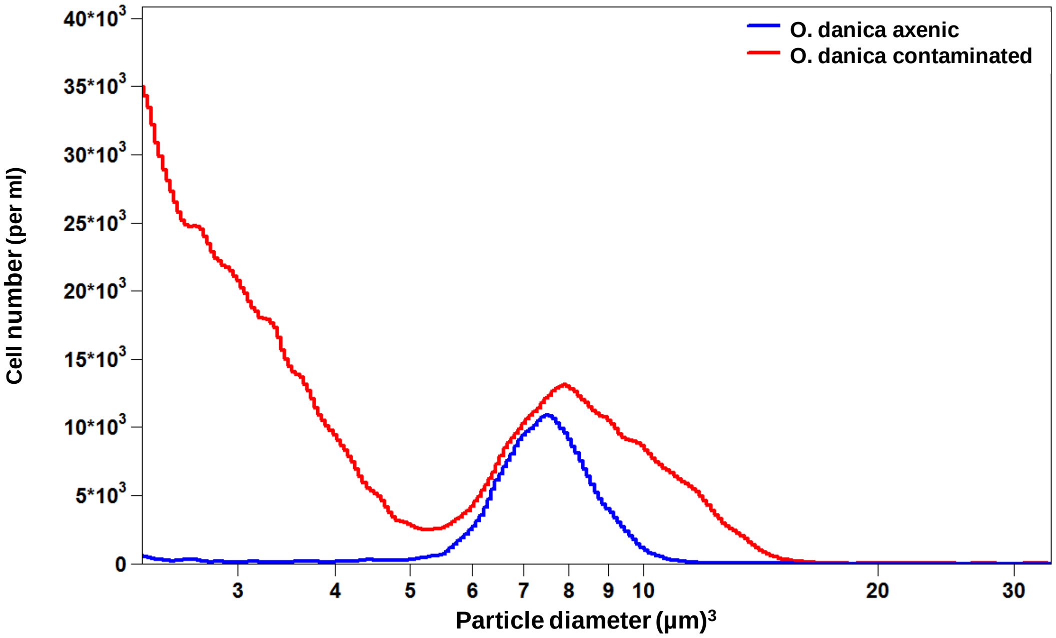

Figure 2.4: Cultures of *Ochromonas danica* in exponential growth phase with (red) and without (blue) bacterial contaminations. In exponential growth phase only the algal peak (5-20 µm) was detected in axenic cultures (blue). When bacterial contaminations grew in the course of an experiment these were visible by a characteristic particle distribution curve (red).

Accordingly, there were no such conspicuous peaks in the region <20 µm³ in non-contaminated cultures of *P. malhamensis* and *O. danica* (Figure 2.3). It should be noted that in the late exponential and stationary growth phases the detection of bacterial contaminations was limited because cell lysis of the algae also produced a peak in the <20 µm³ size range. Het-killed bacteria were detectable by microscopy (Fig. 5B) and by Multisizer III analysis (Figure 2.5B) when a bacterial density of OD_{600}=2 was applied. However, the bacteria were not detectable by microscopy when added to culture aliquots of *P. malhamensis* with OD_{600}=0.05 and OD_{600}=0.03. The bacterial peaks nevertheless already appeared as size distribution peaks during measurements with the Multisizer III at these concentrations (Figure 2.5A).

In summary, size distribution measurements with the Multisizer III not only enable to monitor the growth of algal cultures but also help to survey the cultures for bacterial contaminations in the course of a growth experiment.

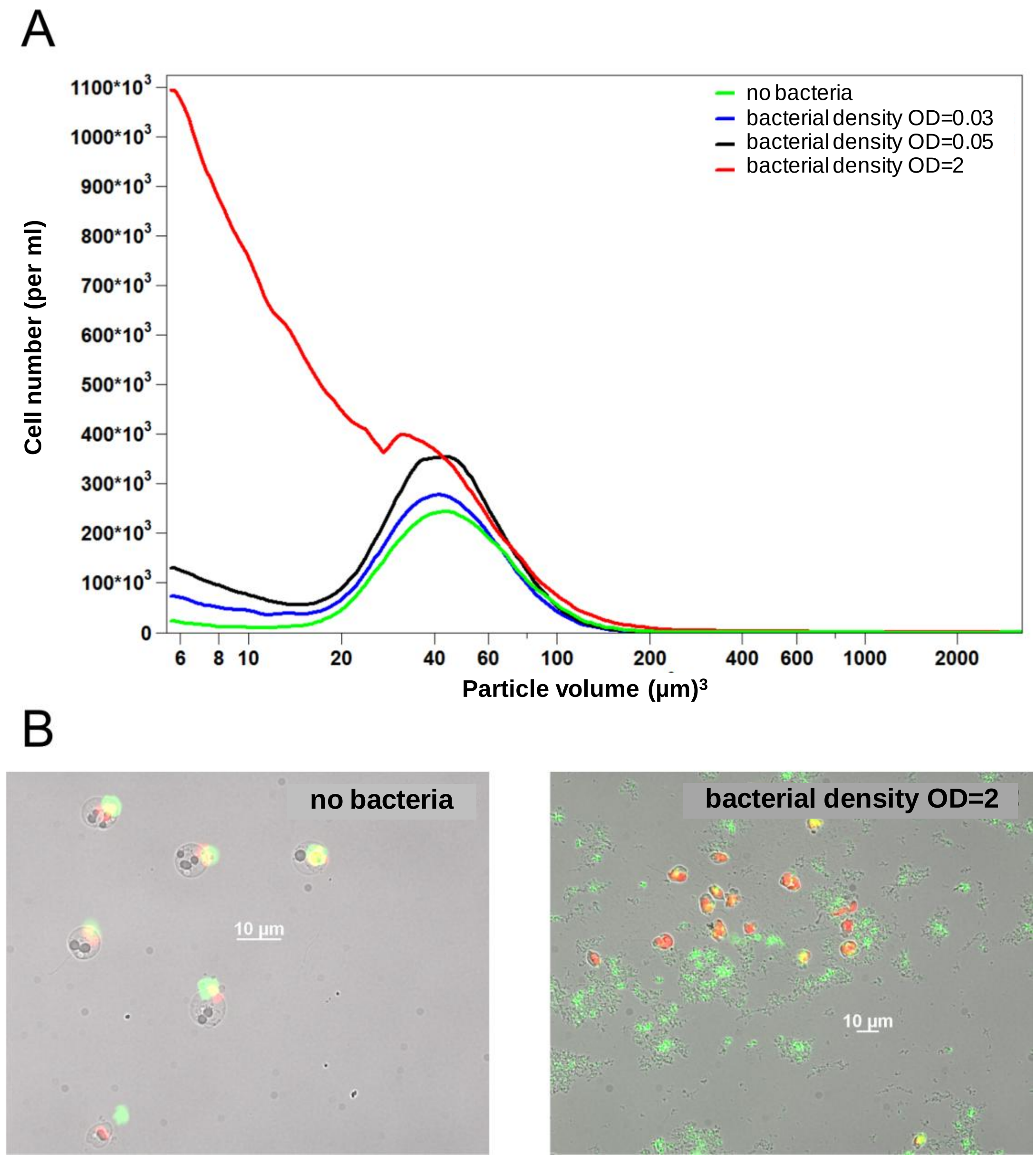

Figure 2.5: Comparison of *Poterioochromonas malhamensis* cultures with and without addition of heat-killed bacteria. A) Distribution of cell volumes without bacteria (green), with bacteria added to an optical density (OD) measured at 600 nm of OD_{600}=0.03 (blue), OD_{600}=0.05 (black) and OD_{600}=2 (red). B) Microscopic detection of bacteria. SYBR-Green stains nucleic acids of algae and bacteria (fluorescence shown in green) and the algal plastids can be detected by their auto-fluorescence (shown in red). In cultures without bacteria (left) any green fluorescence can be assigned to algal cells. In cultures with added bacteria (right), green fluorescence is also detectable outside of the algal cell.

Chapter 3

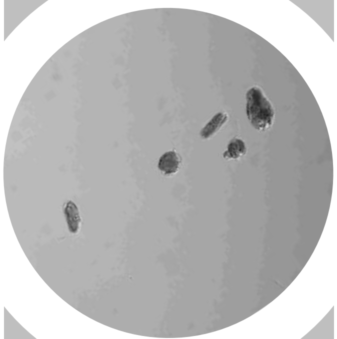

Analysing size variation during light-starvation response of nutritionally diverse chrysophytes with a Coulter counter

by Julia Rottberger, Ansgar Gruber and Peter G. Kroth
contents of this chapter were published as a research article in Algological Studies 141(1):37-51

3. Analyzing size variation during light-starvation response of nutritionally diverse chrysophytes with a Coulter counter

3.1. Abstract

Mixotrophy is a combination of autotrophic and heterotrophic nutrition. The regulation of the nutritional mode in mixotrophic algae is not yet fully understood. Changes in the light regime are likely to affect cell size of autotrophic, mixotrophic and heterotrophic chrysophytes to a varying extend. Here we demonstrate that an automatic particle analyser (Coulter counter) is a helpful tool not only for cell counts, but also for the detection of changes in mean cell size, total cell bio-volume or size distribution of chrysophyte cultures. The method is time saving and therefore allows large comparative studies, however, the method tends to underestimate the absolute size compared to microscopic measurements. The limitations of automated particle analysis opposed to traditional microscopic measurements are discussed exemplarily for *Dinobryon divergens*.

3.2. Introduction

Diversity in morphology and physiology is characteristic for the golden-brown algae (chrysophytes) (Kristiansen and Preisig, 2007). There are completely photoautotrophic representatives (e.g. *Mallomonas sp.*) as well as chemoheterotrophic algae (e.g. *Spumella*-like flagellates) with reduced, colourless plastids. Moreover, a considerable number of morphologically, ecologically and physiologically investigated mixotrophic species, e.g. of the genera *Ochromonas*, *Poterioochromonas* and *Dinobryon* are known. These algae exploit organic carbon sources as well as inorganic carbon (CO_2) for energy production. Growth of mixotrophic chrysophytes depends on the respective external conditions (Butterwick et al., 2005; Kamjunke et al., 2007; Watson and McCauley, 2010), but the regulation of their nutritional mode has not yet been revealed. Growth experiments under conditions which switch or up-regulate different metabolic pathways serve as a basis for the elucidation of the metabolism in mixotrophs. Determination of cell numbers is one measure for growth. Traditionally, cell counting of microorganisms is performed with the help of a haemocytometer. Wallace H. Coulter introduced a new measuring principle in 1953 by measuring changes in electrical resistance across an aperture through which the particle suspension is pumped. This technique, also known as Coulter principle, not only detects a particle, but also measures its size (Gaju et al., 1989). Such automated particle analysers can count large numbers of cells in short time and are very accurate and fast (Elnabarawy and Welter, 1984). The technique offers several advantages (short handling time, precision, etc.) and also has some disadvantages (need for suitable electrolyte, difficulties in distinguishing between living and dead cells) in counting and analysing size distributions of algal cells (Mulligan and Kingsbury, 1968; Elnabarawy and Welter, 1984). Here, we focus on the analysis of chrysophyte cell cultures to obtain nutrient and light dependent growth curves and investigate the advantages and handicaps of Coulter principle based measurements compared to microscopy. The investigated chrysophytes differ in shape but also in their nutritional mode. *Poteriospumella lacustris* is a chemoheterotrophic and *Mallomonas annulata* a photoautotrophic alga, while *Poterioochromonas malhamensis* and *Dinobryon divergens* are mixotrophic. The well-investigated photoautotrophic diatom *Phaeodactylum tricornutum* served as a reference strain. We investigate whether changes in the light regime affect cell size distribution in a way that is detectable with a Coulter counter (Multisizer 3, Beckman Coulter) and compare the Coulter counter results to microscopic data.

3.3. Methods

3.3.1. Standard culturing conditions

Poteriospumella lacustris JBM10 was cultured in modified Inorganic Basal Medium (pH 7.2) (Hahn, 2003) without $NiCl_2$ and with addition of a **d**issolved **o**rganic **c**arbon source **m**ixture (DOCM) of 1 g l^{-1} peptone, 1 g l^{-1} yeast extract and 1 g l^{-1} α-D-glucose. *Dinobryon divergens* FU18K_A and *Mallomonas annulata* WA 18K_M were grown in liquid WC medium (pH 8) (Guillard and Lorenzen, 1972) with modified concentrations of TES buffer (500 µM), $NaHCO_3$ (375 µM), K_2HPO_4 (32 µM), $NaNO_3$ (500 µM) and $MnCl_2$ (0.09 µM). The standard medium for *Poterioochromonas malhamensis* DS was modified Bacillariophycean Medium (BM) (pH 7.2) (Schlösser, 1994) with 236 µM Na_2CO_3, 27 µM Iron(III) citrate hydrate, 214 µM citric acid, 60 nM $MnSO_4$, 200 µg l^{-1} thiamine-HCl, 10 µg l^{-1} biotin and DOCM. *Phaeodactylum tricornutum* UTEX646 was grown in modified f/2 medium (pH 7) (Guillard and Ryther, 1962; Guillard, 1975) with artificial half-concentrated sea salts (16.6 g l^{-1}) and 0.09 µM $MnCl_2$.

Cultures were generally grown at 20 °C in Erlenmeyer flasks without shaking under sterile conditions and a light intensity of 30-40 µmol photons m^{-2} s^{-1} on the surface of the culture flasks. If not stated otherwise, the light:dark cycle was 16:8 h.

Cultures of *M. annulata*, *D. divergens* and *P. tricornutum* were uni-algal but contained bacterial populations. Cultures of *P. malhamensis* and *P. lacustris* were uni-algal and axenic referring to routine microscopic screening (fluorescent staining with SYBR Green and light microscopy) and random plating of culture aliquots on solidified media with dissolved organic carbon sources.

3.3.2. Growth experiments

Growth experiments were performed in triplicates e.g. three culture flasks inoculated from one pre-culture and grown in parallel. In the dark treatments, cultures were grown in the light (16:8 h light:dark cycle) up to a cell density of approximately 50 000-100 000 cells ml^{-1} prior to wrapping flasks into aluminium foil.

3.3.3. Osmolality

Culture samples (1 ml) were taken in time intervals from 1 to 4 days during growth experiments. Cell sedimentation was achieved by centrifugation (<6000 g). The osmotic pressure of the cell-free culture supernatant was measured in 50 µl aliquots with a cryoscopic osmometer (Osmomat 030, Gonotec).

Time series were performed during Coulter counter analysis to investigate possible osmotic effects of the electrolyte on cell size of the algae. Algal cell suspensions were analysed over five minutes every 60 s. Average cell diameters during each measurement were extracted from the size distribution graphs.

3.3.4. Determination of cell numbers

Cell numbers of all cell suspensions were determined with the Multisizer 3 (Beckman Coulter) equipped with a 100 µm-capillary. Directly prior to the measurements, 20-900 µl of a cell suspension were suspended in 12 ml of the electrolyte Isoton II-Diluent (Beckman Coulter) by pipetting. Measurements were performed in triplicates for each sample. The average data of the three measurements was analysed. To reduce background signals from dust, precipitates, fibres and other background particles, a sample with culturing medium or the sterile control was analysed additionally to the cell suspensions. This background measurement was subtracted from the average files using the Multisizer 3 software. To gain the cell density (i.e. cell number per millilitre), the curve area corresponding to the algal cells was calculated via the software. The curve area limits chosen were 3-20 µm for *P. lacustris*, *P. tricornutum* and *P. malhamensis*, 3.5-20 µm for *D. divergens* and 4-20 µm for *M. annulata*. Visual-field counts with the microscope were performed to determine the proportion of living *D. divergens* cells during growth experiments under light and dark conditions (). Here, cells of *D. divergens* were fixed with formaldehyde at a final concentration of 10 % (v/v) prior to microscopic analysis. All loricas were counted and the percentage of loricas with a cell (living cells) was determined.

3.3.5. Determination of cell volume and cell diameter

Cell volume and cell diameters could be extracted from the size distribution graphs after measurements with the Multisizer 3 by choosing “diameter” or “volume” as the x-axis. Fifty average files were chosen randomly from samples in exponential phase under standard conditions for statistical evaluation. Size statistics were set to the corresponding curve area limits of each alga. This way the mean and the standard deviation of each curve under consideration of the respective curve area limits were gained. This mean was considered to represent the average diameter or volume of the cells in the sample. The mean of the 50 standard deviations was considered to represent the average distribution of diameters or volumes in the sample.

For microscopic determination of cell volume and cell diameter, photographs of living cells were analysed. Samples were chosen randomly from cultures in exponential growth phase. Photographs were evaluated concerning diameter or length and width of 100 cells using the software Axiovision (Zeiss). The diameter was determined for *P. malhamensis* and *P. lacustris*. For *M. annulata*, *D. divergens* and *P. tricornutum* length and width of the cells were determined. Loricas of *D. divergens* were surveyed separately. Here, width was determined at the narrowest part of the goblet and the transect lengths from the narrowest point to the end of the goblet and to the end of the stalk were measured (Figure 3.1).

The standard deviation was calculated using the formula “STDEV” in the software Excel, Microsoft-Office 2007 (Microsoft Corporation). Serving as a standard, spherical particles (Flow-Check^{TM} Fluorospheres, Beckman Coulter) with a nominal diameter of 10 µm were measured with the Coulter counter (one sample) as well as by microscopic means (100 particles). T-tests were performed using “t-test” with default parameters in the software SigmaPlot 12.0 (SYSTAT Software).

3.4. Results

During measurements with the Coulter counter the algal peaks were clearly distinguishable from background contaminations when 0.02-0.9 ml of cell suspension within the range of $5*10^3$ to $5*10^7$ cells ml^{-1} were diluted in 12 ml of electrolyte and 500 µl of this dilution were analysed per measurement. The back ground noise could be reduced and peak resolution increased down to concentrations of 1000 cells ml^{-1} by subtraction of signals resulting from particles in the culturing media (dust, fibres, nutrient precipitates, etc.).

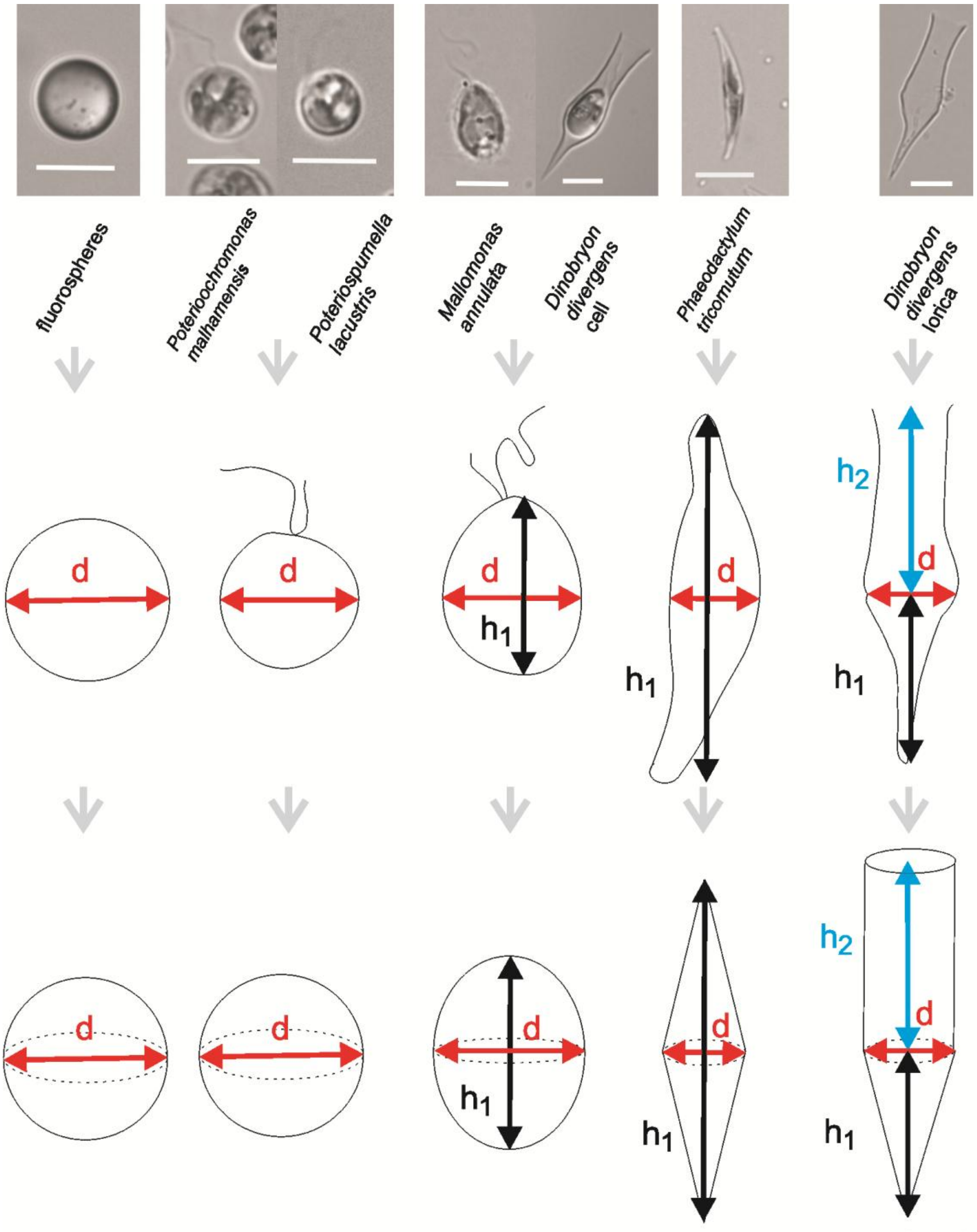

$$V = \frac{\pi}{6} \cdot d^3 \qquad V = \frac{\pi}{6} \cdot d^3 \qquad V = \frac{\pi}{6} \cdot d^2 \cdot h_1 \qquad V = \frac{\pi}{3} \cdot d^2 \cdot h_1 \qquad V = \pi \cdot d^2 \cdot \left(\frac{h_1}{12} + \frac{h_2}{4}\right)$$

Figure 3.1: Transformation of the 2D-data of cell shapes to 3D-data. Width and height of 100 cells per alga were extracted from micrographs (upper row) as demonstrated (middle row). The cell bio-volume (V) of the different alga was calculated from spheres, cones, cylinders and prolated spheres as indicated (lower row).

The particle analyzer extracts cell diameters as "spherical diameter equivalents" automatically from the electronic volume determinations by assuming a spherical cell shape. To test the accurateness of volume and diameter determinations compared to microscopic data, we calculated the bio-volume of single algae by measuring the cell dimensions in micrographs and transferring this 2D-data to a geometrical 3D-shape of the cells (Figure 3.1). Similar to the Coulter counter software, we then extracted spherical diameter equivalents assuming a sphere with the identical volume as the measured cell (Table 3.1). Both methods resulted in equivalent measurements of the spherical diameter for standard particles, with a small and statistically insignificant underestimation (2.8 %, t-test, p=0.558) by the Coulter measurements compared to the microscopic determination.

Table 3.1: Mean spherical diameter equivalents and mean bio-volumes of algal cells extracted from Coulter counter analysis and microscopic analysis.

	Counter (n=50 samples)		**Microscope (n=100 measurements)**	
	diameter [µm]	volume [µm³]	diameter [µm]	volume [µm³]
Mallomonas annulata	7.81±1.82	297.12±202.40	9.10±1.36	418.49±197.23
Dinobryon divergens, cell	6.91±2.49	232.80±228.52	7.78±1.53	276.91±181.68
Dinobryon divergens, lorica	-	-	15.95±0.77	2137.58±314.56
Poterioochromonas malhamensis	6.63±1.25	174.34±117.94	10.54±2.12	688.63±430.89
Poteriospumella lacustris	4.87±0.99	69.75±63.96	5.62±0.64	108.76±84.91
Phaeodactylum tricornutum	4.84±0.67	63.13±43.66	5.76±0.64	103.97±36.18
Fluorospheres	9.73±0.90*	493±119.20*	10.01±0.47	527.89±76.18

**only one sample analyzed*

Cells of the unicellular diatom *P. tricornutum* are fusiform (Figure 3.1 with an organic cell wall that persists a long time after the cells die off. Size distribution peaks of *P. tricornutum* were narrower compared to peaks of the other unicellular algae (Figure 3.2). The peak usually had two maximums with the second at approximately the double bio-volume (~ 90 µm^3, spherical diameters equivalents ~5.5 µm) of the first (~45 µm^3, spherical diameters equivalents ~4.5 µm). The bio-volume of *P. tricornutum* from microscopic cell size determinations was calculated as the sum of two symmetrical cones (Figure 3.1) resulting in bio-volumes of 63.1±43.7 µm^3 (Coulter counter) and (104.0±36.2 µm^3) by microscopic determination (Table 3.1). As expected for a photoautotrophic strain, *P. tricornutum* stopped dividing after cultures had been shifted to the dark (Figure 3.3), and there was only a single maximum in the cell peak of *P. tricornutum* (Figure 3.4*)*. The peak maximum was in the range of the smaller of the two peaks observed in the light treatments but less defined. In contrast to *M. annulata*, *P. tricornutum* was able to recover after three weeks in complete darkness (Figure 3.3).

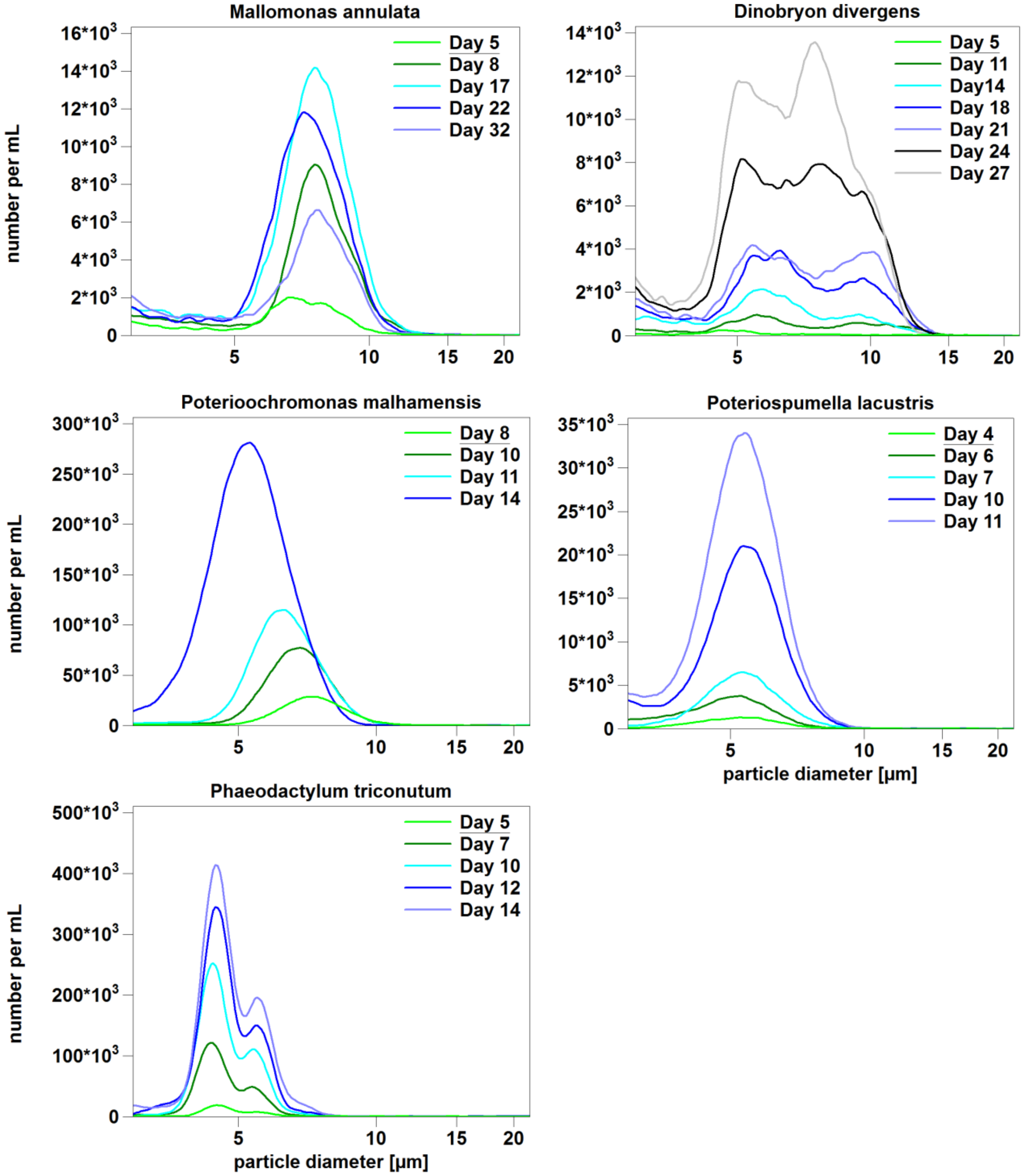

Figure 3.2: Size distribution graphs of the different algae during growth in the light measured with the Coulter counter. Typical size distribution of algal cells (3-20 µm) grown in a 16:8 h light:dark cycle. Only data from the exponential phase is shown except for for which Day 22 and Day 32 fall into the stationary phase.

The photoautotrophic chrysophyte *M. annulata* possesses silica-scaled envelopes. The cells are shaped like prolated spheroids (Figure 3.1). One broad peak was characteristic for the size distribution pattern of *M. annulata* during Coulter counter measurements (Figure 3.2). Particle numbers of *M. annulata* decreased in the late phase of growth experiments (Figure 3.2) and densities of particles smaller than the living alga increased. The increase of small particle abundance in the xenic cultures of *M. annulata* can be explained by two processes: cell lysis of the algal cells which leads to separation of the scales as well as increased bacterial growth due to exudates or cell fragment accumulation. Without systematic microscopic observation the exact composition of the particles <3 µm therefore remains elusive. *M. annulata* had the largest bio-volume (297.12±202.4 µm³) and the largest spherical diameter equivalent (7.8±1.82 µm) of all investigated cells determined by Coulter counter measurements but not from the microscopic surveys (Table 3.1). Shifting cultures to the dark resulted in a growth inhibition and cell death. This was reflected in the size distribution pattern by a loss of definition concerning the form of the algal peak, an increased amount of cell fragments in the range of 3-5 µm and a shift of the peak maximum to smaller spherical diameters equivalents (Figure 3.4). *M. annulata* cultures were not able to recover after 3 weeks in complete darkness (Figure 3.3).

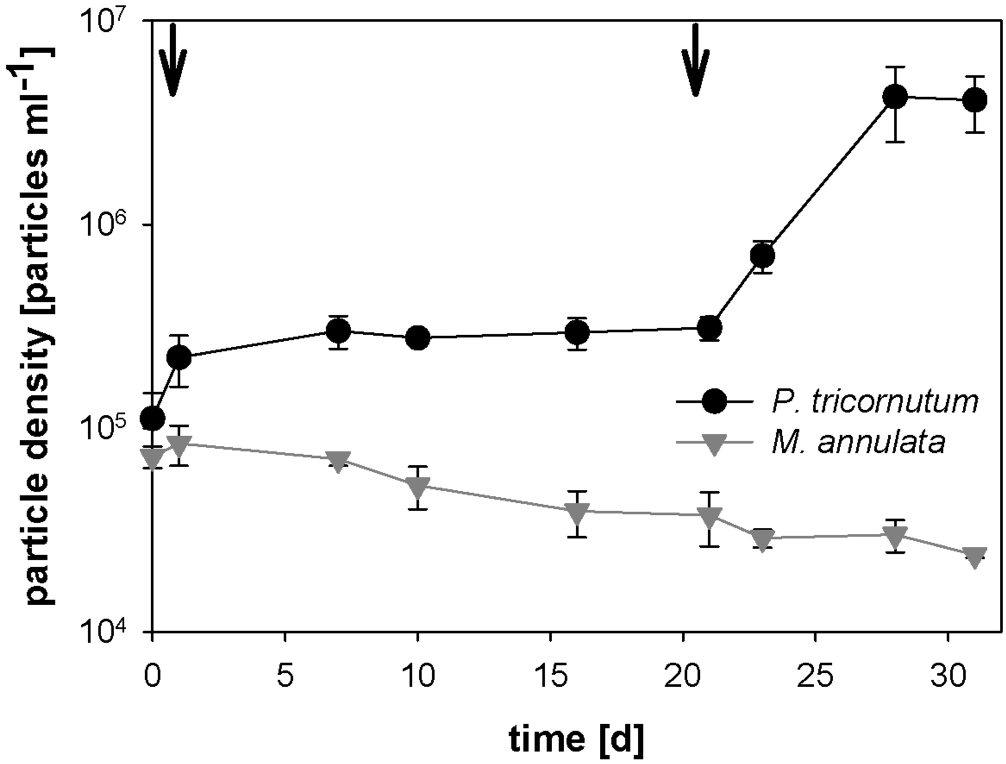

Figure 3.3: Cell densities in *Phaeodactylum tricornutum* and *Mallomonas annulata* cultures during dark treatments. Cultures were grown in a 16:8 h light:dark cycle. On day 2 (first arrow) the cultures were transferred to complete darkness. After 21 days in complete darkness cultures again were grown in a 16:8 h cycle (second arrow). Cell densities of *P. tricornutum* (particles from 3-20 µm) and *M. annulata* (particles from 4-20 µm) were determined by Coulter counter measurements. (n=3)

Cells of the mixotrophic *D. divergens* are seated in a goblet-like cellulose lorica (Figure 3.1). These loricas are very persistent after cells have died. The cells were treated as prolated spheroids for bio-volume determination whereas the volume of the loricas was calculated from a combination of a cone and a cylinder (Table 3.1). Under standard conditions, *D. divergens* was generally present in unicellular form as well as in colonies during the exponential phase. Colonies typically consisted of 2-5 cells whereas larger colonies were present but less frequent. This variability was reflected in a differing amount of peaks showing a size distribution in the range of ~20-2000 µm³ (Figure 3.2). Yet, the peaks were not very distinct from each other so that differentiation into specific colony size was not feasible. Furthermore, separation between living unicellular individuals and the lifeless but rigid solitary loricas caused problems. The mean bio-volume of the mixture of empty and cell-containing loricas of 232.8±228.52 µm^3 determined by Coulter counter analysis was similar (t-test, p=0.201) to microscopic results concerning the cells only (276.91±181.7 µm^3) and much smaller than the microscopically determined bio-volume of the loricas alone (2137.6±314.6 µm³). We performed visual field counts using the microscope in parallel to Coulter counter measurements determining the percentage of living cells (loricas containing a cell) from all counted loricas. For *D. divergens*, the amount of empty loricas in the late exponential phase was 20 % - 30 % under standard conditions and increased steadily in the stationary phase (Figure 3.5). When cells were transferred to continuous darkness, they died completely within 4 days according to microscopic observations (3.5B). Yet, there was no change in cell numbers (3.5A) but only a shift to smaller cell-diameters in the cell-size distribution pattern during Coulter counter measurements (Figure 3.4). The light-treated cultures showed a broad peak with several bumps. In dark-treated cultures, there was only one distinct peak at the lower end of the size distribution range of the light-grown cells.

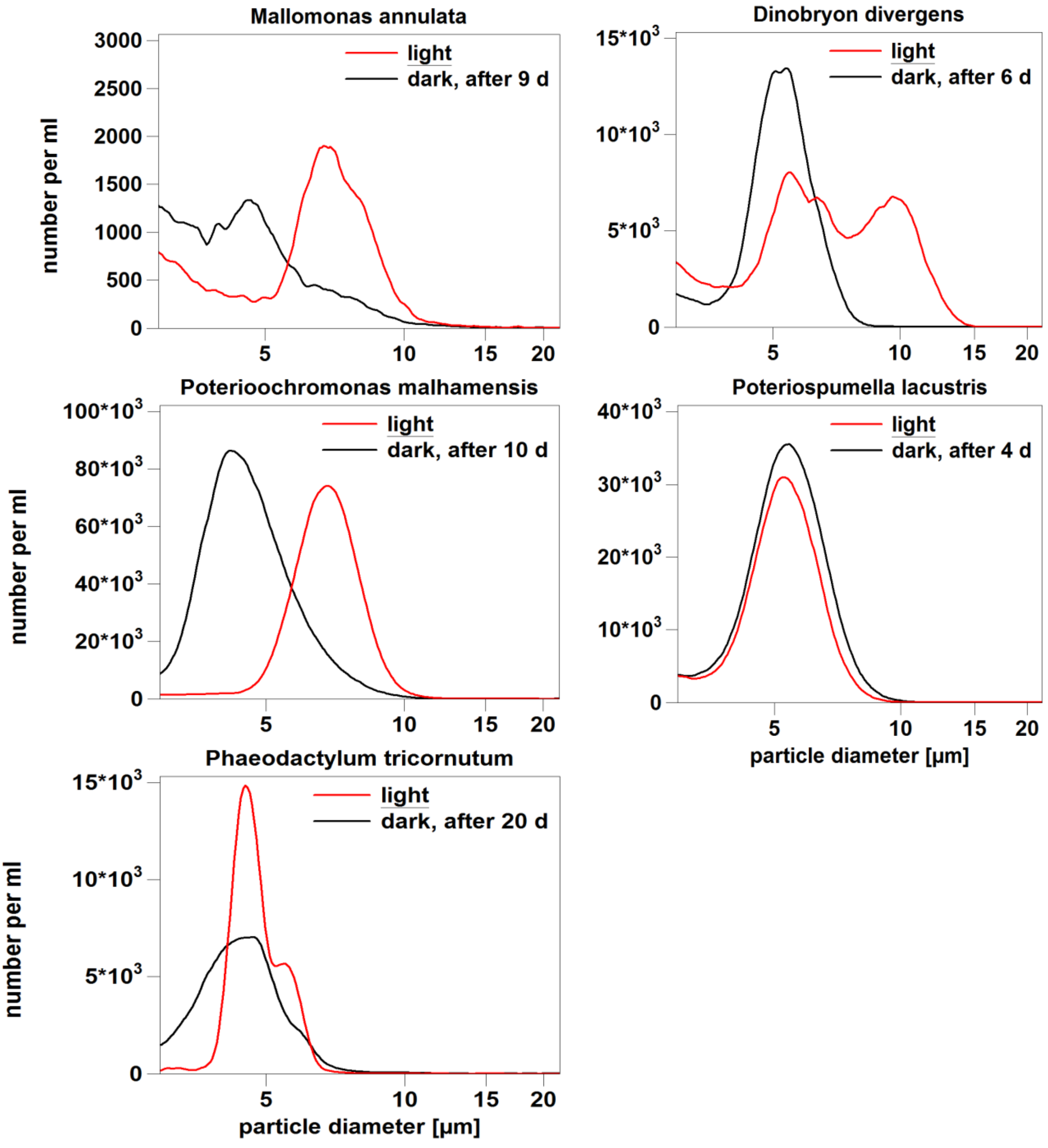

Figure 3.4: Size distribution of the studied algae in the light and in the dark measured with the Coulter counter. Typical size distribution of algal cells grown in a 16:8 h light:dark cycle (grey) and of algal cells shifted to complete darkness for several days (black).

Hence, empty loricas were not separated from cell-containing solitary loricas concerning their electronic volume.

The mixotrophic *P. malhamensis* has a spherical cell shape (Figure 3.1). Some *P. malhamensis* cells may form chitin stalks (Peck, 2010). Individuals with stalks are generally not as mobile as stalk-free cells. We did not observe biofilms on the glass surfaces of the culture vessels, which means that cells generally grew in suspension or only loosely attached to the culturing vessels. Bio-volumes and spherical diameter equivalents of *M. annulata* and *P. malhamensis* differed significantly (t-test, $p<0.008$) between the two strains, measured with both methods. However, according to the microscopic survey *P. malhamensis* had the largest cells within our set of investigated algae, in conflict to the results of the Coulter counter analysis (Table 3.1). Here. *M. annulata* had the largest spherical diameters equivalent and cell volume. Cells of *P. malhamensis* were largest at the beginning (with a mean of 7.10 ± 1.61 µm) and smallest at the end (with a mean of 4.26 ± 1.25 µm) of the exponential phase (Figure 3.2). Cell size also changed in the dark treatments (Figure 3.4), after 10 days the mean of spherical diameters equivalents was 4.57±1.22 µm in the dark compared to 6.69±1.32 µm in the light.

The solitary cells of *P. lacustris* cells were treated as spheres (Figure 3.1). Bio-volumes of *P. lacustris were* 69.8±63.96 µm³ by Coulter counter analysis and 108.8±84.9 µm³ by microscopic means (Table 3.1). As expected from the trophic characteristics, cell-size distribution patterns did not differ between light and dark conditions (Figure 3.4).

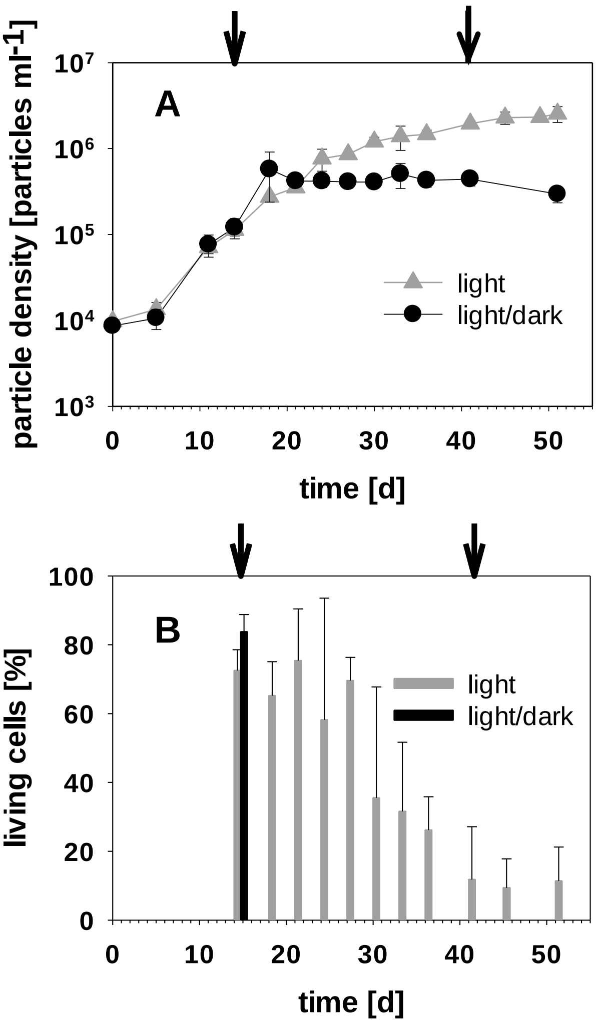

Figure 3.5: Comparison of cell counts in *Dinobryon divergens* cultures performed with the flow cytometer (A) and by visual field counts (B). Cell densities of *D. divergens* (particles from 3.5 µm to 20 µm) were determined by Coulter counter measurements (A) and the percentage of living cells was determined by microscopic visual field counts (B). Cultures were grown in a 16:8 h light:dark cycle. On day 14 (first arrow) some of the cultures (light/dark, black) were transferred to complete darkness whereas conditions remained unchanged for the rest of the cultures (light, grey). After 4 days cells had completely died off in the dark referring to microscopic survey (B, black). After 27 days in the dark (second arrow, day 41) the cultures (light/dark, black) were transferred back to the 16:8 h cycle. (n=3)

Algal cell size distribution varied from 13.8-36.0 % during Coulter counter analysis referring to standard deviations of the peak means (Table 3.1). Standard deviations of spherical diameters equivalents were 11.1-23.3 % for microscopic determinations. Bio-volumes and spherical diameter equivalents were generally significantly underestimated during the Coulter counter measurements (t-test, $p<0.01$) compared to the data generated by microscopic survey. Thus, in contrast to measurements of the standard particles there was a significant difference between the two methods in measurements of living cells.

We performed additional experiments to investigate whether the underestimation of cell size during Coulter counter analysis might be due to changes in the salinity of the culturing media during growth. Osmolality of the WC medium used for *M. annulata* and *D. divergens* was at the lower detection limit of the osmometer (4 mosmol kg^{-1}) and was not influenced by the light conditions throughout the growth experiments. The same observations applied to cultures of *P. lacustris* in NSY (21 mosmol kg^{-1}). Osmolality of the f/2 medium used for *P. tricornutum* increased throughout the experiments from 394 mosmol kg^{-1} to 439 mosmol kg^{-1}, but did not affect cell size (Figure 3.2). The same increase was observed in the sterile control sample containing only f/2 medium but no algal cells. The osmotic pressure decreased from 19 mosmol kg^{-1} to 13 mosmol kg^{-1} during growth of *P. malhamensis*. There were no differences in osmolality comparing light and dark conditions. Osmolality in the sterile control sample was stable over the whole experiment. During Coulter counter analyses three measurements per sample were performed within one minute. Including the sample handling time, contact of cells with the electrolyte was less than two minutes for the whole analysis. As there were considerable differences in osmolality of the medium for the freshwater chrysophytes compared to the electrolyte (300 mosmol kg^{-1}), we performed time dependent cell size analysis for all algae over a time period of 5 min in intervals of 1 min. Cell size distribution patterns of *P. tricornutum* and *D. divergens* did not change over this time period. For *P. lacustris* and *M. annulata* changes in the cell diameter appeared after more than two minutes. For *P. malhamensis* cell shrinkage occurred in the dark as well as in the light. The shrinkage already occurred within the first minute of the time series and the maximum decrease of average cell diameters was 1 µm. We did not observe any correlation of the value of the cell shrinkage to the different growth phases or the different light conditions.

3.5. Discussion

We determined cell dimensions of algae by microscopic and by flow-cytometric means. Our results from micrographs are in accordance with microscopic data from other studies of *P. tricornutum* (Bartual et al., 2008), *P. malhamensis* (Pringsheim, 1955) and loricas of *D. divergens* (Bucka, 2005; Kristiansen and Preisig, 2007).

Standard deviations of spherical diameter equivalents derived from micrographs and Coulter counter analysis were rather high (11.1-36.0 % and 13.8-36.0 %) indicating that cell sizes were very variable. These variations were not due to measuring accuracy because the standard deviations of particles with defined size (4.7 %, microscopically and 9.1 % via Coulter counter analysis) and of lorica dimensions of *D. divergens* were lower (4.8 %, microscopically) than of any population of living cells

Referring to microscopic investigations, cells of the algae with rigid cell envelopes were less variable in size than naked cells. This was reflected by the standard deviations, which were smaller the more pronounced the scaling of the alga was. They were smallest for the persistently coated cells of *P. tricornutum* (11.1 %) and the silica-scaled *M. annulata* (14.3%). The highest standard deviation was observed for the completely naked cells of *P. lacustris*. This correlation was not observed during the Coulter counter measurements. Here, *M. annulata* had higher standard deviations than *P. tricornutum*, *P. lacustris* and *P. malhamensis*. Hence, rigidity of the cell envelopes is not a decisive criterion for size variation measured by the Coulter principle.

A significant underestimation of cell diameters by Coulter counter analyses was observed compared to microscopic analyses (Table 3.1). The underestimation was only partially related to calibration issues as measurements with particles of defined size differed only slightly from their nominal size. A reduction of cell diameters was observed during time series measurements with the Coulter counter within five minutes in culture samples of *M. annulata*, *P. malhamensis* and *P. lacustris*. We did not test electrolytes with lower osmolality, which might have reduced the osmotic effects on the freshwater chrysophytes. The osmotic effects of the electrolyte reduced average cell size up to 1 µm within the measuring time for *P. malhamensis*. Yet, the cell diameter reductions observed for *P. malhamensis* during exponential growth phase or comparing light- to dark- grown cells were larger than 2 µm and are therefore only partially related to osmotic effects. The underestimation of bio-volumes during Coulter counter analysis may also be promoted by too high electrical field strengths (Zimmermann et al., 1976). Independent Coulter counter data was not found for any of the investigated algae. Hence, underestimation of the cell size by Coulter counter analysis cannot be considered a general effect without further independent investigations. Overall, the differences in the two cell diameter determination methods did not affect consistency of the Coulter counter analysis with respect to the scientific questions addressed because they occurred systematically and not randomly.

Surveying the cell-size distribution patterns of algae under different light conditions by Coulter counter measurements revealed individual differences. Generally, mean cell size did not vary in the light during exponential phase in cultures of *D. divergens*, *M. annulata*, *P. tricornutum* and *P. lacustris* (Figure 3.3) but for *P. malhamensis*. The mixotrophic *P. malhamensis* is known to assimilate the major bulk of carbon by phagotrophy or osmotrophy and only to a minor portion by photoautotrophy (Sanders et al., 1990; Boenigk et al., 2006). The cell size reduction in the light might be due to reduction of the photosystems and size of the plastids (Sanders et al., 2001). It also has been shown for the mixotrophic chrysophyte *Ochromonas danica* that plastids are smallest under dark conditions (Maguire et al., 1995). Size reduction of the plastid might explain that cell-size reduction of *P. malhamensis* occurred faster in the dark (Figure 3.4).

Distinguishing between living cells and fragmented dead cells from cell-size distribution graphs was easily possible for *M. annulata*, *P. malhamensis* and *P. lacustris*, while this was problematic for *D. divergens*. Firstly, the quantity of peaks did not always correspond to the size of the colonies of *D. divergens*. We suppose that especially large colonies were disrupted by shearing forces resulting from the current of the pump. Secondly, it was impossible to distinguish empty solitary loricas from living solitary individuals because the electronic volume of the loricas was independent of whether they contained a cell or not.
The electronic lorica volume was smaller than estimated by microscopy, possibly because cellulose particles are not comparable to living cells during Coulter counter measurements in aquatic solutions. In fact, Beckman Coulter recommends acetone or propan-2-ol with ammonium thiocyanate for measuring cellulose particles (Multisizer 3 Operators Manual Appendix). However, due to their cytotoxicity, these solvents were not suitable for our application. Depending on the scientific question addressed these issues might be bypassed by initial calibration of the Coulter counter measurements to an independent method e.g. by microscopic observation as performed in this study.

Interestingly, size distribution graphs of the unicellular diatom *P. tricornutum* showed two peaks in the light, but only one peak after prolonged periods in the dark. Possibly the second peak results from dividing cells, as cell division is light-regulated in *P. tricornutum* and arrested in dark-treated cells (Huysman et al., 2010).

3.6. Summary

Although Coulter counter analysis in our hands did not exactly reflect the results from microscopic surveys (Table 3.1), it is an adequate method to replace time consuming microscopy of living chrysophytes. Furthermore, there are a number of persuasive advantages: (i) in contrast to chlorophyll content determinations, optical density measurements and colony-forming unit counts, Coulter counter analysis was a method suitable to analyse all of the investigated chrysophytes immediately without chemical fixation (Figure 3.2, Figure 3.4); (ii) changes in cell numbers as well as in cell diameters can be obtained in parallel from the same measurement for four out of five algae (Figure 3.2, Figure 3.3, Figure 3.5); (iii) we demonstrated for *P. malhamensis*, *M. annulata* and the diatom *P. tricornutum* that Coulter counter analysis can reveal morphological changes as a reaction to physiological or environmental changes like e.g. light starvation (Figure 3.3, Figure 3.4).

3.7. Acknowledgements

The authors thank Katharina Scholz for the help with the experiments and Prof. Jens Boenigk for providing the chrysophyte strains. The authors are thankful for financial support by the University of Konstanz (Research Initiative “Organismic Interactions in aquatic ecosystems under changing conditions”).

Chapter 4

Influence of nutrients and light on autotrophic, mixotrophic and heterotrophic freshwater chrysophytes

by Julia Rottberger, Ansgar Gruber, Jens Boenigk and Peter G. Kroth
contents of this chapter are in the process of review at Aquatic Microbial Ecology

4. Influence of nutrients and light on autotrophic, mixotrophic and heterotrophic freshwater chrysophytes

4.1. Abstract

Mixotrophy in protists is a noteworthy life style situated between the metabolic modes of photoautotrophy (building biomass from inorganic molecules via photosynthesis) and chemoheterotrophy (building biomass from organic substances via uptake of food). Chrysophyte algae show strong variation regarding their nutritional modes which is especially advantageous in oligotrophic conditions. Re-oligotrophication of lakes may thus result in an increase of mixotrophic chrysophytes in the phytoplankton community. Yet, the capacities and strategies to adapt to changing conditions may vary due to different nutritional requirements of the individual species. In this context, comparative analyses evaluating the physiological range of mixotrophic chrysophytes are important to predict possible changes through re-oligotrophication. We studied four freshwater chrysophytes, *Poteriospumella lacustris*, *Poterioochromonas malhamensis*, *Dinobryon divergens*, and *Mallomonas annulata* under different growth conditions. The diatom *Phaeodactylum tricornutum* served as photoautotrophic reference strain.

We demonstrate active growth of *Poteriospumella lacustris* and the mixotrophic *Poterioochromonas malhamensis* under chemoheterotrophic conditions. Both chrysophytes were not growing photoautotrophically, however, *Poterioochromonas malhamensis* showed some photosynthetic activity and was able to survive longer when kept in the light. *Mallomonas annulata*, *Phaeodactylum tricornutum*, and the mixotrophic alga *Dinobryon divergens* showed light limited growth when kept in inorganic media. Even though *Dinobryon divergens* consumed living bacteria, it did not grow in the dark in the presence of bacteria.

Due to the observed differences in general nutritional preferences between the two mixotrophs *Poterioochromonas malhamensis* and *Dinobryon divergens*, we propose that during re-oligotrophication, *Dinobryon divergens* might primarily compete with photoautotrophs while *Poterioochromonas malhamensis* presumably mainly competes with chemoheterotrophs.

4.2. Introduction

Re-oligotrophication of freshwater habitats is often accompanied by shifts of the phytoplankton composition. In several European lakes mixotrophic algae have attracted considerable attention during the re-oligotrophication process because of their increasing contribution to total phytoplankton biomass (Gaedke, 1998; Anneville and Pelletier, 2000; Dokulil and Teubner, 2005). Mixotrophic algae are able to meet their carbon demands by assimilating inorganic carbon (CO_2) as well as by uptake of organic molecules. This uptake of organic substances is not limited to dissolved molecules (osmotrophy) but can also be accomplished by ingestion of detritus or living bacteria (phagotrophy). Mixotrophy is not synonymous to photoheterotrophy, a lifestyle that involves utilization of light derived energy without assimilating of inorganic carbon.

Chrysophytes (throughout the manuscript this term refers to the chrysophytes *sensu lato*, comprising the classes Chrysophyceae and Synurophyceae (Andersen et al., 1999; Kristiansen and Preisig, 2007; and Iwataki, 2012), are of special interest because their abundance may increase during phases of lake re-oligotrophication (Jeppesen et al., 2005) and because they often dominate mixotrophic phytoplankton populations (De Hoyos et al., 1998; Watson et al., 2001; Kamjunke et al., 2007). Chrysophytes are geographically widespread and abundant in freshwater and marine habitats as well as in soils (Sandgren, 1988; Boenigk and Arndt, 2002; Massana, 2011). While a large number of chrysophyte genera show mixotrophic traits (Porter, 1988; Sanders and Porter, 1988), all different metabolic lifestyles ranging from exclusively chemoheterotrophic to exclusively photoautotrophic nutrition can be found (Raven et al., 1995). Several parameters may affect the growth competitiveness of mixotrophic chrysophytes. Besides carbon and phosphorous availability (Rothhaupt, 1996a) also light (de Castro et al., 2009), pH (Moser and Weisse, 2011a) and temperature (Moser and Weisse, 2011b; Wilken et al., 2013) have been shown to be important factors in laboratory studies. Furthermore some chrysophytes require vitamin supply (Heinrich, 1955). Mixotrophic chrysophytes are thought to be very competitive in oligotrophic waters because some of them may ingest bacteria which are utilized as carbon and phosphorus source (Thingstad et al., 1996; Kamjunke et al., 2007; Unrein et al., 2007). Still, each of the mentioned parameters is likely to affect each chrysophyte species in a different way (Watson and McCauley, 2010; Moser and Weisse, 2011a) making it difficult to predict the success of certain mixotrophic species in re-oligotrophication scenarios.

In this study we compare nutritionally different mixotrophic chrysophyte species to each other as well as to purely photoautotrophic or purely chemoheterotrophic reference species. We thereby want to demonstrate how different chrysophytes are affected by nutritional parameters under identical conditions and by this illuminate and discuss whether the observed differences might influence the competitive fitness of a single species during re-oligotrophication. We tested different culturing conditions to find the most suitable conditions for physiological comparisons. We specified which component of the culturing media limited maximum cell numbers of each protist to make sure that the macronutrients and not the trace metals or vitamins were the limiting factor. Comparative studies were performed examining the influence of light and different carbon sources on all strains. Photosynthetic capacities of all strains were compared by conducting oxygen evolution measurements to complement results from the growth experiments. The results of these experiments allow us to discuss the role of mixotrophs in anticipated lake re-oligotrophication scenarios.

4.3. Methods

4.3.1. Strains and standard culturing conditions

The chrysophytes investigated in this study were isolated from oligotrophic, alpine or pre-alpine freshwaters (Table 4.1) and include two mixotrophic strains, *Dinobryon divergens* FU18K_A (xenic) and *Poterioochromonas malhamensis* DS (axenic).The colourless heterotrophic flagellate *Poteriospumella lacustris* (strain JBM10) (axenic) and the photoautotrophic *Mallomonas annulata* WA 18K_M (xenic) were chosen as reference strains. As a photoautotrophic reference strain we also studied the diatom *Phaeodactylum tricornutum* UTEX646.

Poteriospumella lacustris was cultured in modified Inorganic Basal medium (pH 7.2) (Hahn, 2003) without $NiCl_2$ and with addition of a **d**issolved **o**rganic **m**atter (DOM) of 1 g l^{-1} peptone (Roth, Germany), 1 g l^{-1} yeast extract (Roth, Germany) and 1 g l^{-1} α-D-glucose. *Dinobryon divergens* and *Mallomonas annulata* were grown in liquid WC medium (pH 8) (Guillard and Lorenzen, 1972) with modified concentrations of TES buffer (500 µM), $NaHCO_3$ (375 µM), K_2HPO_4 (32 µM), $NaNO_3$ (500 µM) and $MnCl_2$ (0.09 µM). The standard medium for *Poterioochromonas malhamensis* was modified Bacillariophycean Medium (BM) (pH 7.2) (Schlösser, 1994) with 236 µM Na_2CO_3, 27 µM Iron(III) citrate hydrate, 214 µM citric acid, 60 nM $MnSO_4$, 200 µgl^{-1} thiamine-HCl, 10 µgl^{-1} biotin and DOM. *Phaeodactylum tricornutum* was grown in modified f/2 medium (pH 7) (Guillard and Ryther, 1962; Guillard, 1975) with artificial half-concentrated sea salts (16.6 g l^{-1} Tropic Marin®, Dr. Biener GmbH, Wartenberg, Germany) and 0.09 µM manganese or on solid plates of modified f/2 (with 1.5 % agar) for culture maintenance.

The axenic state of the cultures was monitored regularly by light and fluorescence microscopy, flow-cytometry and by screening of growth of bacterial colonies on solid media (1.5 % agar) including DOM.

Table 4.1: Algal strains investigated in this study.

	Origin	Axenic ?	Reference for strain description	Carbon acquisition	Habitus	Literature reference phagotrophy
Mallomonas annulata WA 18K_M	Lake Wallersee, Austria	no	Boenigk et al., unpublished	autotroph	unicellular	none
Dinobryon divergens FU 18K-A	Lake Fuschelsee, Austria	no	Boenigk et al., unpublished	mixotroph	colonial	Jones & Rees 1994, Veen 1991
Poterioochromonas malhamensis DS	Lake Constance, Germany	yes	Hahn & Höfle, 1998	mixotroph	unicellular, stalks	Hahn & Höfle, 1998
Poteriospumella lacustris JBM10	Lake Mondsee, Austria	yes	Findenig et al. 2010	heterotroph	unicellular	Boenigk et al., 2006
Phaeodactylum tricornutum Bohlin UTEX 646	Baltic Sea, Finland	no	Droop 1954, De Martino et al. 2007	autotroph	unicellular	none

A consortium of several bacterial strains was isolated from *D. divergens* cultures by plating a culture sample on WC medium including DOM and incubating the plate for one week at room temperature. The bacterial consortium was transferred to fresh plates monthly without further purification.
Bacteria were grown in liquid WC medium with DOM for the feeding experiments.

Cultures were generally grown at 20 °C in Erlenmeyer flasks without shaking under sterile conditions and a light intensity of 30-40 µmol photons m^{-2} s^{-1} on the surface of the culture flasks. If not noted otherwise, the light:dark cycle was 16:8 h.

4.3.2. Cell counts of protists

Cell counts and the determination of biovolume of protists were performed by flow cytometry according to the Coulter principle (Multisizer III, Beckman Coulter) using a capillary with an aperture of 100 µm diameter. Directly prior to measurements 100-900 µl of a cell suspension were suspended in 12 ml of the electrolyte Isoton II-Diluent (Beckman) by pipetting. Measurements were performed in triplicates for each sample and averaged. To reduce background signals from dust, precipitates and fibers, a sample of the sterile control was analyzed and subtracted. To gain the cell density (i.e. cell number per milliliter), the curve area corresponding to the algal cells was calculated. The curve area limits were 3-20 µm for *P. lacustris*, *P. tricornutum* and *P. malhamensis*, 3.5 - 20 µm for *D. divergens* and 4-20 µm for *M. annulata*. Cell volume and cell diameters were both extracted from the same size distribution graphs after measurements with the Multisizer III by choosing “diameter” or “volume” as the x-axis.

Except for *D. divergens*, dead cells or cell fragments were clearly distinguishable from living cells by size. To get a better evaluation of the number of living cells of *D. divergens*, we subtracted 30 % of the cell counts representing empty loricas during exponential phases (for details see Rottberger et al., 2013) if actual numbers of living cells were required, but did not do so to determine growth rates.

4.3.3. Cell counts of bacteria

Bacterial cell counts were conducted using a microscope and a micrometer ocular with a total magnification of 640. Cell counts of each sample analyzed were performed in quadruples and averaged.
The concentration of bacteria added during feeding experiments was adjusted according to optical density (OD) measurements at λ= 600 nm. To get an impression of actual bacterial cell numbers the OD measurements were exemplarily correlated to cell counts of living bacteria grown in WC with DOM by one dilution series ranging from OD 0-0.5. Four counts per OD were performed and averaged. Bacterial cell numbers were then calculated by the formula of the linear regression curve over all data points (Supplementary 4.7).
Accompanying, suspended bacteria were counted exemplarily in mid-exponential phase to 47,000 cells ml^{-1} of *D. divergens* and 73,000 cells ml^{-1} of *M. annulata*. Cultures of *D. divergens* and *M. annulata* were inoculated with 1,000 algal cells ml^{-1} and grown under standard conditions in triplicates. Four counts per culture were performed and all twelve counts per alga were averaged. Bacterial densities of *D. divergens* cultures were compared

to an identically treated control culture in which algal cells had been removed by filtration (nitrocellulose, pore size 5 µm) prior to inoculation.

4.3.4. Growth experiments

Growth experiments were performed in triplicates. Protist cultures were inoculated with a start abundance of 1,000-10,000 cells ml^{-1}. Cultures were grown in the light (16:8 h) up to a cell density of approximately 50,000-100,000 cells ml^{-1} prior to exposing them to a 4:20 h (6:20 h for *M. annulata*) or 8:16 h light:dark cycle. For experiments in complete darkness culture flasks were wrapped with aluminium foil directly after inoculation. If aeration was required, dry, double sterile-filtered air (0.2 µm PTFE-filters, Whatman) was bubbled into the culture flasks through silicon plugs. If shaking was required, culture flasks were placed on a horizontal shaker (GFL 3020, 100 rpm).
Feeding experiments were performed with either autoclaved or living bacteria which had been washed twice with 0.9 % sodium chloride.
Autoclaved bacteria were added with OD_{600}=0.01 and living bacteria with OD_{600}=0.05 prior to inoculation with the protists.
Fluorescently labelled living bacteria were generated by staining living cells with SYTO@ 9 Green fluorescent nucleic acid stain (Invitrogen) in a small volume of medium (100 µl) for 1 h. The washed, fluorescently labelled bacteria were added to *D. divergens* cultures in exponential growth phase with an OD_{600}=0.005 corresponding to optical density measurements of an accordingly treated bacterial culture aliquot with non-stained cells.

4.3.5. Maximum yield limitation experiments

Potential limitations on the maximum cell numbers of each investigated strain were tested by increasing the concentration of DOM, glucose, the nitrate source, the phosphate source, the vitamin solution or the trace metal solution during stationary phase to 3 times the standard concentrations under standard conditions.

4.3.6. Oxygen measurements

Cells were harvested during late exponential growth phase and sedimented by gentle centrifugation (< 1500 g). Cell densities were adjusted to >10^6 cells ml^{-1} using a 1:1 mixture of culture supernatant and fresh culturing medium. Oxygen measurements were performed at 20 °C with 1 ml of the cell suspensions in a Clark-type electrode (Hansatech). Samples were acclimatized within the electrode chamber to the respective light intensity (0-1000 µmol photons m^{-2} s^{-1}) for 10 minutes without stirring. Measurements were then performed within 4 minutes of continuous illumination and gentle stirring (30 rpm). The biovolume of the cells in the samples was determined after oxygen measurements with a flow-cytometer (Multisizer III, Beckman Coulter) and rates were then calculated to fmol O_2 μm^{-3} h^{-1}. All oxygen evolution rates were determined from triplicates measured within three successive days.

4.3.7. Statistics

Standard deviations were calculated from triplicates (n=3) using the function “STDEV” in the Excel-software, Microsoft Office 2007 (Microsoft Corporation).

The significance of differences was calculated by p-test performance using SigmaPlot 12.0 (Systat Software). Here, normality distribution was tested by a Shapiro Wilk test with a confidence interval of 95 %, a score of 0.05 and a p-value to reject normality of 0.05.

4.4. Results and Discussion

4.4.1. Selection and characterization of strains

For comparative physiological studies under laboratory conditions we chose two mixotrophic freshwater species of the genera *Poterioochromonas* and *Dinobryon* which both are well-described in the literature (e.g. Bird and Kalff, 1987; Caron et al., 1990; Boenigk et al., 2006; Watson and McCauley, 2010) and compared them to one photoautotrophic (*Mallomonas annulata*) and one heterotrophic chrysophyte (*Poteriospumella lacustris*). In order to compare the results to a physiologically and genetically well-investigated unicellular organism which also belongs to the stramenopiles, we studied the brackish-water diatom *Phaeodactylum tricornutum*.

Bacteria were not detected in cultures of *P. tricornutum* under standard conditions but occasionally appeared when the cells were grown in media containing **d**issolved **o**rganic **m**atter (DOM). *D. divergens* and *M. annulata* were unialgal but not bacteria-free in all media utilized for the experiments. Cultivation of bacteria-free *Dinobryon sertularia* has already been described (Lehman, 1976), however, our attempts to purify *D. divergens* via dilution, single-cell pipetting approach or incubation of culture aliquots with different antibiotics (mainly of the β-lactame group) were unsuccessful. It has been suggested that for *D. cylindricum* the presence of bacteria or organic compounds might be obligatory due to certain unknown growth factors (Caron et al., 1993).

4.4.2. Optimization of culture conditions

Cultures of different chrysophytes have successfully been maintained in batch cultures without agitation (Caron et al., 1993), with occasional agitation (Rothhaupt, 1996a), continuous agitation (Van Donk et al., 2009), with air-bubbling (Maberly et al., 2009) or with

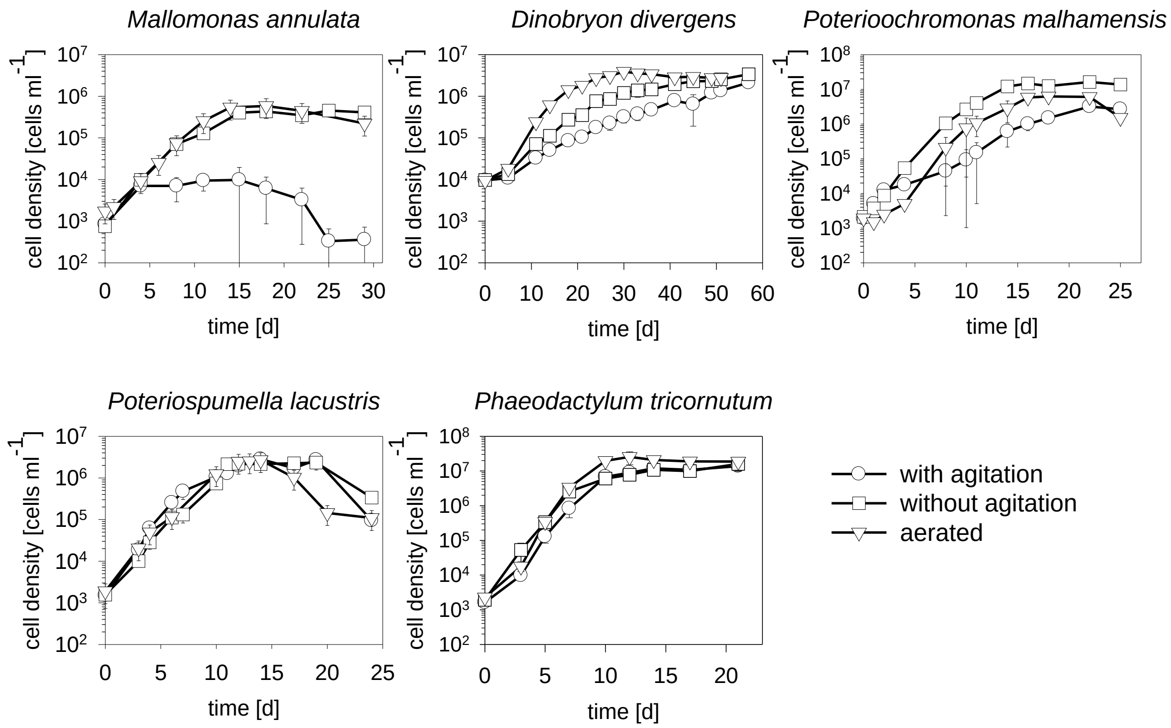

Figure 4.1: Growth curves of the investigated chrysophytes under different culturing conditions. Growth performance of the different protists under aeration and in batch cultures, with and without agitation. Each data point represents the mean of three samples, error bars represent standard deviations.

supply of 4 % CO_2 (Myers and Graham, 1956). In this study we tested no agitation, shaking and aerated conditions (Figure 4.1). Shaking at 100 rpm resulted in slower growth of *M. annulata*, *D. divergens* and *P. malhamensis* (growth rates were reduced by 55.8 %, 32.2 %, and 54.2 %, respectively) than without shaking while *P. lacustris and P. tricornutum* performed equally at all conditions. Specifically *D. divergens* was very sensitive to changes in the experimental set-up (e.g. sensitive to mechanical stimuli, to changes in light regime or in temperature) as demonstrated earlier (Herth and Zugenmaier, 1979; Veen, 1991). Accordingly, colony fragmentation increased the number of unicellular individuals under aerated conditions (Supplementary 4.1). However, no impact on cellular motility and shape of the loricas was observed and growth rates of *D. divergens* were highest during aeration. Taken together, culturing without agitation turned out to be the most convenient unified condition for comparison.

4.4.3. Influence of inorganic carbon

Photoautotrophic organisms convert inorganic carbon (CO_2) into biomass using light energy. In order to demonstrate photoautotrophic growth, we cultured the cells in media that did not contain dissolved organic carbon sources but had a diffusive CO_2 supply. Sustained growth of *P. tricornutum*, *D. divergens* and *M. annulata* was observed under these conditions, while P. *malhamensis* and *P. lacustris* failed to grow (Figure 4.2). As the CO_2 supply might be limiting in non-agitated culture flasks, we aerated the strains and found increasing growth rates for *D. divergens* (from μ=0.23±0.01 d^{-1} to μ=0.39±0.01 d^{-1}) and also slightly for *P. tricornutum* (from μ=1.03±0.05 d-^{1} to μ=1.04±0.03 d^{-1}), while growth of *M. annulata* (from μ=0.57±0.01 d^{-1} to μ=0.50±0.02 d^{-1}) was reduced (Figure 4.1). Aeration enhanced growth of *M. annulata* and *P. tricornutum* in terms of maximum cell densities (by 29.2 % and 59.1 %,

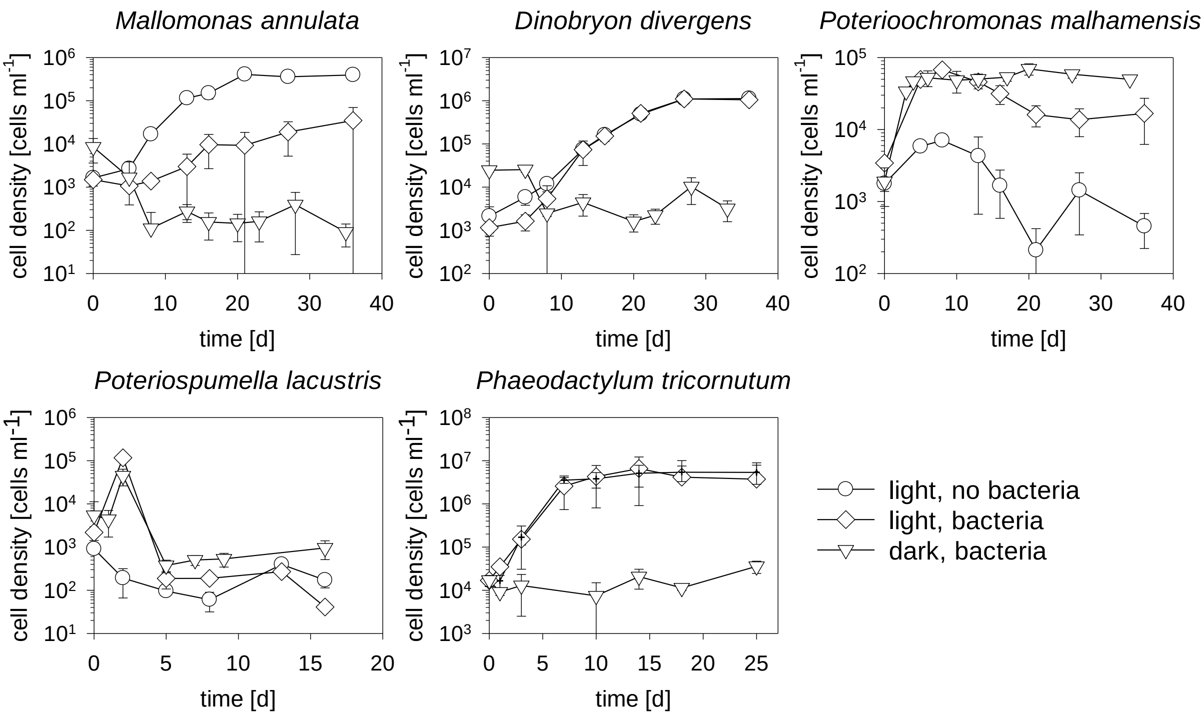

Figure 4.2: Growth of the investigated chrysophytes in the presence of autoclaved bacteria. Growth performances of the different protists cultured with bacteria in the presence or absence of light. No additional carbon sources were added to the media. Each data point represents the mean of three samples, error bars represent standard deviations.

respectively). In contrast to *P. tricornutum* (Johnston and Raven, 1996; Matsuda et al., 2011), chrysophytes including *Mallomonas* species apparently lack effective carbon concentrating mechanisms (CCM) (Maberly et al., 2009; Bhatti and Colman, 2011). Consequently, the investigated chrysophytes are dependent on slow diffusive CO_2 supply in non-agitated cultures which may affect them stronger than other algae.

4.4.4. Nutritional limitations in the stationary phase

In order to identify further limiting factors we examined the role of macronutrients (organic C, N, P) or supplements (vitamins, trace metals) for the maximum yield of cells (Figure 4.3). We found nitrate to be the most limiting nutrient for the photoautotrophic *M. annulata* as cell densities increased by 68 % after addition of 1 mM nitrate during the stationary phase. Nitrate and phosphate concentrations may also influence the growth response of *Mallomonas* species in natural habitats (Scott et al., 2009) and under laboratory conditions (Kim et al., 2009; Lee et al., 2012). Kim et al. (2009) showed that different *Mallomonas caudata* strains had different growth rates at identical nitrate concentrations, suggesting that nitrate turnover might be a key element of growth response in *Mallomonas* spp.. Maximum cell densities of *M. caudata* varied around 10^4 cells ml^{-1} (Kim et al., 2009), whereas we observed up to 5×10^5 cells ml^{-1} for *M. annulata*, indicating that enhanced biomass generation in unialgal laboratory cultures of *Mallomonas spp*. may be accomplished by excessive addition of nitrate to the respective media. However, this hypothesis requires further investigations since the bacteria in cultures of *M. caudata* and *M. annulata* are

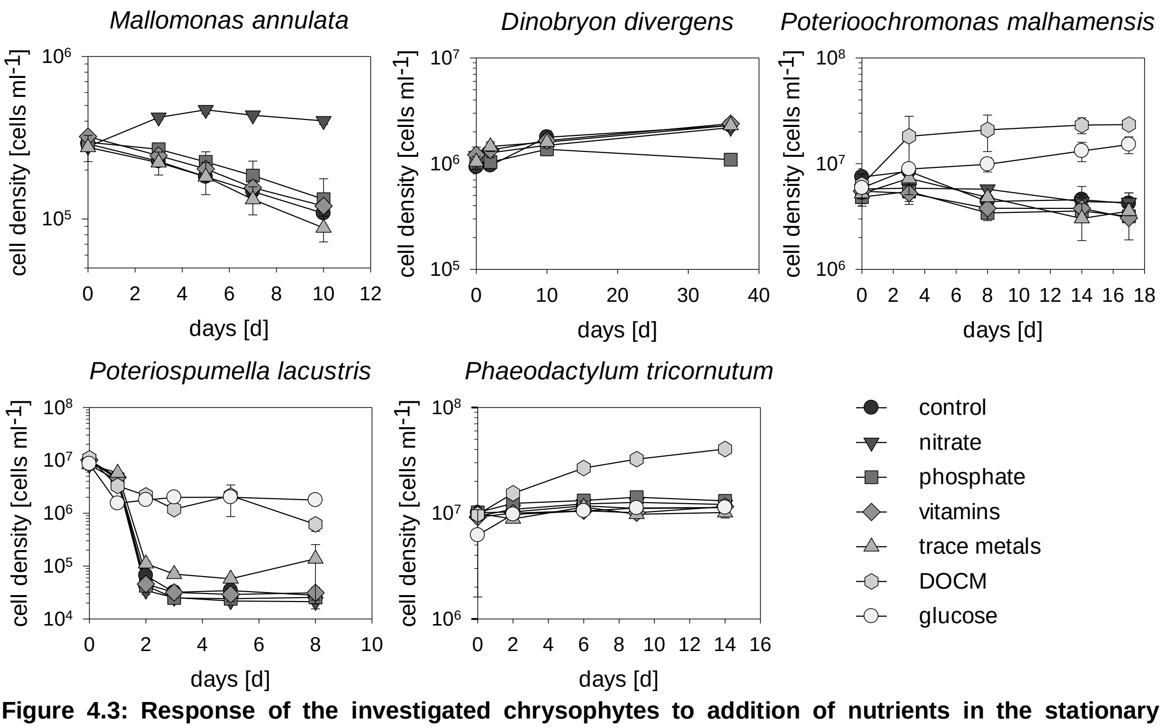

Figure 4.3: Response of the investigated chrysophytes to addition of nutrients in the stationary phase. Growth curves of protists after addition of 2x concentrated (individual concentrations see "Standard culturing conditions" in the "Material and Methods" section nitrate source, phosphate source, vitamin solution, trace metal solution, glucose, and DOM in stationary phase (time point 0). The control was supplemented with 1 ml of sterile double-distilled water in stationary phase. Each data point represents the mean of three samples, error bars represent standard deviations.

additional nitrate consumers, which introduce a possible source of variation in bacterial cell density and nitrate demand between the cultures.

Growth of the heterotrophic *P. lacustris* and the mixotrophic *P. malhamensis* in our experiments was limited by the organic matter (peptone, yeast extract and glucose) (Figure 4.3). As peptone and yeast extract are an undefined mixture of organic compounds this finding alone is difficult to interpret. However, we also could show that organic carbon is one of the limiting compounds in the dissolved organic matter by adding exclusively glucose to stationary phase cultures, which lead to a 2.5-fold increase in maximum cell densities of *P. malhamensis*. Cell densities of *P. lacustris* were stable after the addition of glucose while cell densities decreased rapidly in the control culture without added glucose.

None of the separately tested components (nitrate, phosphate, vitamin solution, trace metal solution) provoked a positive growth response in the stationary phase of *D. divergens* and *P. tricornutum* cultures. Nonetheless it is possible that *P. tricornutum* as well as *D. divergens* were limited by a combination of several elements (e.g. PO_4^{3-} and NO^{3-}) or by other factors not tested (e.g. optimal Ca:Mg ratios (Lehman, 1976)). In fact, a combined depletion of phosphate and nitrate has just recently been shown at the onset of stationary phase for *P. tricornutum* grown in aerated bioreactors at similar growth rates (µ=1.05 deduced from cell densities shown in Figure 1 (Valenzuela et al. 2012)) compared to our aeration experiments (µ=1.04 ± 0.03, Figure 4.1). Addition of potassium phosphate to *D. divergens* resulted in a slight decline of particle numbers (Figure 4.3) and a strong decline of vital cells according to a microscopic survey (Supplementary 4.2). Potassium toxicity would explain the death of the alga but is discussed controversially in the literature (Lehman, 1976; van Donk et al., 1988).

4.4.5. Influence of dissolved organic matter

In contrast to photoautotrophic conditions, *P. lacustris* and *P. malhamensis* grew well when DOM was supplied and they reached maximum cell densities of more than 5×10^6 cells ml^{-1}. In the stationary phase growth was limited by peptone, glucose and yeast extracts (DOM) (Figure 4.3). Different *P. malhamensis* isolates have been shown to assimilate the major bulk of carbon via phagotrophy or osmotrophy and only to a minor portion by photoautotrophy (Pringsheim, 1952; Hutner et al., 1953; Caron et al., 1990; Sanders et al., 1990; Hahn and Höfle, 1998; Zhang and Watanabe, 2001; Boenigk et al., 2006). Our experiments support these results; however, DOM in addition to carbon contains further nutrients that might support growth. In this context, we tested glucose and glycerol as defined organic carbon sources. Dissimilation of glucose by *P. malhamensis* (Reazin, 1956) has been demonstrated within 1-2 days after transfer to an inorganic medium. In our experiments, only very little growth was observed with glucose (µ=0.12±0.05 d^{-1}) or glycerol (µ=0.09±0.02 d^{-1}) as a carbon source in BM medium (Supplementary 4.3) compared to growth with DOM (µ=0.78±0.03 d^{-1}) (Figure 4.1, without agitation). However, the additional supply of glucose in the nutrient limitation experiments increased cell densities of *P. malhamensis* substantially and quickly (Figure 4.3). This indicates the presence of additional growth limiting substances, which might be present either in the yeast extract or the peptone and which might be necessary for sustained growth of *P. malhamensis* with glucose. For instance citric acid cycle intermediates have been proposed to act in this way for *P. malhamensis* (Hutner et al., 1953). We can exclude soil extract as a source for growth limiting substances as its omission did not affect growth rates and maximum cell densities of *P. malhamensis.*

The addition of peptone, glucose and yeast extract to cultures of *M. annulata* and *D. divergens* resulted in intense growth of the bacteria making the determination of algal growth rates difficult. Thus, for these algae, we only tested particulate organic carbon sources.

4.4.6. Influence of bacteria

Feeding with autoclaved bacteria resulted in increased growth of *P. malhamensis* and *P. lacustris*, but not of *D. divergens* and *P. tricornutum* (t-test, p=0.635 and p=0.387) (Figure 4.2). Slower growth rates in the presence of autoclaved bacteria were observed for *M. annulata* (µ=0.57±0.01 reduced to µ=0.11±0.06). Therefore, the autoclaved bacteria apparently were not exploited as a major source of energy and carbon in the light and in the dark by *M. annulata*, *P. tricornutum* and also *D. divergens.*

The accompanying bacteria in cultures of *D. divergens* and *M. annulata* may have affected the outcome of these experiments. When WC medium was inoculated with an alga-free aliquot of *D. divergens* cultures, the bacteria probably utilized the organic buffer as a carbon source and reached maximum bacterial densities of $1*10^7$ cells ml^{-1}. Bacterial densities were 10^7 cells ml^{-1} in cultures of *M. annulata* and $5*10^6$ cells ml^{-1} in cultures of *D. divergens* in mid-exponential phase under standard conditions. Due to feeding on dead algal material there were more bacteria present in later growth phases. Less than 1 ml of exponentially growing algal cultures per 50 ml were used for inoculation in order to adjust a maximum of $1*10^4$ algal cells ml^{-1}. Thus, maximum bacterial densities at the beginning of growth experiments were max. $1*10^5$ cells ml^{-1} in cultures of *D. divergens* and max. $2*10^5$ in cultures of *M. annulata*. $3*10^6$ cells of autoclaved bacteria and $1.5*10^5$ cells ml^{-1} of living bacteria were added, hence, there were around 20 times more dead than living bacteria present at the beginning of experiments with autoclaved bacteria. The dead bacteria provided a source of dissolving organic material for the living bacteria which, thus, probably grew much faster in these experiments than after addition of living or without bacteria. The growing bacteria perhaps depleted some limiting resources (e.g. nitrate) very quickly, so that *M. annulata* grew slower in experiments with autoclaved bacteria (Figure 4.2). Perhaps *D. divergens* could not profit from the increase in living bacteria because ingestion rates were already maximal at standard conditions. Therefore the cause for a slight and significant (t-test, p=0.001) increase of growth rates of *D. divergens* (0.29±0.01 d^{-1}) after addition of living bacteria compared to non-supplied cultures (0.25±0.01 d^{-1}) remains unclear (Supplementary 4.4).

During microscopic survey food vacuoles with undefined particulate structures were visible in *P. malhamensis*, *P. lacustris* and *D. divergens* indicating that they ingested particulate material. It is known that *Dinobryon* sp. is able to ingest bacteria (Jones and Rees, 1994). Discrimination between heat-treated and living bacteria by *D. cylindricum* (Caron et al., 1993) has been proposed to be a consequence of heat-labile growth factors associated with the bacteria. In our experiment, the addition of autoclaved bacteria probably increased the number of living bacteria in the *D. divergens* cultures and thus concentrations of unspecified growth factors should have increased, too. Yet, neither growth rates of *D. divergens* nor maximum yields increased considerably, therefore size discrimination excluding agglomerated autoclaved cells (Supplementary 4.5) could play a role here. Using different fluorescent beads size selection indeed was observed for *Dinobryon* spp. in field studies (Bird and Kalff, 1987) and in lab experiments (Veen, 1991). Hence, a portion of the bacteria might not have been accessible for *D. divergens* simply because the agglomerates were too large to be taken up. However, *P. malhamensis* and *P. lacustris* apparently were able to

exploit the cell agglomerates because both showed growth in the presence of the autoclaved bacteria (Figure 4.2). Accordingly, *P. malhamensis* cells have been found to graze on organisms two to three times larger than their own cell diameter (Zhang and Watanabe, 2001).
Fluorescence labelling of bacteria has been established as a tool to visualize the ingestion of undamaged bacteria (Sherr et al., 1987; Chrzanowski and Simek, 1990). To demonstrate that *D. divergens* actively ingests bacteria rather than just utilizes bacterial exudates, we performed a feeding experiment with living bacteria stained with a fluorescence dye and found the bacteria to be clearly visible inside *D. divergens* cells (Figure 4.4, Supplementary 4.6). In accordance to other studies with *Dinobryon* spp. (Caron et al., 1993; Kamjunke et al., 2007) the increase of growth rates by additional supply with living bacteria was lower than the increase obtained by additional CO_2 supply via aeration, which indicates a stronger limitation by photosynthesis than by organic nutrient sources under the conditions applied. A summary concerning the growth with different carbon sources is given in (Table 4.2).

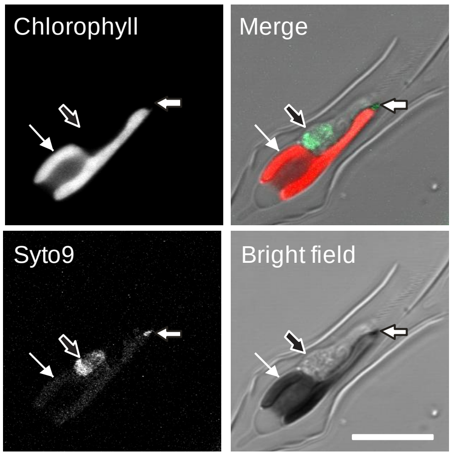

Figure 4.4: Micrographs of *Dinobryon divergens* fed with living fluorescently labeled bacteria. Bacteria were labeled with fluorescent dye (Syto9). Ingested bacteria were visible by green fluorescence inside of the algal cell (black arrow). Additionally, the eyespot of *D. divergens* was found to show green autofluorescence (white thick arrow) while the plastid showed red autofluorescence (white thin arrow). A slight background fluorescence of the chloroplast was visible in the green fluorescence channel (Syto9, see Supplementary 4.6 for additional controls). The scale bar represents 10 µm.

4.4.7. <u>Influence of light</u>

The role of light for growth was investigated by incubating the cells at different light: dark periods and by measurements of oxygen evolution using a Clark electrode Table 4.2. Although oxygen evolution is often normalized to the chlorophyll content of the cells, we chose biovolume (µm³) for normalization because also a non-photosynthetic organism was included here. Maximum oxygen evolution rates of *P. tricornutum* (1.4 fmol O_2 μm^{-3} h^{-1} and respectively 80 fmol O_2 $cell^{-1}$ h^{-1}, pH 7-8, 20 °C, 200 µmol photons m^{-2} s^{-1}) were similar to those obtained in other studies (~40 fmol O_2 $cell^{-1}$ h^{-1} (Patel and Merrett, 1986), ~20-100 fmol O_2 $cell^{-1}$ h^{-1} (Müller and Wilhelm, 1997). All photosynthetic algae in our study reached maximum oxygen evolution rates at light intensities between 150-200 µmol photons m^{-2} s^{-1} (Figure 4.5).

Table 4.2: Summary of growth experiments.

	Growth in inorganic medium	Effect of aeration	Effect of dissolved organic carbon sources	Effect of particulate organic carbon sources	Effect of shortened light periods	Light-dependent oxygen evolution	Survival capacities in the dark
Phaeodactylum tricornutum	yes	increased maximum cell densities	increased maximum cell densities	no effect	decreased growth rates	yes	medium
Mallomonas annulata	yes	increased maximum cell densities	not detectable	decreased growth rates	decreased growth rates	yes	low
Dinobryon divergens	yes	increased growth rates	not detectable	increased growth rates*	decreased growth rates	yes	low
Poterioochromonas malhamensis	no	no effect	increased growth rates	increased growth rates	shortened stationary phase	yes	high
Poteriospumella lacustris	no	no effect	increased growth rates	increased growth rates	no effect	no	high

**only with living bacteria*

As expected *M. annulata* showed photoautotrophic performance with maximum oxygen evolution rates of 1.48±0.31 fmol O_2 µm^3 h^{-1}, which is as high as the maximum oxygen evolution rates of *P. tricornutum* (1.46±0.46 fmol O_2 µm^{-3} h^{-1}) (Figure 4.5). Shortening of the photoperiod resulted in lower growth rates of both algae (Figure 4.6). When cultures were shifted to shorter light periods, cell densities of *M. annulata* (6 h light) decreased by 32.3 % as when compared to a 16:8 h light:dark rhythm, while *P. tricornutum* still showed an increase at 4 hrs light. Thus, *P. tricornutum* apparently is better at coping with light limitation than *M. annulata* (see also Kamp et al., 2011; Rottberger et al., 2013).

While light is obviously indispensable for *M. annulata*, heterotrophic growth rates as well as maximum cell densities of *P. lacustris* were similar in the light (µ=0.63±0.04) and in the dark (µ=0.64±0.04) (Figure 4.6). Also, shortened photoperiods had no negative effects on growth with DOM. Oxygen evolution rates always remained negative due to respiration (–1.5 fmol O_2 µm^3 h^{-1}) independent of light (Figure 4.5).

The mixotrophic *P. malhamensis* is able to grow heterotrophically in the dark and in the light. (Holen, 1999) showed that the ingestion rates of bacteria by a freshly isolated *P. malhamensis* strain were affected by the light intensities applied and thereby differed from other culture strains. We did not observe differences between the growth rates of *P. malhamensis* in complete darkness and under the low-light conditions applied (Figure 4.6). However, we found that the rate of photosynthetic oxygen evolution in *P. malhamensis* depends on the light intensity (Figure 4.5). Possibly the applied light intensity of 3 - 45 µmol quantum m^{-2} s^{-1} in the growth experiments was too low to affect growth rates and

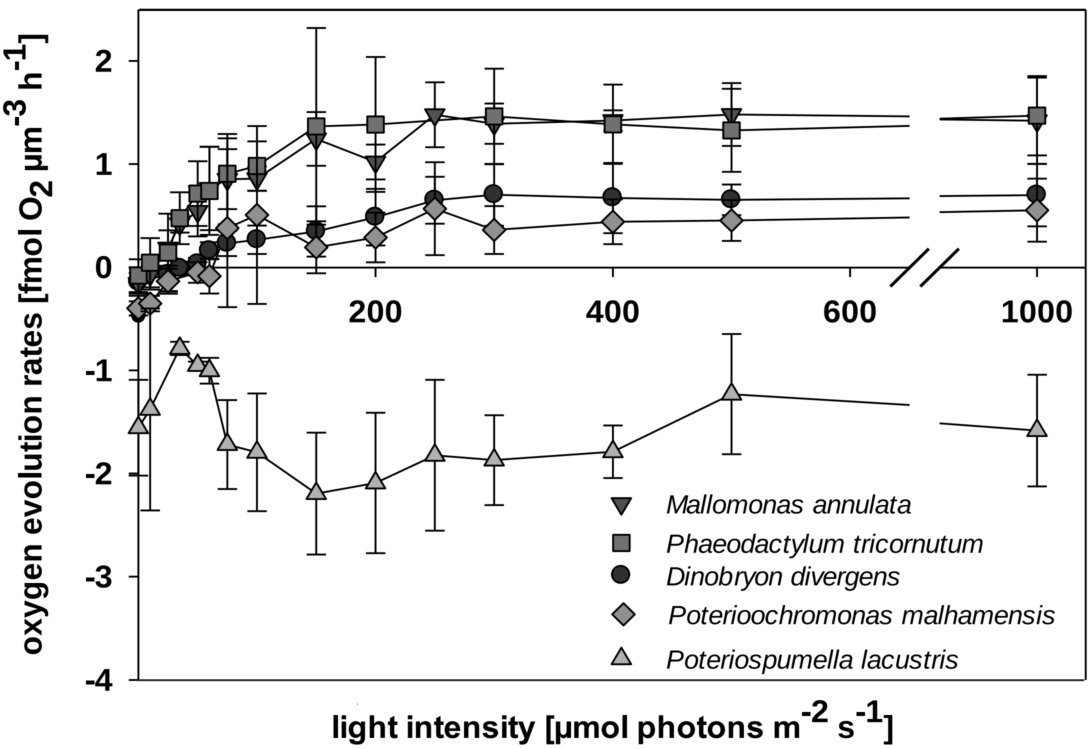

Figure 4.5: Light-dependent oxygen evolution rates of the investigated chrysophytes in late exponential growth phase. Oxygen evolution rates (above zero: O_2 production, below zero O_2 consumption) for the investigated chrysophytes and *P. tricornutum* standardized per biovolume and measured at different light intensities. Each data point represents the mean of three samples, error bars represent standard deviations.

experiments under high-light conditions would have revealed a relationship between light intensity and growth rates.

Prolonged cell maintenance in the stationary phase is only possible if the metabolism can switch to other metabolic pathways which are not dependent on a limited resource or if enough storage resources for survival have been accumulated in the organism before. The period of stationary phase was rather short in all experiments with *P. lacustris* and in dark experiments with *P. malhamensis* growing on dissolved organic carbon sources. Regarding *P. lacustris* this is in agreement with the finding that *Spumella*-like flagellates are typical r-strategists i.e. they have high growth rates if food is available but little starvation tolerance if food is absent (Boenigk et al., 2006). An essential difference between *P. lacustris* and *P. malhamensis* was demonstrated in the stationary phase in media with yeast extract, peptone and glucose. Here, cells of *P. malhamensis* survived much longer in the light than under dark conditions while there was no difference for *P. lacustris* (Figure 4.6). In contrast to *P. lacustris*, *P. malhamensis* is therefore able to compensate organic carbon limitation in the light by switching to a phototrophic maintenance metabolism which allows the alga to survive, but not to proliferate in the presence of light. In the dark this mechanism does not work and the onset of cell mortality appears much earlier in the stationary phase (see also Caron et al., 1990; Zhang and Watanabe, 2001). Altogether, our results show that *P. lacustris* is incapable of photoautotrophy whereas *P. malhamensis* does not grow but sustains cell metabolism with the help of light-derived energy when organic carbon sources are limited.

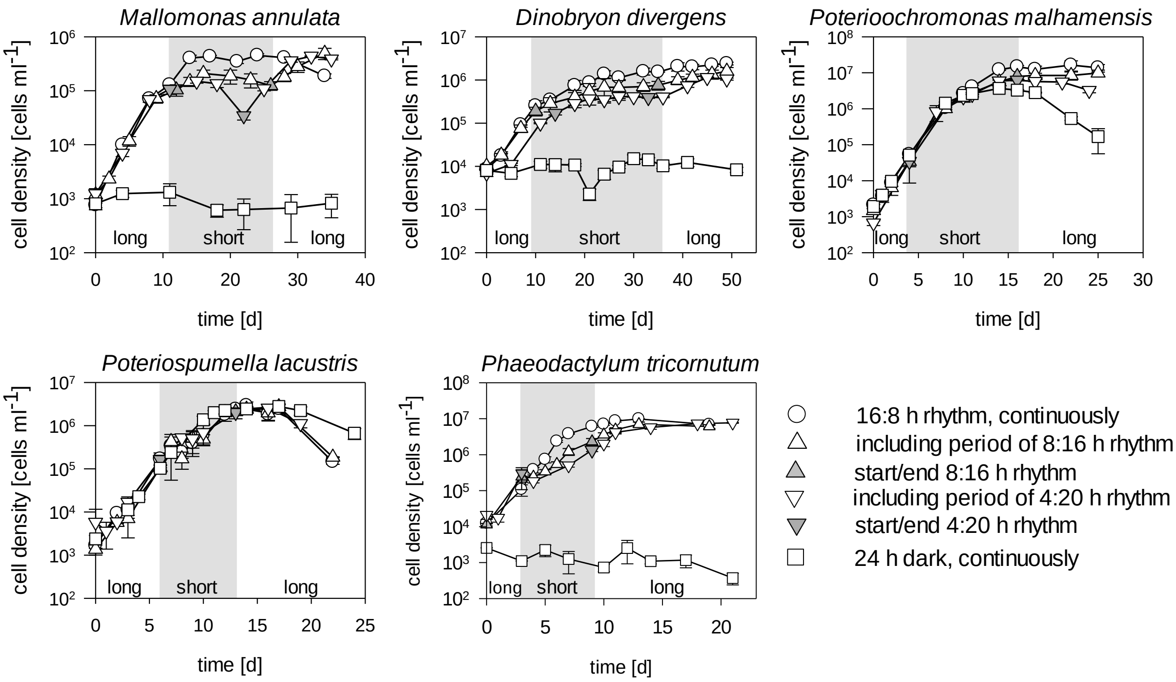

Figure 4.6: Growth of the investigated chrysophytes under different light conditions. Growth performance of cultures grown in a continuous 16 h light : 8 h dark rhythm was compared to those partially grown in a 8 h light : 16 h dark rhythm, a 4 h light : 20 h dark rhythm and in continuous darkness. *M. annulata* was grown under a 6 h light : 18 h dark rhythm instead of 4 h light : 20 h dark. All cultures, besides of those kept continuously in the dark, were initially incubated under 16 h light : 8 h dark conditions (long). Light intervals were then shortened for the cells that were incubated with periods of 4 h (6 h) and 8 h light (short, grey shading) and afterwards the initial rhythm of 16 h light : 8 h dark was re-applied (long). The grey shaded zone represents approximately the incubation period with shortened light intervals; the exact day of beginning and end of the incubation is indicated by filled symbols for each treatment. Each data point represents the mean of three samples, error bars represent standard deviations.

Shortening of the light-period resulted in lower growth rates of *D. divergens* (Figure 4.6) and growth in the dark in presence of particulate organic carbon was not observed (Figure 4.2, Supplementary 4.4). Oxygen evolution rates per biovolume were comparable to *P. malhamensis* (Figure 4.5). Laboratory and field studies support our finding that *Dinobryon* is obligatory light-dependent (Veen, 1991; Caron et al., 1993; Watson et al., 2001; Watson and McCauley, 2010).

Although *M. annulata* has higher maximum oxygen evolution rates than *D. divergens*, both algae grow rather slowly. For unicellular organisms with photoautotrophic abilities growth in terms of increasing cell densities or increasing cell size is coupled to the acquisition of inorganic carbon and oxygen production. There is, however, no direct relation between oxygen production, CO_2 consumption and growth. Oxygen is formed as a product of the photosynthetic light reaction, which provides energy and reduction equivalents for the complete formation of biomass by CO_2 assimilation. In addition to the direct formation of photosynthesis products, there are various direct or indirect metabolic sinks for the reduction equivalents generated in the photosynthetic light reaction that confound the stoichiometry between oxygen production and increase of biomass, most notably further chemical reduction of the overall biomass (e.g. via accumulation of lipids or synthesis of reduced complex secondary metabolites), disposal of carbohydrates via secretion or nitrogen assimilation starting from nitrate. Hence, the differences in growth rates observed for organisms with similar photosynthetic capacities are not necessarily a consequence of different carbon-uptake abilities or strategies. Mixotrophy furthermore increases the independence between growth and oxygen production. Thus, the non-linear relations comparing oxygen evolution rates and growth rates of *P. malhamensis, D. divergens, M. annulata* and *P. tricornutum* to each other might possibly be a result of different exploitation of organic carbon sources but might as well be related to differences in the budgeting of reduction equivalents.

4.4.8. Implications for re-oligotrophication scenarios

In parallel with the decrease of nutrient loads of lake waters during re-oligotrophication, water transparency increases and phosphate becomes limiting (Jeppesen et al., 2005). The ability to exploit bacteria as additional source for carbon and essential nutrients like phosphate may explain the success of mixotrophs in a re-oligotrophication scenario compared to obligate heterotrophs or photoautotrophs. However, looking at *P. malhamensis* and *D. divergens*, this hypothesis has to be differentiated according to the various types of mixotrophic nutrition. We think that the regulation of carbon metabolism in mixotrophic chrysophytes can be a determining factor for the reaction of an organism to environmental changes. Comparative physiological studies may reveal some regulating factors of the carbon metabolism; however, ecologically relevant implications may need further investigation under more natural conditions. In the following, our argumentation is based on maximum nutritional capacities of the organisms examined under laboratory conditions.

Covering the whole spectrum from photoautotrophs to chemoheterotrophs, we identified large differences between the more chemoheterotrophic and mixotrophic *P. malhamensis* and the more photoautotrophic and mixotrophic *D. divergens*. We demonstrated that both mixotrophic algae act within a certain nutritional spectrum so that a total shift from purely heterotrophic to purely autotrophic growth or *vice versa* cannot be induced by varying light availability or different carbon sources. We showed that dead bacteria promote growth of

P. malhamensis, which proliferates independently from light availability, whereas *D. divergens* is obligatory light-dependent in the presence of organic carbon sources. Hence, we would expect *P. malhamensis* and *D. divergens* to populate different vertical layers in a stably stratified lake (without dislocation of the cells via turbulences or currents).

4.4.9. Upper layers of the pelagic zone in oligotrophic lakes

In pelagic oligotrophic habitats in which light is available and particulate organic matter is dominated by living bacteria rather than lifeless material, coexistence and competition of *P. malhamensis* with mixotrophs like *D. divergens* would probably be determined by the clearance efficiencies of both organisms only. In the surface water of the pelagic zone, competition with photoautotrophic organisms is likely and may strongly limit the accessibility of this ecological niche for mixotrophs. Accordingly a sharp restriction of *Dinobryon* to specific water depths in the upper water layers has been reported (Bird and Kalff, 1989; Palsson and Graneli, 2003). *Mallomonas* and *Dinobryon* may co-occur, but apparently *Dinobryon* mostly dominates with respect to abundances. *Dinobryon* and *Mallomonas* species have been found to be present in the same spatio-temporal niche in Lake Sanabria, a glacial lake in Spain, but they occupy different vertical layers (De Hoyos et al., 1998). *Dinobryon* was preferentially located in the upper parts and *Mallomonas* in the deepest layers of the epilimnion. Our results suggest that this stratification is likely to be a consequence of the different capacities of the photosystems. *Mallomonas* - with greater oxygen evolution rates under low light conditions (Figure 4.5) - can possibly exploit deeper layers whereas *Dinobryon* is restricted to upper layers.

Unfortunately, we did not find any field data distinguishing between the genera *Dinobryon*, *Mallomonas* and *Poterioochromonas*. This may be due to the difficulties in distinguishing between the different species of *Ochromonas*-like chrysophytes by light microscopy only. There is some literature evidence for *Dinobryon* and *Ochromonas* populations occurring in the same habitat (Bird and Kalff, 1989; De Hoyos et al., 1998; Olrik, 1998) and at least one study including *Mallomonas,* too (De Hoyos et al., 1998). Though *Ochromonas* representatives generally are mixotrophic, organic carbon acquisition is of varying importance in the single taxa. Hence, it is not possible to deduce a survival strategy during re-oligotrophication for the whole genus.

4.4.10. Deeper pelagic layers and the benthic region in oligotrophic lakes

Dead material from the surface usually sinks to deeper water layers and to the benthic region over time where light is limited and heterotrophic organisms are dominant. Modelling the conditions under which mixotrophs are likely to dominate over heterotrophs has been performed (de Castro et al., 2009). Among other parameters, carbon input, light availability, prey abundance and prey size were taken into consideration. To include mixotrophs in the predictions of the model, photosynthetic capacities need to be known. Due to the presence of bacteria in our cultures, we could not determine absolute photosynthetic capacities of *D. divergens*. On this basis, we did not consider it appropriate to compare *D. divergens* and *P. malhamensis* by the model of de Castro et al.. Nonetheless, mixotrophs with very low photosynthetic growth rates like *P. malhamensis* are predicted to be able to co-exist with heterotrophs under low-light conditions and at relatively high carbon concentrations, which would be in accordance with our expectations.

In deeper layers of the pelagic region where photoautotrophs and mixotrophs with characteristics of *D. divergens* are limited by light-availability and where abundances of heterotrophic eukaryotes like *P. lacustris* are probably lower than in the benthic region, *P. malhamensis* would presumably out-compete *D. divergens*-like mixotrophs. This might not only be connected to different photosynthetic performances but also to the ability of *P. malhamensis* to exploit even agglomerates of dead cells while *D. divergens* apparently is more size selective due to the natural barrier given by the shape and diameter of the lorica. Furthermore, *P. malhamensis* is likely to be more successful than chemoheterotrophic r-strategists like *P. lacustris* under low nutrient conditions because a phototrophic maintenance metabolism secures survival. Heterotrophic r-strategists would probably rather die-off or had to bare the additional metabolic costs of producing endurance forms (e.g. cysts).

4.4.11. <u>Closing remarks</u>

Overall, decoding the complex metabolism of mixotrophic chrysophytes by physiological studies is an ongoing process (Maberly et al., 2009; Watson and McCauley, 2010; Sanders, 2011). To date only a few pioneer studies have dealt with molecular data of mixotrophic chrysophytes (Terauchi et al., 2010), which might nonetheless be a crucial step to entirely understand the regulation of carbon pathways in chrysophytes. In this study, we have compared chrysophytes from pure photoautotrophic to pure chemoheterotrophic nutrition under identical conditions. By this we have build a comparative physiological basis to relate former and future studies on the single species to each other.

4.5. Acknowledgments

We thank Julia Thielicke, Katharina Scholz and Alexander Förderer for help with the experiments and the Universität Konstanz Bio Imaging Center (BIC) for access to a confocal laser scanning microscope. We are very grateful to Prof. Karl-Otto Rothhaupt for support and helpful discussions. This work was supported by the Universität Konstanz (Research Initiative “Organismic Interactions in aquatic ecosystems under changing conditions” to PGK), and by projects FWF P21151 and BO 3245/3-1(DFG) to JB.

4.6. Supplementary Figures

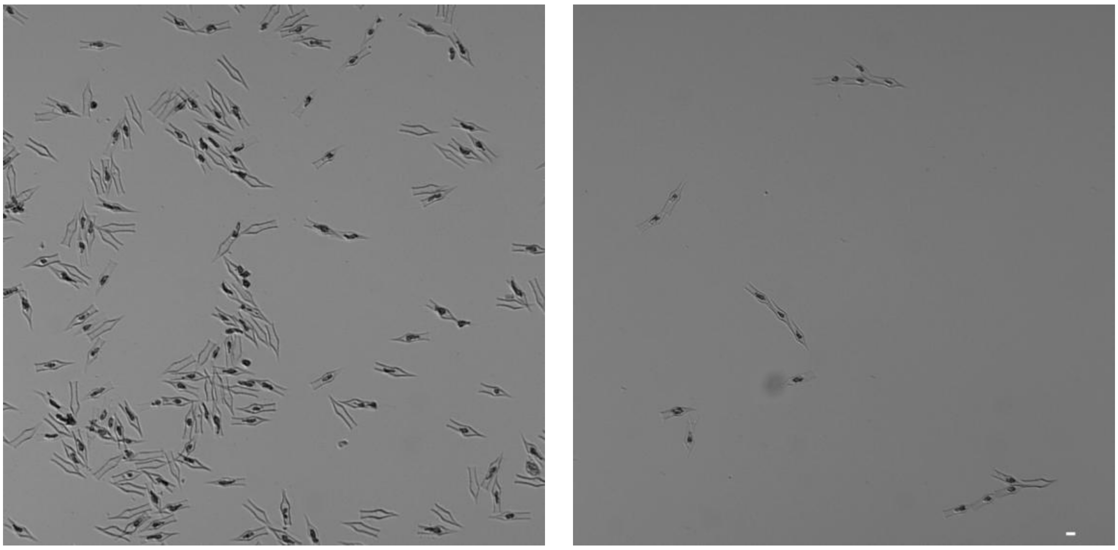

Supplementary 4.1: Cells of *Dinobryon divergens* 18 days after inoculation in aerated cultures(left) and cultures without agitation (right). Cultures without agitation usually contained a higher amount of algal colonies than aerated cultures. The scale bar represents 10 µm.

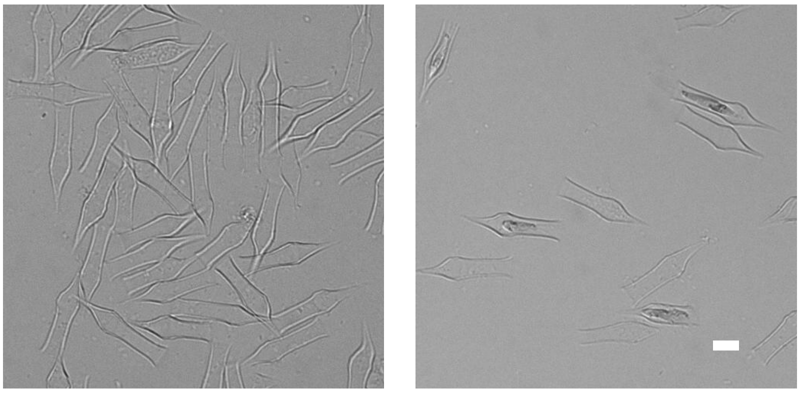

Supplementary 4.2: Cells of *Dinobryon divergens* after addition of phosphate during nutrient limitation experiments (left) compared to cells from the control sample (right). Cell mortality was higher in the phosphate treatment (64 µM added in stationary phase) and therefore more empty loricas were present (left) compared to the control (right). The scale bar represents 10 µm.

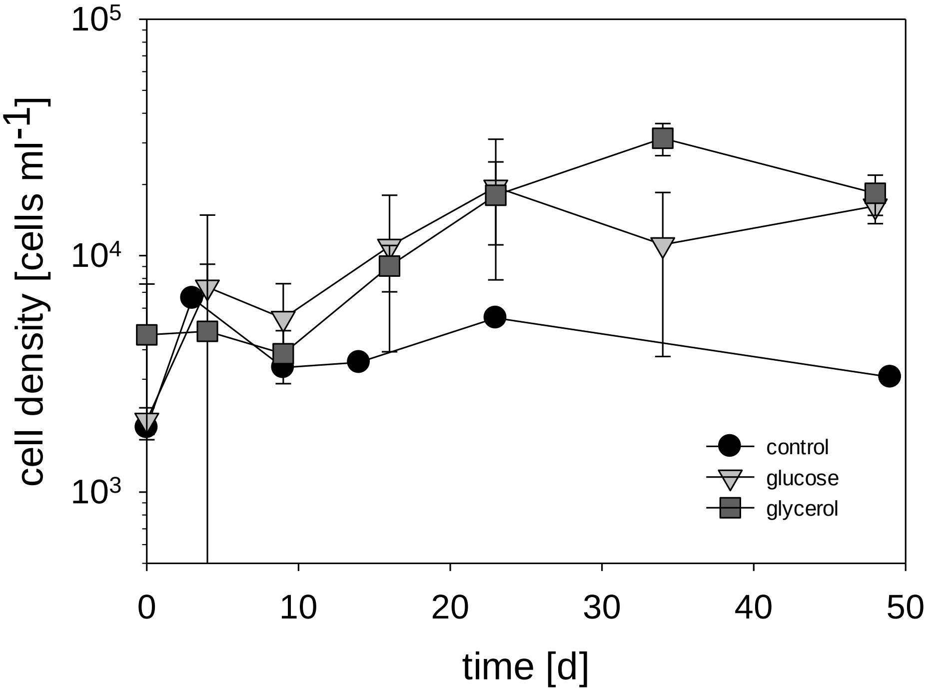

Supplementary 4.3: Limited growth of *Poterioochromonas malhamensis* in the presence of defined organic carbon sources as measured with a Coulter counter. Growth with glucose (3 g l^{-1}) and glycerol (1.5 g l^{-1}) was observed but was very low. For better comparison, particle counts of the sterile control without algal cells were included in the plot. Each data point represents the mean of three samples, error bars represent standard deviations.

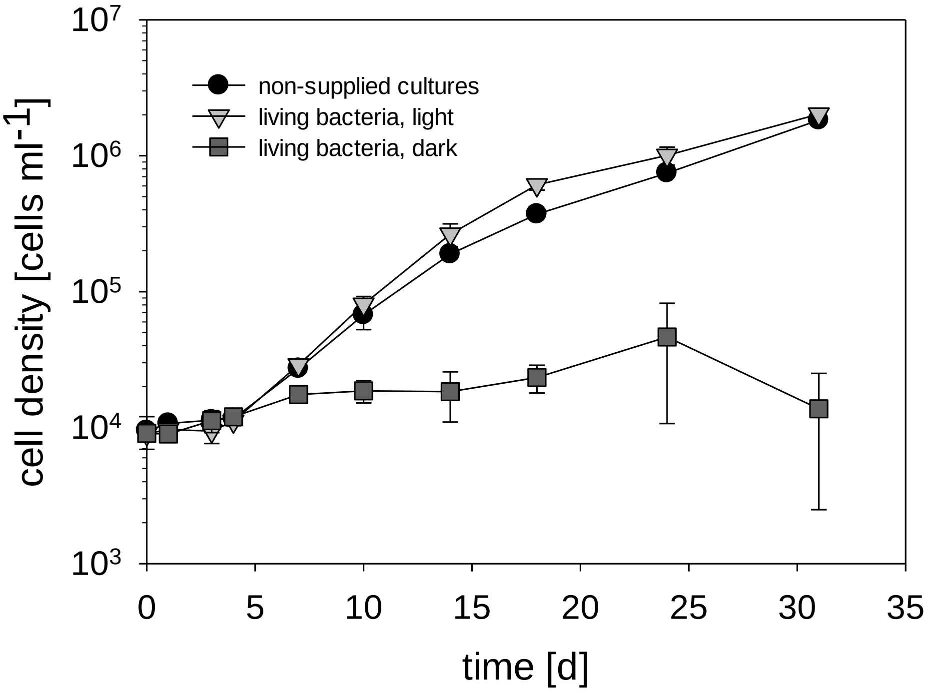

Supplementary 4.4: Growth of *Dinobryon divergens* with and without additional supply of living bacteria. Growth rates of *D. divergens* were slightly but significantly increased in the light when living bacteria were added to the cultures compared to non-supplied cultures. In the dark, the treatment did not support growth of *D. divergens*. Each data point represents the mean of three samples, error bars represent standard deviations.

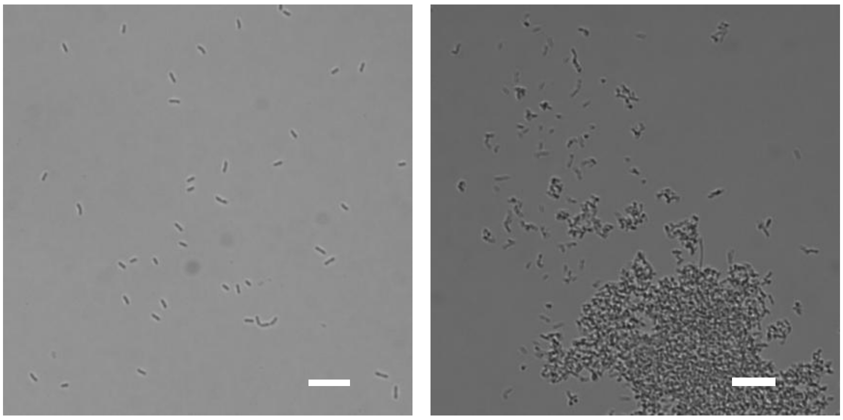

Supplementary 4.5: Phenotype of living and autoclaved bacteria used as prey during feeding experiments. Living cells grew well suspended (left). During autoclaving a portion of bacteria agglomerated (right). The scale bar represents 10 µm.

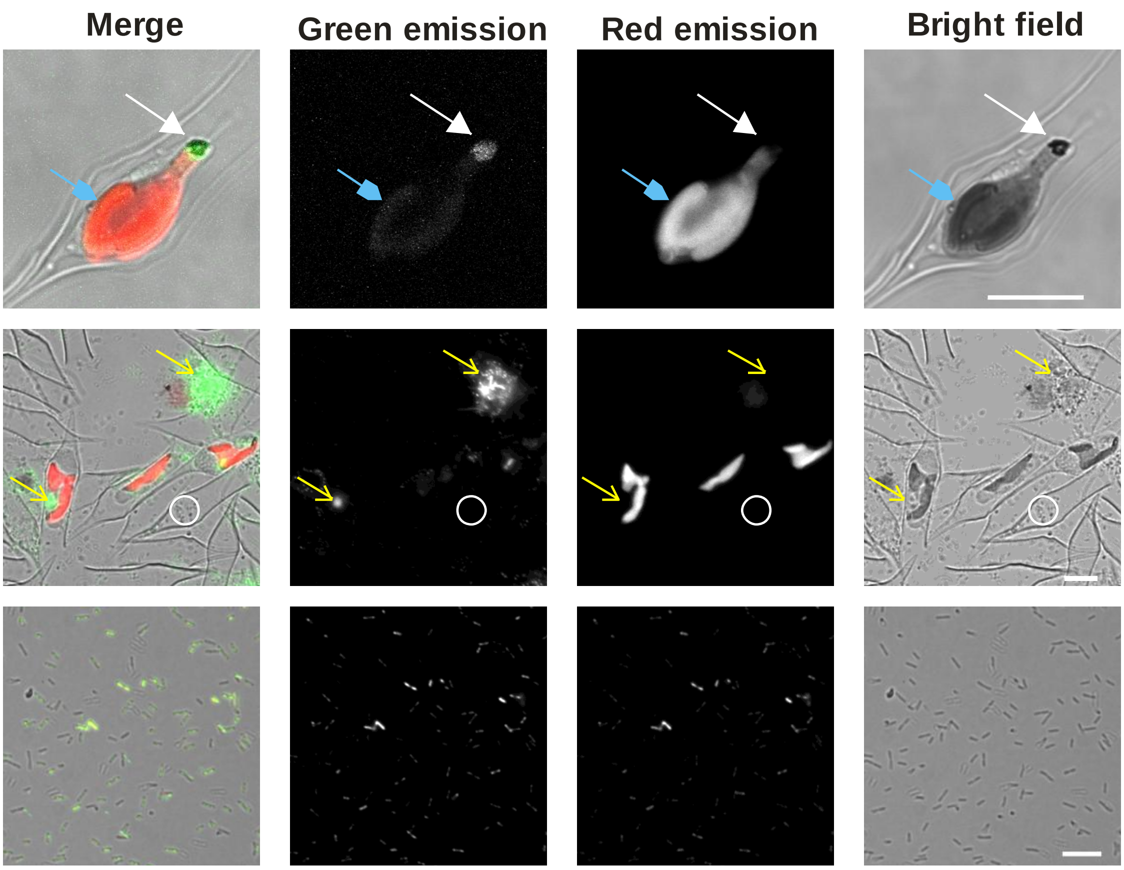

Supplementary 4.6: Micrographs of control samples during feeding experiments of *Dinobryon divergens* with living, fluorescently labeled bacteria. Non-treated cells of *D. divergens* (top row) show green autofluorescence in the region of the eyespot (white arrows) and a weak signal in the plastid region (blue arrows), possibly due to bleed through of autofluorescence from the photosynthesis pigments. Plastids can be identified by their red autofluorescence. Bacteria labeled with Syto9 show a strong green and a weak red fluorescence (bottom row). When *D. divergens* cultures were supplied with Syto9 labeled bacteria, the labeled bacteria were visible by green light emission inside and outside of the algal cells (yellow arrows) apart from the plastid- or eyespot- region (middle row). Due to the xenic state of the culture before addition of the Syto9-labelled bacteria, unstained bacteria were also visible (white circles, middle row). The scale bars represent 10 µm.

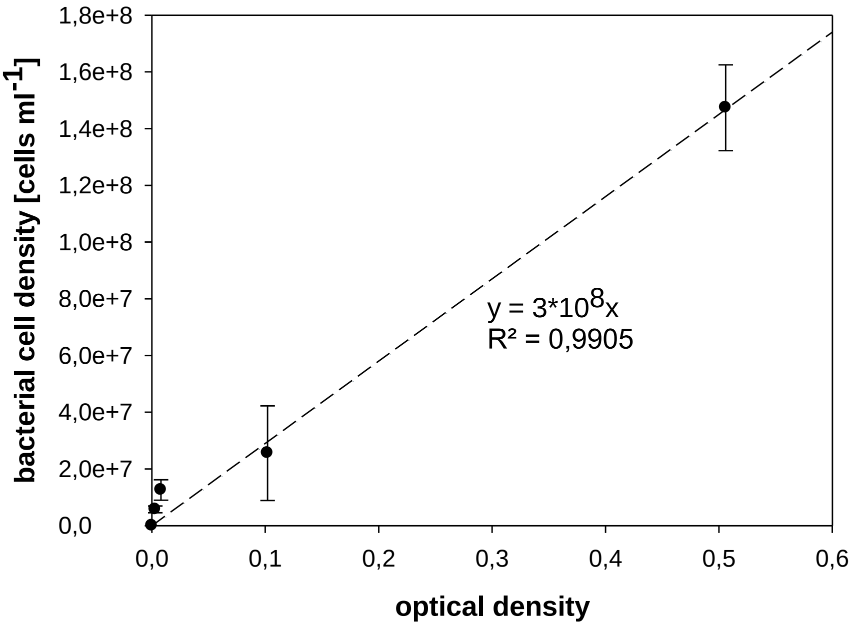

Supplementary 4.7: Correlation of optical density measurements and bacterial cell densities. Bacteria isolated from *D. divergens* cultures were grown in WC medium with DOM. A dilution series of the bacterial culture was prepared and the optical density of samples from the dilution series was measured at λ=600 nm. The numbers of bacteria in samples with an optical density between 0 and 0.5 were counted microscopically. The function of the regression line over all data points (y= $3*10^8*x$) was utilized as the standard function to correlated optical density measurements to bacterial densities. Error bars represent standard deviations (n=4).

Chapter 5

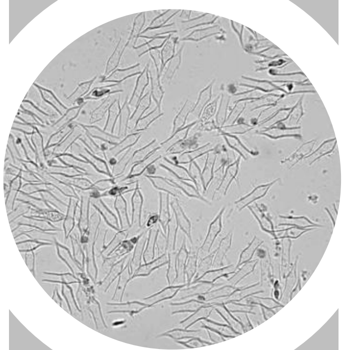

Primary metabolism of autotrophic, mixotrophic and heterotrophic chrysophytes according to *de novo* transcriptomic analysis

by Julia Rottberger, Sabina Wodniok, Carolina Rio Bartulos, Jens Boenigk and Peter G. Kroth
manuscript in preparation

5. Primary metabolism of autotrophic, mixotrophic and heterotrophic chrysophytes according to *de novo* transcriptomic analysis

5.1. Abstract

Chrysophytes are a category of protists marked by the broad nutritional spectrum of its representatives. There are chrysophytes that utilize CO_2 solely as source of carbon (autotrophs) whereas others completely rely on organic substances (heterotrophs). Additionally, there is a great number of species which may utilize both strategies to meet carbon requirements (mixotrophs). The molecular mechanisms enabling the different manifestations of nutrition in chrysophytes have not yet been analysed. In this study transcriptomic analyses and comparison of the freshwater chrysophytes *Mallomonas annulata* (photoautotroph), *Dinobryon divergens* (mixotroph), *Poterioochromonas malhamensis* (mixotroph) and *Poteriospumella lacustris* (organoheterotroph) is performed based on a 454-sequencing approach. A total of 213,361 contigs with an average length of 611 nucleotides were annotated and functionally sorted using BLAST2GO. Manual curations and localization predictions were conducted for 660 contigs putatively involved in major carbon pathways. The transcripts of the pathways of glycolysis, gluconeogenesis and Calvin Cycle and of important intermediary pathways like photorespiration and urea cycle were expressed in the photoautotrophic and both mixotrophic chrysophytes. Many metabolic parallels between *Mallomonas annulata* and the diatom *Phaeodactylum tricornutum* were found. However, the two mixotrophic strains differed from *Mallomonas annulata* by the absence of transcripts for putative key enzymes involved in the oxidative pentose phosphate pathway and certain carboxylating reactions localized in the plastid. These all are enzymes important for photoautotrophic performance. The heterotrophic chrysophyte differed from the other strains by the absence of enzymes assigned to photosynthetic pathways. Nevertheless, a set of glycolytic transcripts was plastid targeted. Thereby a first hint for metabolic activity in the colorless, non-photosynthetic plastid of *Poteriospumella lacustris* is presented. This chrysophyte also expresses a phosphoketolase which is rather uncommon for eukaryotes. Altogether this study lays a profound base for expression analyses of metabolic pathways of chrysophytes and further molecular studies.

5.2. Introduction

Chrysophytes are geographically widespread heterokont algae of the classes Chrysophyceae and Synurophyceae (Andersen et al., 1999; Kristiansen and Preisig, 2007; Jordan and Iwataki, 2012). They are abundant in freshwater, marine habitats and in soils (Sandgren, 1988; Boenigk and Arndt, 2002; Massana, 2011). Chrysophytes are well investigated concerning aspects of their autecology, biogeography and diversity (Andersen et al., 1999; Finlay and Clarke, 1999; Vigna and Siver, 2003). Some taxa affiliated with the genera *Ochromonas*, *Paraphysomonas* and *Spumella* are available from culture collections. Chrysophytes are important paleoindicator organisms due to their sensitivity to eutrophication, acidification, heavy-metal pollution and climate change (Dixit et al., 1999; Pla and Anderson, 2005; Ginn et al., 2010). They display different metabolic lifestyles, ranging from chemoheterotrophy to photoautotrophy (Raven et al., 1995). Organisms utilizing both, CO_2 (autotroph) and organic carbon sources (heterotroph), are called mixotrophic organisms. A large number of chrysophyte genera are described as mixotrophs on account of the presence of a photosynthetically active plastid and their ingestion of particulate organic material (Porter, 1988; Sanders and Porter, 1988). According to the latter definition mixotrophic chrysophytes may be classified into one of four groups (Jones, 2000):

- Group A: Primarily heterotrophic chrysophytes which employ autotrophy only when prey concentration is low.
- Group B: Primarily autotrophic chrysophytes which supplement growth by heterotrophy for additional carbon or energy supply when light is limited.
- Group C: Primarily autotrophic chrysophytes which obtain essential substances besides of carbon by ingestion of organic material (P, N,…).
- Group D: Primarily autotrophic chrysophytes which employ heterotrophy only at very low rates for cell maintenance in periods of prolonged darkness

This classification may be confusing in some cases because Group C mixotrophs do not profit from the carbon in the organic material and thereby are not heterotrophic in a strict sense. However, the classification manifests the main result of physiological studies over the last 60 years: that mixotrophic chrysophytes generally are limited in their ability to switch between autotrophic and heterotrophic metabolism. Instead they obtain a dominant primary mode of nutrition somewhere in between of autotrophy and heterotrophy and profit differently from the ingestion of organic material. A chrysophyte usually associated with Group A for example is *Poterioochromonas malhamensis*, a primarily heterotrophic alga which obtains a photosynthetic maintenance metabolism when organic carbon is not available. Another chrysophyte, *Dinobryon divergens*, is obligatory light-dependent and neither assigned to group A nor group D (Chapter 4). The presence of bacteria during light exposure supports growth (Veen, 1991) suggesting a group B affiliation. However, there is no significant difference in growth rates when *D. divergens* is grown in bacteria-free medium in the light compared to cultures supplied with autoclaved bacteria (Chapter 4), therefore even a group C-strategy is possible.

While there are quite a number of physiological and ecological studies on chrysophytes (for a summary on important studies see Sanders, 2011); only some molecular studies have been performed. The mitochondrial genome of the mixotroph *Ochromonas danica* was the first identified in the chlorophyll a/c group of algae comprising 40 kbp (Coleman et al., 1991). One major expression study of a mixotrophic chrysophyte was published by Terauchi et al. (2010) who identified 400 putative proteins derived from cDNA of *Ochromonas danica*. Also, the expression of single genes or proteins of interest like ribulose-1,5-bisphosphate carboxylase/oxygenase (Lacoste-Royal and Gibbs, 1985) and glyceraldehyde phosphate dehydrogenase (Harper and Keeling, 2003) have been analyzed and genes have been phylogenetically classified (e.g. Boenigk et al., 2005; Cavalier-Smith and Chao, 2006). Still, comprehensive genomic data sets or expression profiles of chrysophyte species are not yet publicly accessible and hence the molecular base to distinguish between the nutritional modes of different species does not exist.

In this study, we aim at differentiating between autotrophic, mixotrophic and heterotrophic chrysophytes on the molecular level. Thus, we established normalized EST-datasets (EST=expressed sequence tags) from mRNA of the mixotrophs *Poterioochromonas malhamensis* and *Dinobryon divergens*, the heterotroph *Poteriospumella lacustris* and the photoautotrophic chrysophyte *Mallomonas annulata* in a next generation sequencing approach (GS FLX , Roche 454 Life Science). Based on annotation and metabolic pathway sorting of the contigs, we present a hypothetical model of chrysophyte metabolism which was derived by merging all of the annotations. This model was developed because datasets of the individual chrysophytes may not represent the complete transcriptome of each organism. By merging their data we intend to demonstrate general metabolic capacities of chrysophytes. We focus on the primary carbon metabolism while comparing this model chrysophyte to the molecular and physiologically well-investigated diatom *Phaeodactylum tricornutum* as a reference. We also deliver specific data by comparing the autotrophic, mixotrophic and heterotrophic chrysophytes to each other and to *P. tricornutum* concerning the cellular distribution of key enzymes in carbon metabolism.

5.3. Methods

5.3.1. Algal material

Poteriospumella lacustris was cultured in modified Inorganic Basal medium (pH 7,2) (Hahn, 2003) without $NiCl_2$ and with addition of a **d**issolved **o**rganic matter (DOM) of 1 g l^{-1} peptone, 1 g l^{-1} yeast extract and 1 g l^{-1} α-D-glucose. *Dinobryon divergens* and *Mallomonas annulata* were grown in liquid WC medium (pH 8) (Guillard and Lorenzen, 1972) with modified concentrations of TES buffer (500µM), $NaHCO_3$ (375 µM), K_2HPO_4 (32 µM), $NaNO_3$ (500 µM) and $MnCl_2$ (0.09 µM). The standard medium for *P. malhamensis* was modified Bacillariophycean Medium (BM) (pH 7,2) (Schlösser, 1994) with 236 µM Na_2CO_3, 27 µM Iron(III) citrate hydrate, 214 µM citric acid, 60 nM $MnSO_4$, 200 µgl^{-1} thiamine-HCl, 10 µgl^{-1} biotin and DOM. *P. tricornutum* was grown in modified f/2 medium (pH 7) (Guillard and Ryther, 1962; Guillard, 1975) with artificial half-concentrated sea salts (16,6 g l^{-1}) and 0,09 µM manganese or on solidified plates (1,5 % agar) of the modified f/2 for culture maintenance.

Culturing conditions were chosen in order to support maximum growth (Chapter 4). All cultures were grown at 20 °C in Erlenmeyer flasks under sterile conditions and a light intensity of 30-40 µmol photons m^{-2} s^{-1} on the surface of the culture flasks. The light:dark cycle was 16:8 h. Cultures of *P. lacustris* and *P. malhamensis* were grown on a horizontal shaker at 100 rpm and harvested during exponential phase. Cell material of *D. divergens* and *M. annulata* was gained from cultures grown under aeration and static conditions and was harvested during exponential as well as during stationary phase. The algal cells were pelleted from the liquid cultures by gentle centrifugation in 50 ml Falcon tubes at 1200-2000 g and 4°C for 3 min in a swinging bucket rotor (SS34, Beckman Coulter). The supernatant was discarded and the tubes containing the algal cell pellets were frozen in liquid nitrogen immediately.

5.3.2. Total RNA extraction

During one round of extraction RNA of 100-200 ml of the algal cultures with cell densities between $5*10^5$ and $5*10^6$ cells ml^{-1} were processed. The frozen algal material was grounded in nitrogen cooled mortars.

Total RNA of *P. lacustris*, *P. malhamensis* and *M. annulata* was then extracted following the standard protocol for TRIzol@ reagent, using 1 ml of TRIzol@ per extraction. Total RNA yield using the TRIzol-protocol was much lower for *D. divergens* compared to the other three Chrysophytes. Therefore, a modified protocol according to Kirk Apt et al. (1995) was used for RNA extraction from *D. divergens* cells. The grounded powder from 100-200 ml of liquid culture with cell densities around $5*10^5$ cells ml^{-1} was added to 10 ml of sterile-filtered extraction buffer pH 8 (1,4 M NaCl; 100 mM Tris pH 7.5; 20 mM EDTA; 2% CTAB) with 100 µl of freshly added β-mercaptoethanol. Thorough mixing was performed manually for 10 min. One volume of chloroform-isoamyl alcohol (24:1) was added and extraction performed for 10 min. After centrifugation (10.000 g; 20 °C; 20 min) the aqueous phase was transferred to a fresh tube and mixed thoroughly with 0.25 volumes of 12 M LiCl and 1% β-mercaptoethanol. For RNA precipitation the mixture was incubated overnight at -20°C. After centrifugation (10.000 g; 4 °C; 35 min) the supernatant was discarded. The pellet was dissolved in 0.7 ml of TE with a pH of 7.5 on ice and transferred to a 2 ml reaction vessel. Extraction with 0.7 ml phenol-chloroform-isoamylalcohol (25:24:1) was performed by inverting the tube for ~2 min followed by centrifugation (10.000 g; 4°C; 20 min). The aqueous phase was then transferred to a fresh tube on ice. Extraction was performed with 0.7 ml of chloroform-isoamylalcohol by vigorous shaking (~ 10) sec and centrifugation (10.000 g; 10 min; 4 °C). The aqueous phase was transferred to a fresh tube on ice and 0.1 volumes of 3 M sodium acetate were added. The RNA was precipitated by inverting the tube several times after adding 2 volumes of 100 % ethanol and incubating the mixture at -20°C for at least 6 h. The total RNA was then pelleted by centrifugation at 10.000 g and 4 °C for 30 min and the pelleted RNA was briefly washed with 70 % ethanol. The RNA pellet was then re-suspended in 20-30 µl of nuclease-free water.

Quality of the RNA was monitored by agarose-gel-electrophoresis, photometric analysis (Genequant) and fluorometric analysis (Qubit). Quality control revealed DNA contaminations in the total RNA of *D. divergens*. Therefore DNA digestion and precipitation was performed for *D. divergens* RNA-samples using the Turbo-DNAse Kit (Ambion).

Several aliquots of total RNA were pooled after extraction and quality analysis to gain a total of 25 µg RNA per alga. Total RNA concentrations were determined by fluorometric analysis (Qubit).

5.3.3. cDNA library construction

The cDNA library construction was performed by Eurofins, Ebersbach, Germany. Briefly, quality of the total RNA was re-checked by capillary electrophoresis (Shimadzu MultiNA) and poly(A)+ RNA was extracted, thus gaining only the eukaryotic, nuclear mRNA. First strand synthesis was performed with a N6 randomized primer, before 454-adapters were ligated to the 5' and 3' ends of the cDNA. PCR amplification was carried out (11-16 cycles) using a proof reading enzyme.

Normalization was carried out by one cycle of denaturation and re-association of the cDNAs. Re-associated double-strand cDNA was separated from the remaining single-strand cDNA by a hydroxylapatite column. The cDNA was amplified with 10-11 PCR cycles after normalization. The cDNAs in the size range of 500-700 bp (including 50 bp of adapters and barcodes) were eluted from preparative agarose- gels and utilized for sequencing.

5.3.4. Sequencing and *de novo* assembly

Sequencing and assembly of the cDNA libraries was performed by Eurofins MWG Operon, Ebersberg, Germany. The 454-sequencing was performed on a GS FLX system (Roche 454 Life Science) with 1/2 segment of a full plate per alga using Titanium series chemistry. Trimming of the raw-data was performed by calculating a quality score for each base based on the signal properties relative to the statistical distributions of the control DNA fragment signals. Starting with a 10 base window at the 3' end of the read an average base quality score was calculated and the Q_{20} test was applied for trimming of the raw data (average base quality score >20). Trimming back from the 3' end occurred until the 10-base window passed the Q_{20} test. If present, primer sequences were also clipped-off. Clustering and assembly according to Smith-Wareman into contigs were performed using the MIRA assembler. The minimal read-overlap was 40 bp with a minimal sequence identity of 90 %.

5.3.5. Functional automatic annotation of the EST-data

All steps for automatic functional annotation were performed using the BLAST2GO tool (Conesa et al., 2005). Annotation was performed for all contigs but not for singletons i.e. reads which were unique and could not be assembled to any other read.
All contigs were translated and compared to the NCBI non-redundant (nr) protein database (April 2011) (http://blast.ncbi.nlm.nih.gov/Blast.cgi) for sequence similarities using the BLASTX algorithm. The search was performed with relatively low stringency (e-value cut-off 10^{-3}) extracting the 20 most similar hits per sequence.
Mapping was performed by retrieving Gene Ontology terms (GOs) from the NCBI BLAST-Hits and associating them to the corresponding contig. Annotation of the mapped sequences was performed with annotation parameters set to an e-value-hit-filter of 10^{-6}, an annotation cut-off of 55, a GO weight of 5, and a HSP-Hit coverage cut-off of 40 %.
Additionally, all contigs were searched for protein signatures via InterPro Scan (http://www.ebi.ac.uk/Tools/pfa/iprscan/) which includes the databases BlastProDom, FPrintScan, HMMPIR, HMMPfam, HMMSmart, HMMTigr, ProfileScan, HAMAP, PatternScan, SuperFamily, SignalPHMM, TMHMM, HMMPanther and Gene3D. GO-terms associated to the InterPro hits were merged to the annotations.
Based on the merged GO annotations enzyme category (EC) number acquisition was performed for the contigs.
Metabolic pathway analysis of chrysophytes was based on the automatic sorting of these ECs according to the Kyoto Encyclopaedia of Genes and Genomes (KEGG) (http://www.genome.jp/kegg/pathway.html).

5.3.6. Numeric comparison of functional annotations

Numeric comparison between the individual chrysophytes and *Phaeodactylum tricornutum* was performed by extracting the total number of sequences assigned to ECs within one metabolic KEGG-pathway map from BLAST2GO annotations or from the JGI database for the diatom *Phaeodactylum tricornutum* (http://genome.jgi.doe.gov/cgi-bin/metapathways?db=Phatr2 and http://genome.jgi.doe.gov/cgi-bin/metapathways?db=Phatr2_bd).

5.3.7. Comparison of metabolic pathways of the chrysophytes to other stramenopiles

Distribution of enzymes within glycolysis/gluconeogenesis (map 00010), pentose phosphate pathway (map 00030) and carbon fixation in photosynthetic organism (map 00710) was compared to other stramenopiles. EC annotations were extracted from the KEGG annotation database of the Joint Genome Institute (JGI) for *Aureococcus anophagefferens* (http://genome.jgi.doe.gov/cgi-bin/metapathways?db=Auran1), *Phaeodactylum tricornutum* (http://genome.jgi.doe.gov/cgi-bin/metapathways?db=Phatr2), *Phytophthora sojae* (http://genome.jgi.doe.gov/cgi-bin/metapathways?db=Physo3) and *Thalassiosira pseudonana* (http://genome.jgi.doe.gov/cgi-bin/metapathways?db=Thaps3). EC annotations for *Saccharina latissima* are referred to as published by Heinrichs et al. (2012) Table S5. EC annotations for *Ectocarpus silicolosus* were withdrawn from Cock et al. (2010). Supplementary Table 21 and by checking the BLAST results of chrysophyte contigs assigned to an EC number for similarity to gene sequences from *Ectocarpus silicolosus* (Supplementary Table S 5.3).

5.3.8. Manual curation of automatically annotated contigs

Manual curation of chrysophyte contigs was performed for the contigs assigned to gene products of glycolysis/gluconeogenesis (map 00010), pentose phosphate pathway (map 00030) and carbon fixation in photosynthetic organism (map 00710). Here, contigs were extracted from the dataset via their EC annotations according to KEGG pathway sorting. The longest open reading frame (ORF) based on the six frame amino acid translation of each contig was extracted with BLAST2GO. The individual ORFs were validated manually by re-blasting (BLASTp) the putative amino acid sequence and by monitoring the hit and the query amino acid sequences for coverage (> 40 %) and conformity with annotation results gained on the nucleotide sequence level. In a few cases, the BLAST-results based on the longest ORF resulted in a high e-value and a hit description differing from the automatic annotation. In all cases, this conflict was resolved by changing to one of the remaining five ORFs which then had a lower e-value during re-blast and the original hit description from automatic annotation. The ExPasy translation-tool (http://web.expasy.org/translate/) was utilized to gain the remaining five amino acid reading frames from the nucleotide sequence. Contigs usually represented only fragments of the complete transcript. This occasionally led to ambiguous or misleading assignment of ECs. If it was not possible to curate such conflicts logically, contigs were removed from the dataset.

5.3.9. Analysis of the sub-cellular localization of putative enzymes based on semi-automatic predictions

Localization predictions were performed for manually curated chrysophyte contigs of gene products involved in glycolysis/gluconeogenesis (map 00010), pentose phosphate pathway (map 00030) and carbon fixation in photosynthetic organism (map 00710). Pre-sequences of nucleus encoded plastid proteins in diatoms and cryptophytes consist of a signal peptide followed by a transit peptide-like domain (Pancic and Strotmann, 1993; Gschloessl et al., 2008). Localization predictions for the chrysophytes were performed corresponding to procedures applied for diatoms and cryptophytes. Based on similarities to proteins of other organisms (blastp search, http://blast.ncbi.nlm.nih.gov/) the ORFs were screened for beginnings of putative proteins and the presence of a methionine at a likely starting position. All amino acids up-stream of the putative start methionine were deleted for subcellular localization predictions via TargetP 1.1 (non-plant, no cut-offs, cleavage site prediction). TargetP (http://www.cbs.dtu.dk/services/TargetP/) predicts the presence of N-terminal pre-sequences coding for mitochondrial targeting peptides (mTP) or secretory pathway signal peptides (SP). A prediction of the cleavage site of the SP was performed using SignalP 3.0 (http://www.cbs.dtu.dk/services/SignalP-3.0/). Target P is trained on the prediction of chloroplast transit peptides for green plants but is not trained for heterokont algae (Emanuelsson et al., 2007). The plastids of heterokonts are more complex than those of green plants and protein transfer into their plastids follows different rules. For heterokonts, prediction of a SP includes that the putative subcellular destination either is the endoplasmatic reticulum, the periplastidic space or the stroma of the plastid. To identify gene products destined to the plastid stroma, all amino acids up-stream of the predicted cleavage site of the signal peptide were deleted and a second TargetP analysis was performed with the remaining fragment. If a second SP or mTP was predicted and a phenylalanine, tryptophan, tyrosine or leucine was the first amino acid up-stream of the cleavage site (“ASAFAP motif” and variations, (Gruber et al., 2007)), the putative subcellular destination of

the predicted gene product was considered to be the stroma of the plastid (Kilian and Kroth, 2005) .
Localization predictions of putative enzymes of the chrysophytes were compared to *P. tricornutum* based on literature records (Kroth et al., 2008).

5.3.10. Phylogenetic Analyses

Chrysophyte sequences with similarities to glyceraldehydes-phosphate dehydrogenase (GAPDH) according to BLAST analyses were translated into the corresponding amino acid sequence. They were added to an existing sequence set of C-type GAPDH from different algae and plants (Rio Bartulos, C. and Brinkmann, H., manuscript in preparation). To achieve sequence alignments the web-based ClustalW program at GenomeNet (http://www.genome.jp/tools/clustalw/) was performed with default settings for slow/accurate alignment and Phylip as the output format. Refinements on the alignment were executed manually, obtaining 350 amino acid positions. Maximum likelihood analysis was performed using PhyML 3.0 online (http://www.atgc-montpellier.fr/phyml/) (Guindon et al., 2010) with default settings (LG substitution model (Le and Gascuel, 2008), 4 substitution rate categories). Bootstrap analyses with 100 replicates were executed.
The graphical display was conducted by import of the resulting tree in FigTree v1.4.0 (http://tree.bio.ed.ac.uk/software/figtree/) to perform midpoint rooting and to collapse sequences of minor interest. Final colouring and labelling was implemented using CorelDRAW X5 (Corel Corporation, Ottawa, Ontario, Canada).

5.4. Results

5.4.1. RNA extraction

The first step in order to generate EST-datasets of the chrysophytes was to establish total RNA extraction procedures. The application of the TRIzol protocol according to manufacturer's advices yielded 110 - 470 µg of total RNA per 1 g fresh material of *Mallomonas annulata*, *Poterioochromonas malhamensis* or *Poteriospumella lacustris*.

However, this protocol was not applicable to *Dinobryon divergens*. During the chloroform treatment there was a relatively large interphase which contained the cellulose envelopes (loricas) of *D. divergens*. Yet, even when optional steps for organisms with high contents of polysaccharides or extracellular material were performed, total RNA yields were marginal compared to the other three chrysophytes. Hence, we applied a modified version of the phenol-chloroform extraction procedure according to Apt et al. (1995) for *D. divergens*. Here, the cellulose envelopes did not interfere with the phase separation and sufficient amounts of nucleotide acids were yielded. Yet, the amount of contaminating DNA was increased compared to the TRIzol protocol. Thus, a DNA digestion was performed for *D. divergens* after RNA extraction. In the end, the yield was 14 µg DNA-free RNA per 1 g fresh *D. divergens* material.

The adjusted total RNA extraction procedures resulted in sufficient quantities (25 µg per chrysophyte) to perform the sequencing approach. Quality and integrity of the total RNA was monitored by agarose-gel electrophoresis, optical density measurements (A_{260}/A_{280} ratios) and fluorometric measurement. Additionally, the quality of RNA samples was counterchecked prior to the cDNA library construction by Eurofins MWG Operon, Ebersberg.

Contamination by bacterial RNA fragments and transcripts of genes encoded on the plastid genome and the mitochondrial genome were minimized during construction of the cDNA library by the enrichment of poly(A)+ RNA from the total RNA.

5.4.2. Library, sequencing data and assembly statistics

Sequencing of the random-primed, normalized cDNA libraries of *M. annulata*, *D. divergens*, *P. malhamensis* and *P. lacustris* was performed applying 454 technologies. Sequencing resulted in 609,509 high quality reads for *M. annulata* to 714,488 high quality reads for *P. lacustris* (Table 5.1). These reads were assembled into 34,194-64,107 contigs, leaving 62,700-219,870 single reads. We did not further analyse the remaining singletons as they include non-assembled, short reads for which recognition of potential sequencing errors is impossible without a reference genome.

The average coverage over all contigs ranged from 4.09 for *P. malhamensis* to 8.83 for *P. lacustris* (Table 5.1.). Average contig size was between 336-385 nt. The largest contig was found in the dataset of *M. annulata* with 10470 nt, however, this contig does probably not encode any functional gene product as it did not produce any hits during BLAST search and during InterPro scan. The longest contigs of *P. lacustris* (7683 nt), *D. divergens* (4467 nt), and *P. malhamensis* (3146 nt) showed highest similarity to a hypothetical protein, a zinc-finger protein and an ABC-transporter, respectively. Contigs composed of 10 reads or less constituted 58.9-84.4 % of the datasets, whereas 0.31-2.1 % of the contigs were build from 100 reads or more. The most common transcript (Supplementary Table S 5.1) in *P. lacustris* (2360 reads) was annotated as putative calmodulin, had highest similarity to a phospholipase b like protein in *P. malhamensis* (366 reads) but did not fulfil annotation criteria and did not produce any BLAST Hit in *D. divergens* (584 reads) and *M. annulata* (605 reads).

Table 5.1: Summary of the sequencing, the assembly and the annotations statistics for the investigated chrysophytes

	Mallomonas annulata	*Dinobryon divergens*	*Poterioochromonas malhamensis*	*Poteriospumella lacustris*
Sequencing				
reads in total	609509	675231	669323	714488
average read length	367 nt	355 nt	336 nt	385 nt
Assembly and clustering				
number of contigs	53858	64107	61202	34194
number of singletons	49762	162082	204605	50109
average contig length	671 nt	531 nt	509 nt	735 nt
average coverage	4.7	4.5	4.1	8.8
% contigs built of >100 reads	0.5	0.4	0.3	2.1
% contigs built of < 10 reads	73.5	83.3	84.4	59.0
Annotation				
% contigs with BLAST-results	42.0	40.2	42.2	50.0
% contigs with BLAST GOs	34.0	32.2	35.1	41.7
% annotated contigs via BLAST	7.1	5.5	7.6	13.5
% contigs with InterPro results	49.2	73.0	26.3	52.9
% contigs with InterPro GOs	21.4	16.3	20.8	25.7
% annotated contigs total	23.2	18.0	22.7	30.2
% contigs with EC numbers	4.6	4.0	5.3	6.4
longest contig	M_ann_c27	D_div_c2548	P_mal_c3853	S_JBM_c1257
length of longest contig	10470 nt	4467 nt	3146 nt	7683 nt
annotation of longest contig	no hit	zinc-finger protein	abc transporter	hypothetical protein
most common transcript (reads)	M_ann_c27 (605)	D_div_c2607 (584)	P_mal_c2189 (366)	S_JBM_c50 (2360)
annotation of most common transcript	no hit	no hit	not annotated	calmodulin

5.4.3. Functional annotation based on BLAST performance

Automatic annotation was performed to assign proteins putatively to the contigs. First, a low stringency similarity search with an e-value cut-off set to 10^{-3} against the NCBI database (April 2011) was performed and yielded at least one BLAST-Hit for 40-50 % of the chrysophyte contigs (Table 5.1). The top 20 BLAST-Hits were taken into consideration for GO-mapping. The acquisition of GO-terms is the key element for functional annotation using the BLAST2GO application. Based on the low stringency BLAST search, 32.2-41.7 % of the contigs were assigned to one or more GO-terms. Yet, settings chosen for annotation reduced the amount of sequences with significant BLAST matches and GO classification to being 6-13 %. Settings for annotation were chosen in a way to ensure balance between too stringent and too insignificant by annotating a test set of 1 % randomly chosen contigs from the *D. divergens* dataset (Scholz, 2011). Default settings were shown to be adequate in this respect except for the HSP cut-off filter which was changed from 0 % to 40 % in order to reduce the number of short sequences annotated. Interestingly, the species with the most and best BLAST matches to each of the four chrysophytes was the brown alga *Ectocarpus siliculosus*. Other organisms delivering many sequences with high similarity were photosynthetic and non-photosynthetic heterokonts, followed by plants, mosses, green algae, colourless protists and bacteria. *Homo sapiens* hits ranged on position 12-14 looking at the species delivering the most hits, but were not among the first 30 of the species delivering the most similar hits. Altogether, five species delivered 14-16 % of all matches and

49-53 % of all top-hits (Figure 5.1). A more detailed study of global gene similarities is difficult due to the relatively small number of algal genomes in the NCBI database.

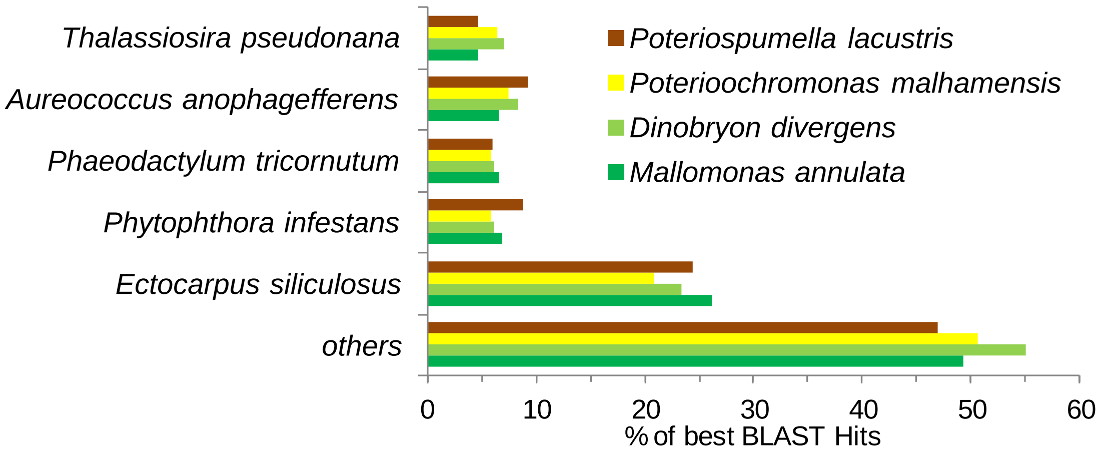

Figure 5.1: Amount of top-hits after BLAST performance.

5.4.4. Functional annotation based on InterPro Scan

Assignment of protein signatures and the associated GO terms was performed independently from BLAST based on an InterPro Scan. A protein domain signature was found for 26-73 % of the contigs, of which 16-26 % yielded a GO term. Note, that InterPro annotation in principle is a true/false decision and that there is no possibility to increase or decrease stringency. The newly gained GO annotations were then merged to the BLAST derived GO annotations resulting in a total of 18-30% functionally annotated contigs.

5.4.5. General comparison of metabolic pathways from chrysophytes to *P. tricornutum*

KEGG PATHWAY is a collection of manually drawn maps representing known metabolic interaction and reaction networks on the enzyme level (http://www.genome.jp/kegg/pathway.html). An enzyme category (EC) number has to be assigned to successfully sort enzymes of interest into the different maps. EC numbers are unique; nevertheless the same EC might produce several pathway map entries because it is involved in several metabolic pathways. EC acquisition for the chrysophytes was performed based on the functional GO annotations from BLAST and InterPro analysis and yielded 2199-3264 contigs with one or more ECs. These contigs produced a total of 944-1082 pathway entries in 131 different maps (organismal systems (2), environmental information processing (2), genetic information processing (1), metabolism (126)). The pathway map entries were assigned to 363-415 unique ECs. The number of pathway map entries and unique ECs found for the photoautotrophic strain *M. annulata* and the chemoheterotrophic strain *P. lacustris* was higher than of each of the two mixotrophic strains. As a reference, we compared our pathways analyses to KEGG annotations available from the Joint Genome Institute performed for the diatom *P. tricornutum* of November 2012. Here, 1438 pathway entries with 620 ECs were associated with 148 maps. *P. tricornutum* shared 120 pathway maps and 304 ECs with the chrysophytes.

The quantity of distinct pathway map entries was generally lower for the single chrysophytes than for *P. tricornutum* (Supplementary Table S 5.2). This is most likely related to the fact, that unlike the investigated chrysophytes, KEGG annotations of *P. tricornutum* are based on a fully sequenced genome and several EST-datasets. Diversity of whole metabolic pathways between *P. tricornutum* and the chrysophytes was highest regarding secondary metabolites, biodegradation of xenobiotics and glycan biosynthesis whereas carbohydrate pathways were corresponding.

5.4.6. A model for primary metabolism in chrysophyte

Annotated sequences of *M. annulata*, *D. divergens*, *P. malhamensis* and *P. lacustris* were merged into one joint model in order to demonstrate general metabolic capacities of chrysophytes as a group. The model is based on EC annotations. The model does not take metabolic modes of the chrysophytes and subcellular localizations of putative enzymes into account (Figure 5.2).

When merging the data, many metabolic pathways like glycolysis, oxidative and reductive pentose phosphate pathway, fatty acid metabolism, citrate cycle and glyoxylate cycle were completely annotated. One or more important genes for enzymes were still missing in other major metabolic pathways like e.g. gluconeogenesis, histidine and isoleucine biosynthesis, nitrogen fixation, sulphur fixation or nucleotide and amino sugar metabolism. Pathways of secondary metabolism like e.g. vitamin or hormone biosynthesis were very fragmented and annotated enzymes within were scattered. This states that some putative enzymes involved in the respective pathways are present, yet integrity of these pathways cannot be claimed.

The ornithine-urea cycle in *P. tricornutum* and *T. pseudonana* is thought to be one of the major intermediary pathways between photorespiration, tricarboxylic acid cycle and protein metabolism (Allen et al., 2011; Bender et al., 2012). The key enzyme of the urea cycle, carbamoylphosphat-synthetase (EC 6.3.4.16), was only annotated for the autotroph *M. annulata*. Other essential enzymes as the ornithine-, urea-, arginosuccinate- and fumarate-forming enzymes were found in all four chrysophytes whereas the citruline-forming ornithine transcarbamoylase (EC 2.1.3.3) and the urease (EC 3.5.1.5) were not present in the dataset of the heterotrophic strain.

Photorespiration is commonly found in photosynthetically active cyanobacteria, algae and plants (Bauwe et al., 2010; Raven et al., 2012). It is the process of 2-phosphoglycolate conversion into less toxic compounds and occurs during oxygenase activity of RuBisCO. In higher plants, one molecule of 2-phosphoglycolate emerges for each molecule of 3-phosphoglycerate generated from ribulose-1,5-bisphosphate during photorespiration (Bauwe et al., 2010). During this process energy and reduction equivalents are consumed, CO_2 is released and, in higher plants, 3-phospho-glycerate may re-enter the Calvin Cycle (Bauwe et al., 2010). Enzymes catalyzing the key steps during photorespiration were annotated for the chrysophytes (Figure 5.3).

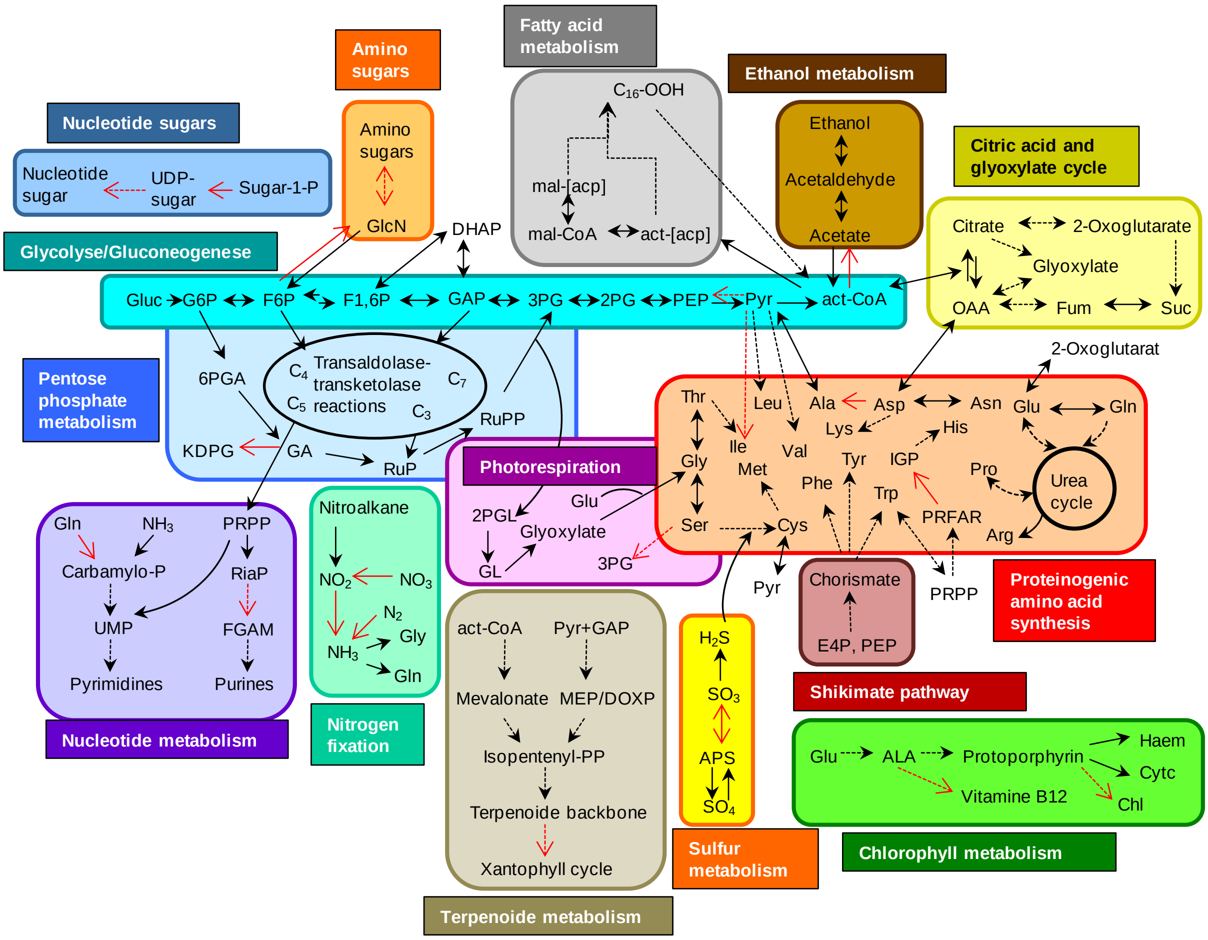

Figure 5.2: Schematic overview of principal primary metabolism for a model chrysophyte. The model was derived by merging KEGG metabolic pathway mappings of all four investigated chrysophytes. Arrows and cycles indicate putative enzymes found by EC annotation of contigs. Black color indicates that putative enzymes were found (solid: single step, broken: multiple steps, cycle: multiple steps), red colored arrows with open tips indicate incomplete pathways (solid: single step, broken: multiple steps). Reversible (double arrow) and irreversible (simple arrow) reactions are distinguished from each other.

-P: -phosphate; 2PG: 2-phosphoglycerate; 2PGL: 2-phosphoglycolate; 3PG: 3-phosphoglycerate; 6PGA: 6-phospho-gluconolacetone; acp: acyl-carrier-protein; act: acetyl-; ALA: 5-aminolevulinate; C_n: sugars with number of constituting carbon molecules subscribed; Cytc: cytochrome c; DHAP: dihydroxyacetone phosphate; DOXP: 1-deoxy-D-xylulose 5-phosphate; E4P: erythrose-4-phosphate; F1,6P: fructose-1,6-bisphosphate; F6P: fructose-6-phosphate; FGAM: formylglycinamidine-ribonucleotide; Fum: fumarate; G6P: glucose-6-phosphate; GA: 6-phospho-gluconat; GAP: glyceraldehyde-3-phosphate; GL: glycolyte; GlcN: glucoseamine-6-phosphate; Gluc: glucose; IGP: imidazole glycerole-3-phosphate; KDPG: 2-keto-3-desoxy-6-phosphogluconate; mal: malonyl; MEP: 2-C-methylerythritol 4-phosphate; OAA: oxalacetate; PEP: phosphoenolpyruvate; PPRP: phosphoribosyl diphosphate; PRFAR: N´-[(5´-phosphoribulosyl) formimino]-5-aminoimidazole-4-carboxamide; Pyr: pyruvate; RiaP: ribosylamine-5-phosphate; RuP: ribulose-5-phosphate; RuPP: ribulose-1,5-bisphosphate; Suc: succinate; UDP: uridine diphosphate; UMP: uridine monophosphate.

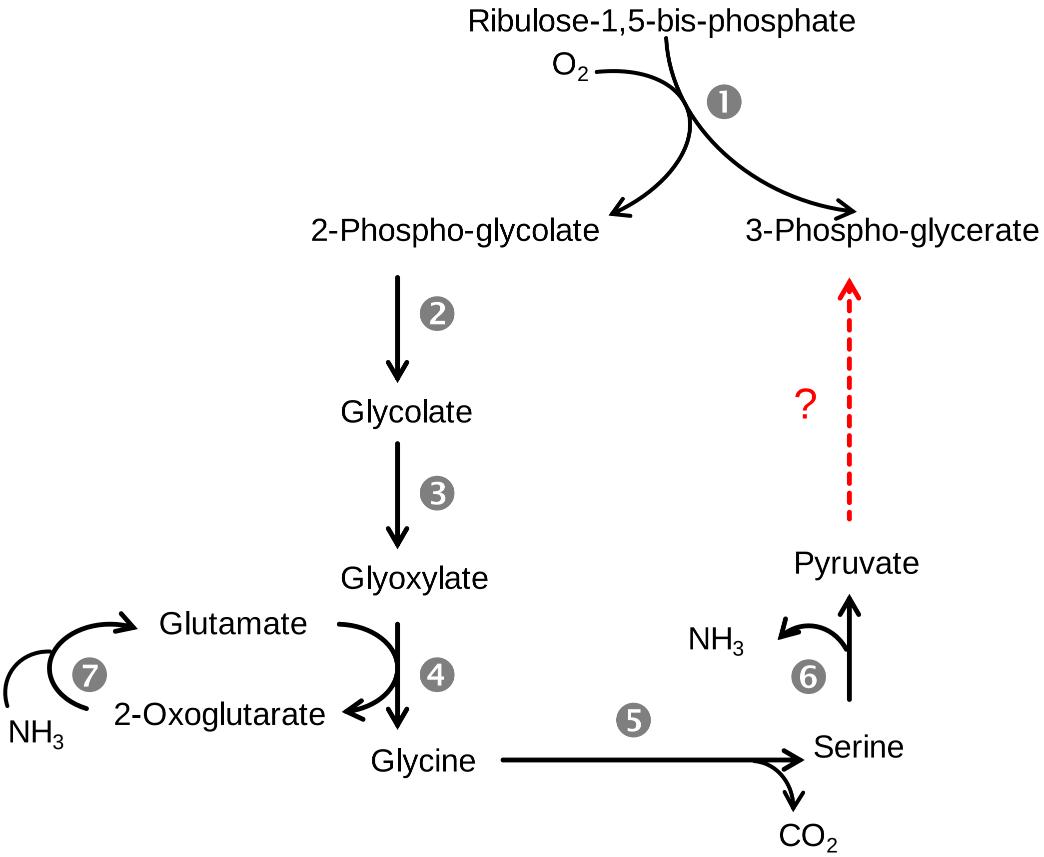

Figure 5.3: Schematic overview of important intermediates and reactions involved in the photorespiratory pathway. A black arrows indicates that an enzyme (number) catalyzing the respective reaction was found in at least one of the chrysophytes; the red broken arrow indicates that multiple steps are necessary and that enzymes were only partially found for the investigated chrysophytes. 1) Ribulose-bisphosphate carboxylase/oxygenase, EC 4.1.1.39; 2) Phosphoglycolate phosphatase, EC 3.1.3.18; 3) Glycolate oxidase, EC 1.1.3.15; 4) Glutamate-glyoxylate aminotransferase, EC 2.6.1.4; 5) Glycine decarboxylase complex, EC 1.4.4.2, EC 2.1.2.10, EC 1.8.1.4, EC 2.1.2.1; 6) Serine dehydratase, EC 4.3.1.17 or 4.3.1.19; 7) Glutamate dehydrogense 1.4.1.2.

5.4.7. Autotrophic carbon fixation

So far, six natural carbon fixation pathways are known (Fast and Papoutsakis, 2012): the Calvin-Benson-Bassham-Cycle or reductive pentose phosphate cycle (rPP, Calvin Cycle), the reductive citrate cycle (rCC), the Wood-Ljungdahl pathway or reductive acetyl-CoA pathway (WL), the 3-hydroxypropionate cycle (HP), the 3-hydroxypropionate/4-hydroxbutyrate cycle (3HP/4HP) and the dicarboxylate/4- hxdroxybutyrate cycle (DC/HP). Due to the oxygen sensitivity of some enzymes WL and DC/4HB are restricted to organisms living under anoxic conditions whereas rPP, rCC, 3HP/4HB and HP have been found in organisms from aerobic environments. Based on available EC annotations for *P. tricornutum* and our analysis for the chrysophytes none of the CO_2-fixation pathways seems to be complete, except for the rPP (Figure 5.4). Nevertheless, several of the CO_2-fixating enzymes have been annotated (Table 5.2). The conversion of CO_2 into bicarbonate may be catalyzed by carbonic anhydrases. Putative carbonic anhydrases (EC 4.2.1.1) were annotated for all four chrysophytes.

Table 5.2: Important putative carboxylating and decarboxylating enzymes of the chrysophytes and *Phaeodactylum tricornutum*. Ma: *Mallomonas annulata*; Dd: *Dinobryon divergens*; Pm: *Poterioochromonas malhamensis*; Pl: *Poteriospumella lacustris*; Pt: *Phaeodactylum tricornutum*.

Association	EC number	Name	Ma	Dd	Pm	Pl	Pt
Involved in CO_2 fixing reactions							
3HP and 3HP/4HB cycle	6.4.1.2	Acetyl-CoA carboxylase	x	x	x	x	x
3HP and 3HP/4HB cycle	6.4.1.3	Propionyl CoA carboxylase	x	x	x	x	x
Calvin cycle	4.1.1.39	Ribulose-1,5-bisphosphate carboxylase	x	x	x	-	x
Dicarboxylate/4HB cycle	1.2.7.1	Pyruvate synthase	-	-	-	-	-
Dicarboxylate/4HB cycle	4.1.1.31	Phosphoenolpyruvate carboxylase	x	x	x	x	x
Gluconeogenesis	6.4.1.1	Pyruvate carboxylase	x	-	-	-	x
Photosynthetic carbon fixation	4.1.1.31	Phosphoenolpyruvate carboxylase	x	x	x	x	x
Reductive Acetyl-CoA pathway	1.2.1.43	Formiate dehydrogenase	-	-	-	-	-
Reductive Acetyl-CoA pathway	1.2.7.4	CO- dehydrogenase (ferredoxin)	-	-	-	-	-
Reductive Acetyl-CoA pathway	2.3.1.169	CO-methylating acetyl CoA synthase	-	-	-	-	-
Reductive citrate cycle	1.2.7.3	2-oxoglutarate:feredoxin oxidoreductase	-	-	-	-	-
Reductive citrate cycle	1.1.1.42	Isocitrate dehydrogenase	x	x	x	x	x
Urea cycle	6.3.4.16	Carbamyl-phosphate synthetase	x	-	-	-	x
Various pathways	4.2.1.1	Carbonic anhydrase	x	x	x	x	x
Involved in CO_2 releasing reactions							
Citrate cycle	1.1.1.42	Isocitrate dehydrogenase	x	x	x	x	x
Oxidative pentose phosphate cycle	EC 1.1.1.44	6-phosphogluconate dehydogenase	x	-	-	-	x
Photorespiration	1.4.4.2	Glycine dehydrogenase	x	x	x	x	x
Pyruvate metabolism	1.1.1.38/39/40	Malic enzyme	x	-	x	-	x
Urea degradation	3.5.1.5	Urease	x	x	x	-	x
Various pathways	4.1.1.49 /32	Phoshoenolpyruvate carboxykinase	-	x	x	x	x

5.4.8. Carbohydrate metabolism of chrysophytes

One of the aims of this study was to find major differences in the carbohydrate metabolism of mixotrophic chrysophytes compared to heterotrophic and autotrophic representatives. Some obvious differences regarding the heterotroph *P. lacustris* were expected, like for example the lack of ribulose-1,5-bisphosphate carboxylase/oxygenase (RuBisCO, EC 4.1.1.39) or phosphoribulokinase (Prk, EC 2.7.1.19) which are enzymes involved in the Calvin Cycle (Figure 5.4). Other findings were less predictable like for example the missing of complete maps for individual chrysophytes in lipid metabolism, metabolism of other amino acids, glycan biosynthesis, biosynthesis of secondary metabolism and others (Supplementary Table S 5.2).

Due to normalization of the EST-libraries quantitative transcript expression analysis is not applicable for the datasets. However, given that biosynthetic reactions may be controlled on the transcriptional level, it is anticipated that the number of distinct pathway map entries will be higher if a metabolic pathway is active than if the pathway was down-regulated or inactive. Therefore, a qualitative analysis might yet hint at the relevance of certain metabolic reactions for an organism. The number of pathway map entries according to KEGG sorting differed between the organisms (Supplementary Table S 5.2). A ranking from purely photoautotrophic to purely chemoheterotrophic nutrition according to physiological observations results in the order of *M. annulata* → *D. divergens* → *P. malhamensis* → *P. lacustris* (Chapter 4). Screening the KEGG maps for pathways with entry counts that reflected this ranking (i.e. highest number of entries for *M. annulata* and lowest for *P. lacustris* with a minimum difference of 5 entries) was performed (Table 5.3). We detected biosynthetic pathways of plant hormones, terpenoids, porphyrine and the amino acids valine, leucine and isoleucine to correlate with the ranking. Reciprocally, glycolysis and sucrose metabolism may be related to the importance of chemoheterotrophy for the algae because entry counts were declining from *P. lacustris* to *M. annulata*.

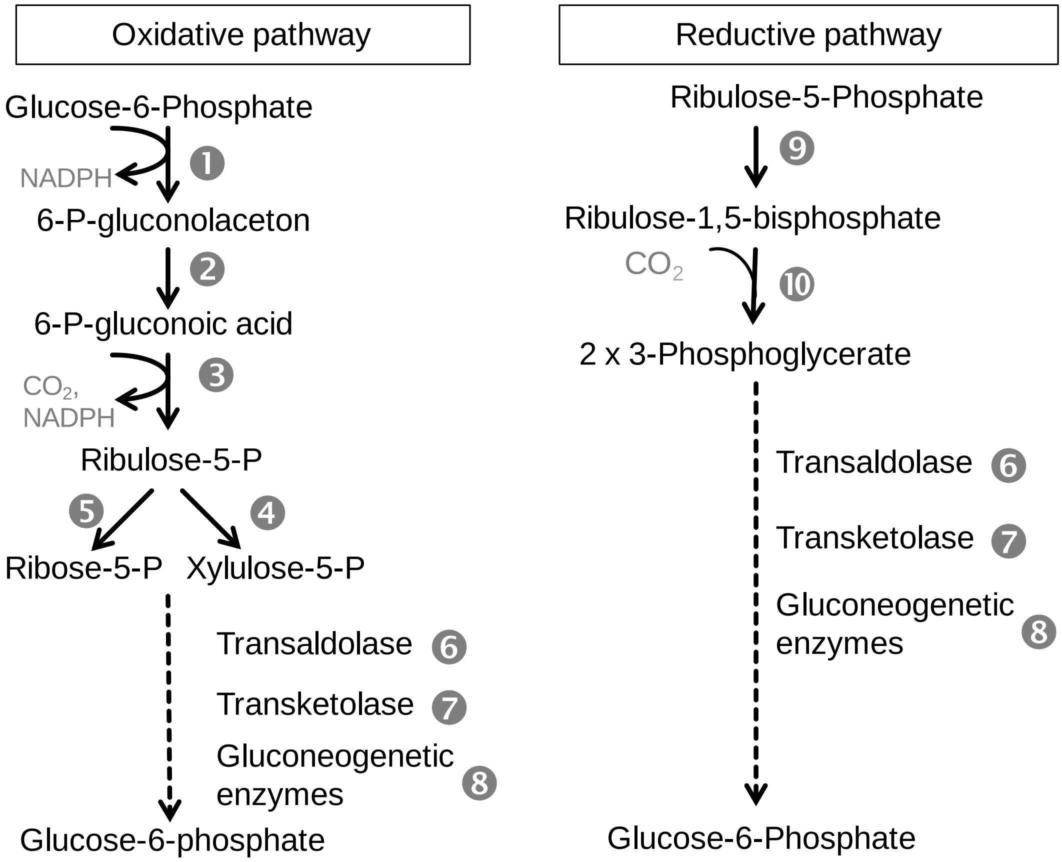

Figure 5.4: Schematic overview of important intermediates and reactions involved in the oxidative (left) and the reductive (right) pentose phosphate cycle. A black arrows indicates that an enzyme (number) catalyzing the respective reaction was found in at least one of the chrysophytes. Solid arrows indicate single step and dashed arrows multiple step reactions. 1: Glucose-6-phosphate dehydrogenase (EC 1.1.1.49); 2: Gluconolacetonase (EC 3.1.1.31); 3: 6-phospho-gluconate dehydrogenase (EC 1.1.1.44); 4: Ribulose-phosphate 3-epimerase EC 5.1.3.1;5: Ribose-5-phosphate isomerase EC 5.3.1.6; 6: Transaldolase EC 2.2.1.2; 7: Transketolase (EC 2.2.1.1); 8: see Figure 5.2or Figure 5.6 starting from 3-phosphoglycerate; 9: Ribulose-5-phosphate kinase (EC 2.7.1.19); 10: Ribulose-bisphosphate carboxylase/oxygenase (EC 4.1.1.39).

The chrysophyte data was compared to other protists regarding putative enzymes involved in glycolysis, gluconeogenesis, the pentose phosphate pathways and photosynthetic carbon fixation (Table 5.4). The only unique chrysophyte enzymes were found for *P. lacustris* with two contigs (S_JBM_c1109; S_JBM_c2509) annotated as phosphoketolases (EC 4.2.1.9; EC4.1.2.22). These contigs showed high sequence similarity on the protein level (74-77 %) to phosphoketolase from green sulfur bacteria and cyanobacteria.

In the course of localization predictions, manual curation of annotations was performed for a subset of 660 chrysophyte contigs putatively involved in glycolysis, gluconeogenesis, the pentose phosphate pathways and photosynthetic carbon fixation. Here, approximately 10 % of the contigs were removed from the dataset because the InterPro based annotations turned out to be too insignificant. Approximately 2 % of the contigs had gained wrong or bivalent EC annotations and were re-annotated. Localization predictions were successfully performed for 169 contigs. The remaining 491 contigs encoded open reading frames (ORFs) which were incomplete at the 5'-end. During analysis of ORFs assigned to glycolytic enzymes, a putative start methionine was found for ~15 % of the ORFs of *D. divergens* and *P. malhamensis*, in contrast to ~50 % for *M. annulata* and *P. lacustris.*

Table 5.3: Metabolic pathways which correlate with the gradient from autotrophic to heterotrophic lifestyle by entry counts. Numbers represent KEGG pathway map entries. Red= lowest number of pathway entries, dark green= highest number of pathway entries, light green=second highest number of pathway entries, yellow= third highest number of pathway entries. Ma= *Mallomonas annulata* (autotroph), Dd= *Dinobryon divergens* (mixotroph), Pm= *Poterioochromonas malhamensis* (mixotroph), Pl= *Poteriospumella lacustris* (heterotroph). Pathway map entries of *P. tricornutum* (Pt) serve as a reference and coloring indicates the range of entries compared to the chrysophytes.

Pathway map	Ma	Dd	Pm	Pl	Pt
Linked to autotrophy					
Biosynthesis of plant hormones	76	64	64	58	74
Biosynthesis of alkaloids derived from terpenoid and polyketide	40	37	37	34	40
Porphyrin and chlorophyll metabolism	18	17	12	10	24
Terpenoid backbone biosynthesis	14	13	12	8	13
Valine, leucine and isoleucine biosynthesis	9	7	7	2	12
Linked to heterotrophy					
Glycolysis / Gluconeogenesis	18	19	20	23	20
Glutathione metabolism	9	9	11	15	17

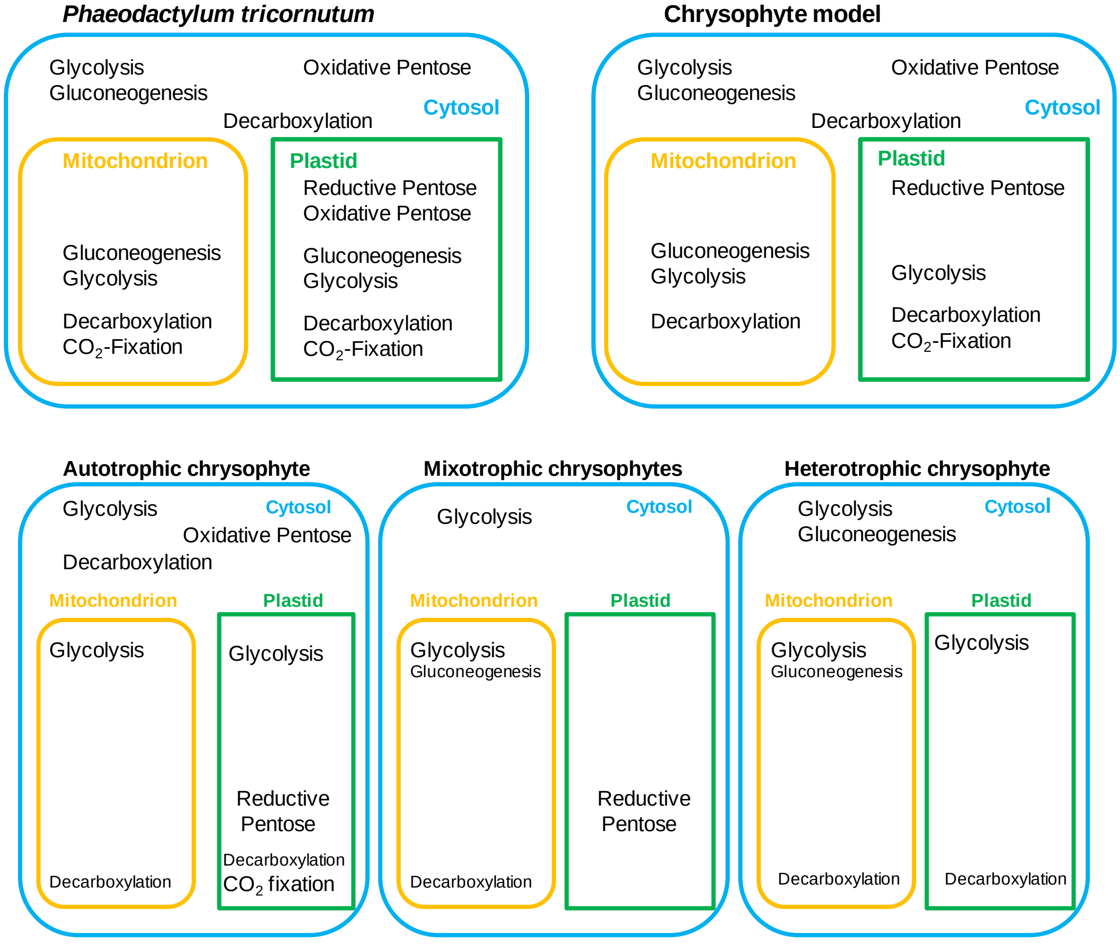

Figure 5.5: Schematic overview of carbon pathways in the different compartments of the cell of chrysophytes and *Phaeodactylum triconutum*. Distribution of autotrophic, mixotrophic and heterotrophic chrysophytes (lower part) are merged to a chrysophyte model and opposed to *P. tricornutum* (upper part). Allocations were performed regarding the subcellular localization predictions of key enzymes and distinct carboxylating and decarboxylating enzymes only (Supplementary Table S 5.5). Note, that assignments made for the plastid also include predictions of enzymes dedicated to the periplastidic space and the chloroplastidic endoplasmatic reticulum. Pentose = pentose phosphate pathway.

In the following, we consider the subcellular localization of the key enzymes in a pathway as the major criterion for the subcellular localization of the whole pathway (Supplementary Table S 5.5). Generally, our localization predictions reflect a similar distribution of reactions in the different compartments compared to *P. tricornutum* (Kroth et al., 2008; Gruber et al., 2009). Still, there are some significant differences (Figure 5.5). Photosynthetic carbon fixation in *P. tricornutum* takes place in the plastid but, due to the presence of certain enzymes like pyruvate carboxylase (EC 6.4.1.1) and phosphoenolpyruvate carboxylase (EC 4.1.1.31), can also take place in the mitochondrion. So far, there is no evidence for mitochondrial CO_2 fixation from the partial chrysophytic dataset analyzed.
Similar to *P. tricornutum*, the oxidative pentose phosphate pathway (Figure 5.4) is probably only expressed in the cytosol of *M. annulata* cells. Strikingly, no sequences coding for the key enzymes of the oxidative pentose phosphate pathway were found for the mixotrophic chrysophytes and carboxylating plastid targeted enzymes were missing, too. However, intracellular distribution differences based on lacking isoforms in the mixotrophic subsets have to be considered with caution due to the relatively low amount of non-truncated sequences in the two subsets and because transcriptomes may not be complete.
Some of the sequences of the heterotroph *P. lacustris* had a signal and a transit peptide and are therefore dedicated to the non-photosynthetic plastid or the endoplasmatic reticulum. Such plastid-targeted sequences were found for all of the enzymes that catalyze the steps

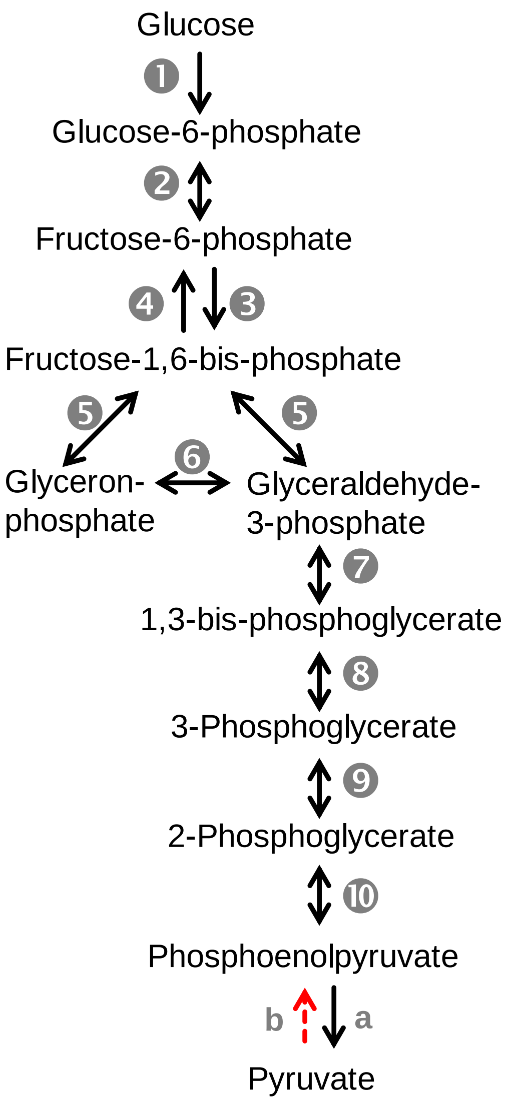

Figure 5.6: Schematic overview of important intermediates and reactions involved in glycolysis and gluconeogenesis. A black arrow indicates that an enzyme (number or letter) catalyzing the respective reaction was found in at least one of the chrysophytes; a red arrow indicates that the enzyme was not found for any of the investigated chrysophytes. 1: Hexokinase (EC 2.7.1.1); Glucokinase (EC 2.7.1.2); 2: Glucose-6-phosphate isomerase (EC 5.3.1.9); 3: 6-phosphofructokinase (EC 2.7.1.11); 4: Fructose-bisphosphatase (EC 3.1.3.11); 5: Fructose-bisphosphate aldolase EC 4.1.2.13; 6: Triose-phosphate isomerase EC 5.3.1.1; 7: glycer-aldehyde-3-phosphate dehydrogenase (EC 1.2.1.12, EC 1.2.1.13; EC 1.2.1.9; EC 1.2.7.6 or EC 1.2.1.59); 8: Phosphoglycerate kinase (EC 2.7.2.3); 9: Phosphoglycerate mutase (EC 5.4.2.1); 10: Phosphopyruvate hydratase (EC 4.2.1.11); a: Pyruvate kinase (EC 2.7.1.40), b: Pyruvate, water dikinase (EC 2.7.9.2), pyruvate, phosphate dikinase (EC 2.7.9.1), pyruvate carboxylase (EC 6.4.1.1) and phosphoenolpyruvate carboxykinase (EC 4.1.1.32/49).

from fructose-6 phosphate to phosphoenolpyruvate during glycolysis (Figure 5.6). Additionally, we found a putative malate dehydrogenase, which is a decarboxylating enzyme, with a signal and a transit peptide.
So far, phylogenetic analyses have shown that the sequences of plastid-targeted glyceraldehydes-3-phosphate dehydrogenases (GAPDHs) of the chromalveolates differ from those of plants, green algae, red algae, *Euglena* and *Pycrocystis* and from cyanobacterial sequences (Harper and Keeling, 2003). Moreover, it is possible to distinguish the plastid-targeted GAPDHs of heterokonts from cytosolic and mitochondrial-targeted homologues (Liaud et al., 2000; Harper and Keeling, 2003). Thus, phylogenetic analyses of GAPDH sequences are a suitable and independent method to proof findings regarding subcellular localization predictions for the chrysophytes. We added the translated amino acid sequence of all contigs annotated as GAPDHs in the chrysophyte datasets to an existing alignment of GAPDH sequences (Rio, C and Brinkmann, H, manuscript in preparation). We found that the sequences from this study clustered with sequences of other chrysophytes, namely *Mallomonas rasilis* and *Ochromonas danica* (Figure 5.7) Moreover, all GAPDHs with a signal-peptide prediction clustered into the plastid-targeted branch of the tree, including the sequences of the heterotrophic *P. lacustris*. Accordingly, sequences with mitochondrial localization prediction clustered into the mitochondrial branch. None of the analyzed new sequences clustered outside of the mitochondrial and the plastidic branch. Hence, results of subcellular localization predictions were matching results of phylogenetic analyses.

5.4.9. Polysaccharides and fatty acids in chrysophytes

Organisms generally conserve superfluous carbon by producing various storage compounds among which polysaccharides and fatty acids are the most prominent. Synthesis of polysaccharides depends on the availability of nucleotide-bound sugars like UDP-, GDP- or ADP- sugars. Chrysolaminarin is a primary storage polysaccharide of chrysophytes and other alga (Beattie et al., 1961; Goddijn and van Dun, 1999). The reactions involved in chrysolaminarin biosynthesis have not yet been completely revealed (Wan et al., 2012; Chauton et al., 2013), but synthesis is probably initiated starting from UDP-glucose. Yet, the only gene for a putative UDP-sugar pyrophosphorylase found in the chrysophyte datasets was UDP-N-acetylglucosamine pyrophosphorylase (EC: 2.7.7.23) for the heterotroph *P. lacustris*. Pathway map entries concerning biosynthesis of all nucleotide sugars and possible condensation reactions were very fragmented for all four chrysophytes.
According to annotated pathway map entries the biosynthesis of long chain fatty acids palmitic acid (16:0) and myristic acid (14:0) is possible in chrysophytes. Biosynthetic pathways of other saturated and unsaturated fatty acids were incomplete.

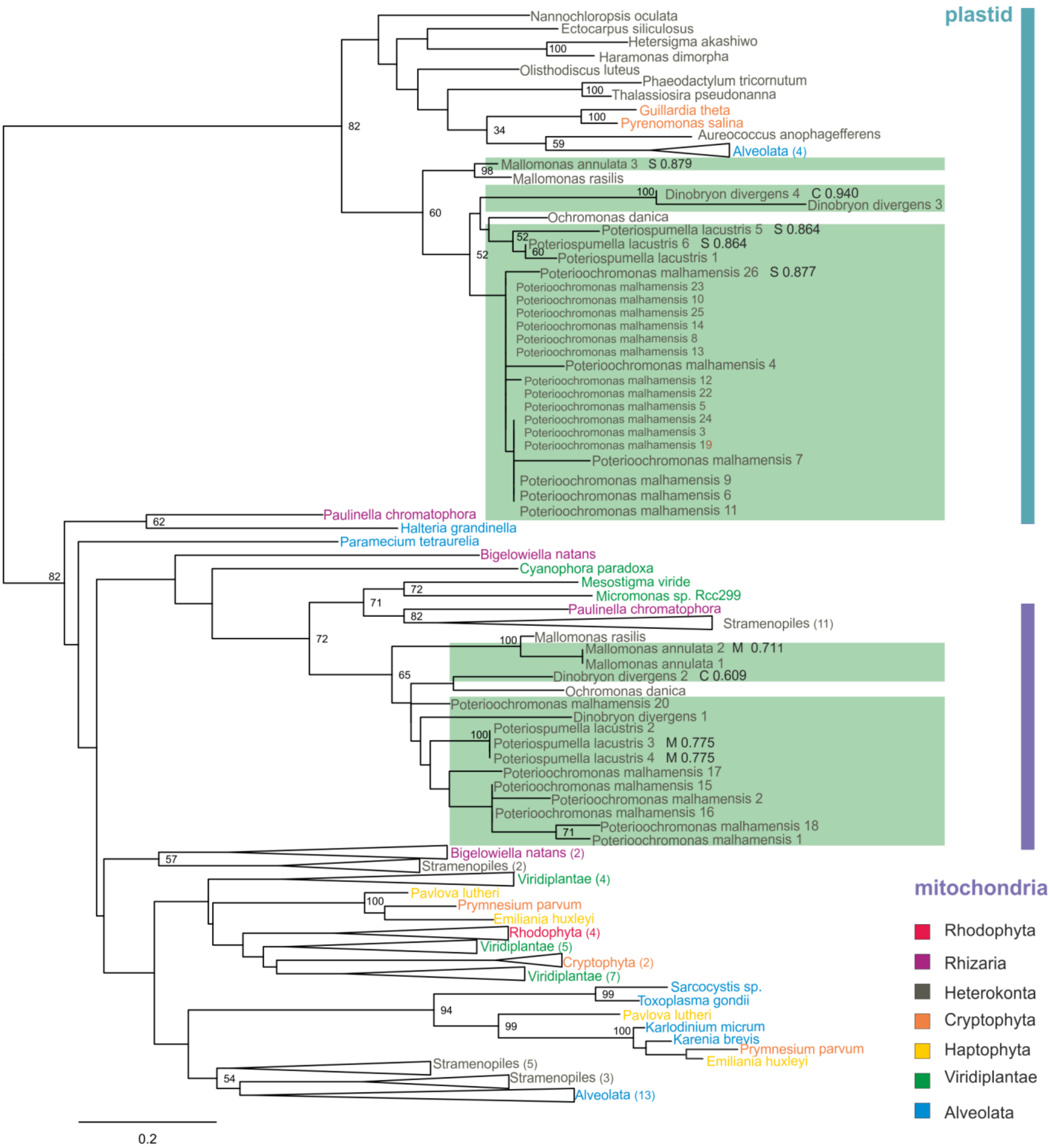

Figure 5.7: Maximum likelyhood phylogenetic tree of GAPDH (GAPDH C) sequences using PhyML with 132 sequences and 350 amino acid positions. Chrysophyte sequences from this study are highlighted by green shading. If applicable, results of subcellular localization prediction analysis are presented behind the sequences (C= cytosolic, M= mitochondrial, S= signal peptide). Numbers at nodes of subtrees correspond to bootstrap values greater than 50 %. All sequences gained in this study clustered either into the mitochondrial (purple bar) or the plastidic branch (turquoise bar), no cytosolic variants were found. Interestingly, sequences of the heterotroph *Poteriospumella lacustris* with a signal peptide accordingly clustered into the plastidic branch of the tree. This implies that the origin of sequences is the same as for other plastidic targeted genes of GAPDHs and demonstrates reliability of the localization predictions. Contig numbers of sequences from this study are listed in the Supplementary Table S 5.4.

5.5. Discussion

5.5.1. Methodical issues

Integrity and purity are two major criteria for a good quality of RNA preparations. Degradation usually is more severe at the 5'-end of nuclear encoded eukaryotic mRNAs since they are not protected from RNA degrading enzymes by multiple adenosine nucleotides (polyA). Though intra-organismic RNAse activity is inhibited during the extraction procedure a certain degree of RNA degradation is inevitable. In relation to the total amounts of contigs analysed manually, the subsets of the autotroph *M. annulata* and the heterotroph *P. lacustris* contained more ORFs with a putative start methionine than those of the mixotrophs. Therefore, the amount of degraded RNA sequences in samples of *P. malhamensis* and *D. divergens* may have been higher.
Enrichment of nuclear encoded mRNA was performed during library production exploiting the binding affinity of polyA-tails to a suitable matrix. However, any RNA- or DNA-fragment with polyA-stretches may contaminate the normalized library. Such contaminations may severely affect analysis of transcriptomic datasets, especially quantitative aspects. The analyses of final total RNA samples regarding contaminations by DNA were negative. We therefore consider DNA contaminations to be low. This study was not designed to analyse gene expression quantitatively, but to provide a qualitative overview of possible metabolic pathways in chrysophytes. A low amount of contaminations by nuclear DNA fragments from the protists do not affect our metabolic overview substantially.
Plastidic and mitochondrial RNA and DNA may introduce a bias regarding the localization predictions performed. We found 14 transcripts putatively coding for large and small subunits of RuBisCO (ribulose-1,5-bisphosphate carboxylase/oxygenase) for *M. annulata*, *D. divergens* and *P. malhamensis*. RuBisCO is active in the plastid or chloroplast of photosynthetic eukaryotes. Yet, we did not find any plastidic targeting signals encoded within the contigs though some encoded the complete 5' region of the transcript. Thus, we consider our findings to be plastidic DNA contaminations. Plastid encoded genes of algae have been found to be AT-rich and contain a rather high amount of homopolymeres (Ravi et al., 2008) which is a plausible explanation for contaminations. Apart from the RuBisCO sequences, we did not find any other contaminating sequence.
Bacterial nucleic acids in samples of *M. annulata* and *D. divergens* may introduce a bias, too. Transcripts were not analysed in respect to general codon usage, which is a possibility to distinguish DNA of prokaryotic origin (including also the plastidic and mitochondrial genomes) from eukaryotic DNA. Anyway, since bacteria did not produce suspicious amounts of hits during BLAST analysis, bacterial contaminations were considered to be marginal.

Transcripts with low expression rates may be sequenced with a lower probability compared to housekeeping genes in non-normalized libraries or might even not be sequenced at all. Thus, we performed normalization of cDNA to increase the abundance of rarely expressed sequences compared to housekeeping genes. A possible hint concerning quality of normalization is the character of the high read number composed contigs. In our case normalization for *P. lacustris* was probably not very successful as within the 20 highest read number composed contigs, putative ribosomal proteins, which generally are considered as housekeeping genes, were over-represented whereas the data was more diverse for the remaining algae (Supplementary Table S 5.1). We suppose the less successful normalization of the *P. lacustris* library compared to the other chrysophytes is based on separating the double strand cDNA fragments too early from the single strand cDNA during the normalization procedure.

A complete transcriptome includes all sequences which may be expressed under different conditions. Evaluation of completeness, however, is not that simple. As there is no suitable reference genome available for chrysophytes the total number of putatively expressed genes remains unknown. Anyway, the total of expressed genes usually differs from the number of coding genes and varies from organism to organism. For *P. tricornutum* (Bowler et al., 2008) and *A. anophagefferens* (Gobler et al., 2011), for example, 86% and 98% of the predicted genes found had EST-support.

In order to minimize methodical errors, each nucleotide of a contig's sequence should be represented by more than one nucleotide during the assembly. This is usually called coverage referring to a single position and average coverage referring to the whole contig. Here, it is necessary that the individual nucleotide sequences truly represent different reads originating from first strand synthesis and not different amplificates resulting from the PCR steps performed. Using random primed cDNA libraries, only PCR amplificates are likely to show completely identical length and composition. Thus, to minimize the bias introduced by PCR amplificates, clustering is performed prior to the assembly. During clustering reads of identical sequence composition (min. 98 %) and length are summarized by one cluster representative. Assembly and calculation of the average coverage is then performed with the distinct cluster representatives found. Yet, and unlike to genome sequencing approaches, high average contig coverage is no criterion for the completeness of a transcriptome, especially using random-primed, normalized libraries. Evaluation might instead be performed by looking at the sequencing depth. This means to screen the dataset for transcripts with ensured low expression. If such transcripts are found, sequencing depth was high and the probability that the majority of transcripts are represented by the dataset is high, too. However, finding a suitable evaluation transcript at the current knowledge on chrysophytes is not reasonable.

In this case, sequencing approaches may be performed under several culturing conditions until the number of newly found contigs per sequencing step is marginally low. In this study, cell harvest was performed in exponential as well as stationary phase, however, we chose growth promoting conditions for each alga and did not include non-favourable conditions e.g. nutrient depletion, light stress etc. Therefore, it is unlikely that the whole transcriptome of any of the chrysophytes investigated is represented in the datasets.

Hence, at the present state of analysis, the only possible estimation of the completeness of the chrysophyte transcriptomes is a comparison to gene numbers of other algae. For the brown alga *Ectocarpus siliculosus* (Cock et al., 2010), the pelagophyte *Aureococcus anophagefferens* (Gobler et al., 2011) and the diatom *Phaeodactylum tricornutum* (Bowler et al., 2008) there are about 16,200, 11,500 and 10,400 genes predicted in the nuclear genome. The average transcript length is 2400 nt, 1600 nt and 1500 nt, respectively. It is therefore very likely, that the number of contigs found for the chrysophytes (~34,000-64,000) does overestimate the actual number of genes. The average contig length (500-700 nt) is less than 50% of the average transcript length of the upper set of alga which may be a result of RNA degradation during preparation. The high number of contigs per protist in relation to expected numbers of expressed genes may be due to non-overlapping short sequences. Nevertheless, even partial sequences of transcripts (>100 nt) are sufficient to ensure a good quality of annotation results during sequence similarity search as performed in this study.

To relate our data to a good reference, we chose the diatom *P. tricornutum* since its genome is fully sequenced and EST support gained under various conditions is available. The genome of *E. siliculosus* might have been a better reference judged by the BLAST similarities (Figure 5.1), however, the EC annotations for the *E. siliculosus* genome are not publically available which was a decisive criterion for the comparisons performed in this study. Nevertheless, re-annotation of the *E. siliculosus* genome has been performed including EC assignment via BLAST2GO and has also been compared to *P. tricornutum* (Heinrich et al., 2012).

Annotation rates were below 30 % while up to 70 % of the contigs did not produce a hit during sequence similarity search to proteins in the NCBI non-redundant database or during search for protein domain signatures. *De novo* annotation rates of 20-50 % are also reported for other algal EST-datasets (Hackett et al., 2005; Stanley et al., 2005; Bayer et al., 2012; Heinrich et al., 2012). The no-hit-category of sequences might not only represent uncharacterized, new proteins but may additionally include fragments of non-coding RNA (like e.g. the 5' and 3'UTR), other regulatory RNA, rRNA, DNA and assembly artefacts. We did not further investigate the character and composition of these contigs.

Several sequences of *P. lacustris* assigned to glycolytic enzymes were predicted to enter its non-photosynthetic plastid due to their signal peptide. This included sequences assigned to GAPDH enzymes. The phylogenetic analysis showed that these sequences were homologous to sequences of plastid-targeted GAPDHs of other heterokonts (Figure 5.7). Thus, *P. lacustris* may perform a partial glycolysis in the reduced plastid. Here, the localization of the glycolytic enzymes in the plastid of *P. lacustris* needs to be confirmed experimentally for example by the application of *in situ* hybridization techniques combined with electron microscopy.
Phylogenetic analyses were performed with all of the chrysophyte sequences assigned to GAPDH by sequence similarity. We did not exclude nearly identical sequences from the analyses because it is not possible to distinguish between allele-variants, PCR duplicates or sequencing artifacts in the dataset. This strategy may have introduced certain biases affecting the bootstrap values and formation of clades. First, some of the clades comprising several sequences of one chrysophyte exclusively might be “pseudo-clades”. This is because nearly identical sequences naturally assort into the same clade, independent of whether they are truly homologues or if sequence differences are assembly artifacts. Second, the amount of chrysophyte sequences was quite large compared to the whole dataset. This probably caused the separation of chrysophyte branches from other heterokonts which was not observed in the original dataset. Third, some of the sequences were relatively short (<100 aa) which affects the reliability of formed branches, too. Accordingly, one of the short sequences of *P. malhamensis* was removed from the dataset because it formed a separate long branch.
Nevertheless, these biases did not affect the clustering of the new sequences with chrysophyte sequences from other studies. Also, good bootstrap support (> 70%) of the new sequences within the plastid-targeted chromalveolate GAPDH clade and the mitochondrial-targeted clade was given.

5.5.2. Carbon turnover in chrysophytes

Differences in the metabolic pathways were mainly found in the secondary metabolism (Supplementary Table S 5.2) and thereby affect compounds which are known to vary greatly from species to species in photosynthetic organisms like e.g. pigments, terpenoids, hormones or defense intermediates. Some pathways were completely lacking for the individual chrysophyte strains like e.g. biotin biosynthesis for the mixotroph *P. malhamensis*. Vitamin deficiencies of chrysophytes have been taken advantage of by utilizing them as sensitive indicator organisms for e.g. the presence of vitamin B12, biotin and thiamin in solutions (Heinrich, 1955). However, pathway map entries concerning vitamins and cofactors were scarce compared to *P. tricornutum* (with some exceptions like e.g. one carbon pool by folate), making interpretations difficult and speculative. The presence of one or two enzyme within a whole pathway does not imply actual biosynthetic relevance of the pathway for an organism and the absence of the corresponding contig in another organism might still mean that it was actually expressed but simply not present in the dataset. Thus, further investigation on all of the findings with only one or two annotated enzymes in a complete pathway are necessary. Yet, we considered an enzyme absent if the putative enzyme was not found in any of the four chrysophytes.

Previous studies have shown that carbon fixation in individual chrysophytes is ineffectively performed compared to other algae (Maberly et al., 2009). Interestingly, we found all major pathways of carbon metabolism of *P. tricornutum* in the chrysophytes (with the obvious exception of the Calvin Cycle in the heterotroph *P. lacustris*). It has been suggested, that the photosynthetic handicap of chrysophytes in general might be a consequence of missing external carbonic anhydrases (Bhatti and Colman, 2008). These enzymes catalyze the reversible interconversion from CO_2 to bicarbonate and do exist in soluble or membrane associated isoforms. Under physiological conditions in chloroplasts of plants the reaction from bicarbonate to CO_2 is favored and the resulting increase of the CO_2 concentration is beneficial for the activity of RuBisCO (Badger and Price, 1994). In chrysophytes, RuBisCO is thought to depend on diffusive supply with CO_2 probably making carbon fixation less effective (Bhatti and Colman, 2011). Interestingly, we found several putative carbonic anhydrases in our EST-dataset. Further studies on localization and functionality of the corresponding proteins would present an important step regarding the approval of these theories.

Comparing the photoautotrophic strain to the remaining chrysophytes, the gluconeogenetic CO_2-fixing enzyme pyruvate carboxylase and carbamylo-phosphate synthetase involved in the urea cycle may be promoted as potential candidates for the effectiveness of photosynthesis. This is because they were only found for the photoautotrophic *M. annulata*. Additionally, transcripts for the key enzymes of the oxidative pentose phosphate pathway were not expressed in the two mixotrophic and the heterotrophic strain. The oxidative pentose phosphate pathway serves to form ribulose-5-phosphate from glucose-6-phosphate and NADPH. These are important anapleurotic processes which need to be compensated for in the mixotrophic and the heterotrophic chrysophyte.

The presence of an active Entner-Doudoroff pathway has attracted considerable attention in *P. tricornutum* (Fabris et al., 2012). Similar to the oxidative pentose phosphate cycle (Figure 5.4) phosphogluconate is an important intermediate of the Entner-Doudoroff pathway. Yet, there is no formation of ribulose-5-phosphate, but pyruvate and glyceraldehyde phosphate are formed from the characteristic compound 2-keto-3-desoxy-6-phosphogluconate (KDPG). In chrysophytes, this pathway is probably not active, as we did not find the key enzymes of KDPG-synthesis (EC 4.2.1.12 and EC 4.1.2.14) in any of the chrysophytes investigated.

Opposing pathways like glycolysis and gluconeogenesis or oxidative and reductive pentose phosphate pathways do not lead to a net gain of energy or carbon if they operate in the same compartment at the same time. One way of regulation, which might possibly even result in different physiological phenotypes, is a differential intracellular distribution of pathways. Hence, ineffective carbon fixation in chrysophytes might probably not be a consequence of the absence of important enzymes but instead be related to different subcellular distribution of carbon fixation metabolism compared to other algae. Analyzing the genome of the diatom *P. tricornutum* has revealed an unusual intracellular distribution of enzymes compared to higher plants and non-photosynthetic eukaryotes (Kroth et al., 2008; Gruber et al., 2009). One of the remarkable findings in this context is that gene products involved in pathways of CO_2-Fixation and carbon intermediate degradation are located in all compartments of the unicellular organism. This also implies the presence of a complex and effective regulatory machinery controlling the intracellular carbon flux. The overall distribution of the enzymes also anticipates a high degree of shuttling of metabolic intermediates between the different compartments. Thus, demonstrating the functionality of required membrane transporters and shuttling systems is one of the scientific hot spots in completing the metabolic puzzle for *P. tricornutum*. Basically, carbon metabolic pathways were distributed within all cell compartments of the chrysophytes (Figure 5.6) showing many parallels to *P. tricornutum*. Interestingly, we did not find the carbon-fixing enzymes pyruvate carboxylase (EC 6.4.1.1) and phosphoenolpyruvate carboxylase (EC 4.1.1.31) with a mitochondrial localization prediction in any of the chrysophytes. If not biased by the incompleteness of the transcriptomes, this might be a major aspect concerning ineffectiveness of autotrophy in chrysophytes.

No favorable storage polysaccharide could be manifested from the transcriptomic datasets of the chrysophytes. Nevertheless, biosynthesis of the disaccharide trehalose may be performed by *P. lacustris* and *P. malhamensis* due to the presence of trehalose 6-phosphate synthase (EC 2.4.1.15) and the dephosphorylating trehalose 6-phosphatase (EC 3.1.3.12). Trehalose-6-phosphate synthase catalyzes the formation of trehalose-6-phosphate from UDP-glucose and glucose-6-phosphate. Trehalose is known as a storage compound in plants. Yet, putative trehalose cleaving enzymes were not found in the datasets of the chrysophytes suggesting that trehalose breakdown was either not performed at the time of cell harvest or that trehalose has a different function. This might be a heat- or freezing-protective function as has been postulated for other organisms (Goddijn and van Dun, 1999; Elbein et al., 2003).
Loricas of *D. divergens* and stalks of *P. malhamensis* are both build of polysaccharides, namely cellulose (Herth and Zugenmaier, 1979) and chitin (Herth et al., 1977). However, neither cellulose synthase (EC 2.4.1.12) nor chitin synthase (EC 2.4.1.16) were annotated. The lorica of *D. divergens* and the silica scale of *M. annulata* help to sustain their shape while cells of *P. malhamensis* and *P. lacustris* are rather deformable due to the lack of a stabilizing cell wall. Here, cell shape may be maintained by structural polysaccharides. Keratan sulfate is a structural carbohydrate found in bones and cartilage in humans and belonging to the highly hydrosylated glycosaminoglycans. It is a linear polymer that consists of repeating disaccharide units composed of galactose and N-acetylglucosamine. UDP-galactose-glycoprotein galactosyltransferase (EC 2.4.1.38) which is involved in chain extension during keratan sulfate biosynthesis was found for *P. lacustris* and *P. malhamensis*. This may hint at biosynthesis of keratan sulfate or other polysaccharides made of galactose and N-acetylglucosamine.

Poteriospumella lacustris is a non-photosynthetic *Spumella*-like flagellate. The clade of *Spumella*-like flagellates is polyphyletic, probably arising twice by the loss of photosynthesis as sister clades to the likewise secondary endocytobionts *Uroglena* and *Chrysolepidomonas* (Boenigk et al., 2005; Cavalier-Smith and Chao, 2006). Morphologic studies have proven the presence of leucoplast in *Spumella* sp. (Zwart and Darbyshire, 1992). We found putative glycolytic and decarboxylating gene products with plastidic destination for *P. lacustris*. This represents a first evidence for putative metabolically active enzymes in the colorless plastid of *Spumella*-like flagellates. Non-photosynthetic secondary endocytobionts are thought to keep their plastids despite of the loss of photosynthetic capabilities if the host cell depends on other plastid functions. In *Apicomplexa* reactions catalyzing isoprenoid biosynthesis proofed metabolic activity of the complex, non-photosynthetic plastids (Waller et al., 1998; Jomaa et al., 1999). Here, the intermediate isopentenylpyrophosphate can be synthesized by two metabolic pathways which might be active in parallel or independently. The genes coding for the respective enzymes of both pathways are encoded in the nuclear genome. Still, the pathways are usually localized in different cell compartments, namely the cytosol (mevelonate pathway) and the plastids of plants and algae (non-mevelonate pathway) (Lange et al., 2000; Grauvogel and Petersen, 2007). The non-mevelonate pathway was found to be active in the colorless plastid of *P. falciparum*, a malaria pathogen belonging to the *Apicomplexa* (Jomaa et al., 1999). In heterotrophic chrysophytes the role of the plastid seems to be a different one since we found putative enzymes of both pathways for the three photosynthetically active chrysophytes but only the cytosolic mevelonate pathway for the heterotroph *P. lacustris*. The localization and expression of glycolytic enzymes in the apicoplast has been shown for *Toxoplasma gondii*. It has been hypothized that the relocation of central glycolytic reactions into the apicoplast would lead to a net transfer of ATP and the reduction power from the cytosol to the apicoplast in order to perform fatty acid synthesis (Fleige et al., 2007; Lim and McFadden, 2010). To evaluate if similar implications might be true for *P. lacustris*, fatty acid metabolism needs to be studied in greater detail. A possible hint for an actual need of plastid encoded gene products during fatty acid biosynthesis might be that pathways of palmitic acid and myristic acid biosynthesis were the only pathways found to be completely nuclear encoded.

5.5.3. Intermediary and other pathways

The occurrence of photorespiration in chrysophytes has been demonstrated experimentally (Bhatti and Colman, 2011). In *P. tricornutum* the N-donor to produce glycine from glyoxylate during photorespiration is proposed to be serine by serine-glyoxylate transaminase (EC 2.6.1.45) (Kroth et al., 2008). This enzyme was not found for any of the chrysophytes. Thus, different from *P. tricornutum* glycine is probably produced via glutamate-glyoxylate aminotransferase (EC 2.6.1.4, Figure 5.3). Here, the regeneration of glutamate may be performed on the level of 2-oxoglutarate by a glutamate dehydrogenase (EC 1.4.1.2). Two molecules of glycine are converted to serine under decarboxylation and desamination by the glycine decarboxylase complex (EC 1.4.4.2, EC 2.1.2.10, EC 1.8.1.4). In *P. tricornutum*, the next step regarding the conversion of serine to 3-phospho-glycerate usually is a conversion of serine into hydroxypyruvate by serine- or alanine-aminotransferases (EC 2.6.1.51 or 2.6.1.45) (http://www.diatomcyc.org/DIATOM/new-image?type=PATHWAY&object=PWY-181) which both are absent in chrysophytes. No other transcript for hydroxypyruvate converting or forming enzymes was found in the dataset of the chrysophytes. In plants and also in *P. tricornutum*, hydroxypyruvate is usually converted into glycerate by hydroxypyruvate reductase (EC 1.1.1.81) and then 3-phosphoglycerate is produced via glycerate kinase. A putative glycerate kinase (EC 2.7.1.31) was present in the dataset of the heterotrophic chrysophyte alga only. Thus, the photorespiratory pathway probably ends with serine production or conversion into pyruvate and NH_3 takes place by serine dehydratase (EC 4.3.1.17 or 4.3.1.19). By conversion to acetyl-CoA, pyruvate may enter a variety of other pathways like e.g. the citrate cycle or fatty acid biosynthesis. It might as well be true, that serine is the main product and that photorespiration, thus, may link carbon to amino acid metabolism. Yet, the regeneration of 3-phospho-glycerate from 2-phosphoglycolate (Figure 5.3) is probably not possible in chrysophytes.

Interestingly, most enzymes hypothetically involved in photorespiration were also present in the heterotroph *P. lacustris*. Even the initial step is performed according to the annotation of phosphor glycolate phosphatase (EC 3.1.3.18). Activity of this enzyme has previously been found in heterotrophic organism without RuBisCO activity (Pellicer et al., 2003; Kim et al., 2004) as a response to 2-phosphoglycolate formation during oxidative stress. Currently, it remains unanswered if the photorespiratory chain serves a different purpose in the heterotroph chrysophyte than in the remaining chrysophytes. Photorespiration in higher plants and algae usually includes steps in the chloroplast, the peroxisome and the mitochondrion (Bauwe et al., 2010). Thus, the different intermediates need to be shuttled between the compartments. To proof photorespiration in chrysophytes subcellular localization of the enzymes and confirmation of the presence of the respective transporters are necessary next steps.

Phosphoketolase is one of the key enzymes during heterofermentative lactic acid formation. Lactic acid fermenting bacteria are lacking fructose-1,6-bisphosphat-aldolase (EC 4.1.2.13) and, thus, may use the phosphoketolase pathway in several variations to generate ATP and NADH from hexoses and pentoses (Fuchs and Schlegel, 2007). The reaction catalyzed by phosphoketolase (EC 4.1.2.9) produces glyceraldehydephosphate and acetyl-phosphate from pentose phosphate whereas fructose-6-phosphate phosphoketolase (EC 4.1.2.22) produces erythrose-4-phosphate and acetyl-phosphate from fructose-6-phosphate. Thus, the phosphoketolases reaction in *P. lacustris* may serve to generated important anaplereutic intermediates like glyceraldehyde phosphate, erythrose-4-phosphate or acetyl-phosphate but might as well serve the purpose of ATP generation from pentoses. Phosphoketolase is found among cyanobacteria but is no common enzyme in eukaryotes (Sanchez et al., 2010). Interestingly, a putative phosphoketolase pathway has just recently been discovered by *in silico* prediction of metabolic pathways in *P. tricornutum* (Fabris et al., 2012). Together with our findings this may demonstrate that the phosphoketolase pathways may be more common in heterokonts than in other eukaryotes.

The case of phosphoketolase also demonstrates that the JGI KEGG-database of *P. tricornutum* does not include all information available on metabolic pathways. Thus, our comparisons to other algae in the JGI database represent the best possible analysis based on the currently available resources but we cannot claim a 100 %-integrity.

Xanthophylls are pigments belonging to the carotenoids serving the purpose of non-photosynthetic quenching under light-stress conditions and thereby prevent cells from oxidative damage. Reduction and interconversion of xanthophylls is performed in the so called xanthophylls cycle. Phylogenetically, the xanthophylls cycle is abundant in the higher plants, green algae and “green secondary or tertiary endocytobiotic algae” i.e. those algae which arose by engulfing a green alga. The xanthophylls cycle has not yet been found in cyanobacteria and red algae (Takaichi, 2011). Violaxanthin de-epoxidase (EC 1.10.99.3), a violaxanthin reducing enzyme involved in the xanthophylls cycle, was annotated for the autotrophic as well as for the two mixotrophic chrysophytes. Chrysophytes are usually associated with the “red endocytobiotic linage” i.e. algae that arose by engulfing a red alga. Thus, the expression of violaxanthin de-epoxidase contradicts with evolutionary theories at first sight. Nevertheless, similar findings have been made for the diatom *P. tricornutum* (Lohr and Wilhelm, 2001) which also belongs to the red endocytobiotic linage. Horizontal gene transfer from green algae into the red secondary endocytobiotic linage is still heavily discussed throughout literature (Frommolt et al., 2008; Dorrell and Smith, 2011).

5.6. Conclusion

Until today, chrysophytes like *Ochromonas sp.* and *Dinobryon sp.* have attracted considerable attention due to their feature to benefit from autotrophic and heterotrophic nutrition. In the past decades mixotrophic chrysophytes have often been the target of research because they were found to increase in their contribution to phytoplankton biomass in parallel with declining nutrient concentrations in lakes (e.g. during re-oligotrophication) though such conditions are only favourable for few phototrophic species (Gaedke, 1998; Anneville and Pelletier, 2000; Kamjunke et al., 2007). Re-oligotrophication is a designated target of drinking water management and thus, understanding the physiology and ecology of chrysophytes is getting more and more important to understand their role in freshwater ecosystems. In fact, physiology and ecology of individual mixotrophic chrysophytes are fairly well understood. However, the gained knowledge has so far not led to a holistic understanding of this lifestyle. Due to their individually different sensitivity to numerous environmental factors, characteristic traits are not easily transferable between species by physiological approaches. All the more, looking at things from a different angle might be a crucial step to gain deeper insights into this lifestyle. Despite of the physiological varieties between *M. annulata*, *D. divergens* and *P. lacustris* (Chapter 4) their molecular metabolic carbon pathway apparatus is in large parts identical. This implies that the different nutritional phenotypes are rather developed by post-transcriptional or post-translational regulation of gene products or, as displayed on the basis of some examples in this study, by differential intracellular compartmentation of pathways. This hypothesis is also promoted by our findings regarding glycolytic isoenzymes sequences with plastidic destination in the heterotroph *P. lacustris*. Though this alga has lost its photosynthetic activity there appears to be some kind of relevance in preserving glycolytic activity in the reduced plastid. Here, future studies will need to deal with the verification of the *in silico* distribution predictions and with expression analysis under different nutritional conditions. Additionally, it might be helpful, to establish a model organism for molecular analysis because over-expression or silencing of genes may provide new insights into pathway regulation. The unicellular chrysophyte *P. malhamensis* might be a suitable candidate in this regard due to the detailed physiological information available, short doubling times and the ability to grow in bacteria-free cultures. The transcript datasets also provide information on gene products known to be regulated by external factors like for example the light-regulated fucoxanthin-chlorophyll-binding proteins or the cobalamin-dependent methionine synthase (EC 2.1.1.13). The promoter regions of this kind of inducible genes are utilized as molecular tools for other algae (Fernandez et al., 1989; Apt et al., 1996) and might as well be suitable for chrysophytes. Altogether, this work has laid the base for a profound study of expression data in different chrysophytes.

5.7. Acknowledgements

The authors thank Ansgar Gruber and Bernard Lepetit for helpful discussions and Dariia Bova for her assistance during listing and counting of KEGG annotated sequences.

Table 5.4A: Presence of enzymes putatively involved in glycolysis and gluconeogenesis for different stramenopiles. EC numbers are listed according to KEGG pathway map 00010 "Glycolysis/Gluconeogenesis". "x" marks that a putative enzyme was found, "-" marks that no putative enzyme was found. Data was retrieved from KEGG pathway mapping performed in this study for the four chrysophytes and from the JGI database for all other stramenopiles except for *Ectocarpus siliculosus* for which data originates from Cock et al. (2010) and BLAST (blastx) search against the NCBI database with query sequences from the chrysophytes (see also Supplementary Table S 5.3). Ma: *Mallomonas annulata*; Dd: *Dinobryon divergens*; Pm: *Poterioochromonas malhamensis*; Pl: *Poteriospumella lacustris*; Pt: *Phaeodactylum tricornutum*; Tp: *Thalassiosira pseudonana*; Sl: *Saccharina latissima*; Es: *Ectocarpus siliculosus* Ps*: Phytophthora spp.*; Aa: *Aureococcus anophagefferens*.

EC number	Name	Ma	Dd	Pm	Pl	Pt	Tp	Sl	Es	Ps	Aa
1.1.1.1	alcohol dehydrogenase	-	-	x	x	x	x	-	-	x	x
1.1.1.2	alcohol dehydrogenase (NADP+)	-	-	-	-	x	x	x	-	x	x
1.1.1.27	L-lactate dehydrogenase	-	-	-	-	-	-	-	-	-	-
1.1.2.7	methanol dehydrogenase (cytochrome c)	-	-	-	-	-	-	-	-	-	-
1.1.2.8	alcohol dehydrogenase	-	-	-	-	-	-	-	-	-	-
1.2.1.12	glyceraldehyde-3-phosphate dehydrogenase	x	x	x	x	x	x	x	x	x	x
1.2.1.3	aldehyde dehydrogenase (NAD+)	-	x	x	x	x	x	-	-	x	x
1.2.1.5	aldehyde dehydrogenase (NAD(P)+)	x	x	x	x	x	-	-	-	x	x
1.2.1.59	glyceraldehyde-3-phosphate dehydrogenase (NAD(P)+)	-	-	x	x	-	-	x	x	-	-
1.2.1.9	glyceraldehyde-3-phosphate dehydrogenase (NADP+)	x	x	x	x	x	-	-	x	x	x
1.2.4.1	pyruvate dehydrogenase (acetyl-transferring)	x	x	x	x	x	x	-	x	x	x
1.2.7.1	pyruvate synthase	-	-	-	-	-	-	-	-	-	-
1.2.7.5	aldehyde ferredoxin oxidoreductase	-	-	-	-	-	-	-	-	-	-
1.2.7.6	glyceraldehyde-3-phosphate dehydrogenase	-	-	-	-	-	-	-	-	-	-
1.8.1.4	dihydrolipoyl dehydrogenase	x	x	x	x	x	x	x	x	x	x
2.3.1.12	dihydrolipoyllysine-residue acetyltransferase	x	x	x	x	x	x	-	x	x	x
2.7.1.1	hexokinase	-	-	-	-	-	-	-	-	-	-
2.7.1.11	6-phosphofructokinase	x	x	x	x	x	x	x	x	-	-
2.7.1.146	ADP-specific phosphofructokinase	-	-	-	-	-	-	-	-	-	-
2.7.1.147	ADP-specific glucokinase	-	-	-	-	-	-	-	-	-	-
2.7.1.2	glucokinase	x	x	x	x	x	x	-	x	x	x
2.7.1.40	pyruvate kinase	x	x	x	x	x	x	x	x	x	x
2.7.1.41	glucose-1-phosphate phosphodismutase	-	-	-	-	-	-	-	-	-	-
2.7.1.63	polyphosphate-glucose phosphotransferase	-	-	-	-	-	-	-	-	-	-
2.7.1.69	protein-phosphohistidine-sugar phosphotransferase	-	-	-	-	-	-	-	-	-	-
2.7.2.3	phosphoglycerate kinase	x	x	x	x	x	x	x	x	x	x
3.1.3.10	glucose-1-phosphatase	-	-	-	-	-	-	-	-	-	-
3.1.3.11	fructose-bisphosphatase	x	x	x	x	x	x	x	x	x	x
3.1.3.13	bisphosphoglycerate phosphatase	-	-	-	-	-	-	-	-	-	-
3.1.3.9	glucose-6-phosphatase	-	-	-	-	-	-	-	-	-	-
3.2.1.86	6-phospho-beta-glucosidase	-	-	-	-	-	-	-	-	-	-
4.1.1.1	pyruvate decarboxylase	-	-	-	-	-	x	-	-	-	-
4.1.1.32	phosphoenolpyruvate carboxykinase (GTP)	-	-	-	-	-	-	-	-	-	-
4.1.1.49	phosphoenolpyruvate carboxykinase (ATP)	-	x	x	x	x	x	x	-	x	x
4.1.2.13	fructose-bisphosphate aldolase	x	x	x	x	x	x	x	x	x	x
4.2.1.11	phosphopyruvate hydratase	x	x	x	x	x	x	x	x	x	x
5.1.3.15	glucose-6-phosphate 1-epimerase	-	-	-	-	-	-	-	-	-	-
5.1.3.3	aldose 1-epimerase	-	-	-	-	-	x	-	-	x	x
5.3.1.1	triose-phosphate isomerase	x	x	x	x	x	x	x	x	x	x
5.3.1.9	glucose-6-phosphate isomerase	x	x	x	x	x	x	x	x	x	x
5.4.2.1	phosphoglycerate mutase	x	x	-	x	x	x	x	x	x	x
5.4.2.2	phosphoglucomutase	x	x	x	x	x	x	-	x	x	x
5.4.2.4	bisphosphoglycerate mutase	-	-	-	-	-	-	-	-	-	-
6.2.1.1	acetate-CoA ligase	x	-	-	x	x	x	-	x	x	x
6.2.1.13	acetate-CoA ligase (ADP-forming)	-	-	-	-	-	-	-	-	-	-
		auto	mixo		hetero						
		Chrysophytes				Diatoms		Brown algae		Oomycetes	Pelagophytes

Table 5.4B: Presence of enzymes putatively involved in pentose phosphate pathways for different stramenopiles. EC numbers are listed according to KEGG pathway map 00030 “Pentose phosphate pathway”. “x” marks that a putative enzyme was found, “-“ marks that no putative enzyme was found. Data was retrieved from KEGG pathway mapping performed in this study for the Chrysophytes and from the JGI database for all other stramenopiles except for *Ectocarpus siliculosus* for which data originates from Cock et al. (2010) and BLAST (blastx) search against the NCBI database with query sequences from the Chrysophytes (see also Supplementary Table S 5.3). Ma: *Mallomonas annulata*; Dd: *Dinobryon divergens*; Pm: *Poterioochromonas malhamensis*; Pl: *Poteriospumella lacustris*; Pt: *Phaeodactylum tricornutum*; Tp: *Thalassiosira pseudonana*; Es: *Ectocarpus siliculosus*; Sl: *Saccharina latissima*; Ps: *Phytophthora* spp.; Aa: *Aureococcus anophagefferens*.

EC number	Name	Ma	Dd	Pm	Pl	Pt	Tp	Es	Sl	Ps	Aa
1.1.1.215	gluconate 2-dehydrogenase	-	-	-	-	x	-	-	-	-	x
1.1.1.43	phosphogluconate 2-dehydrogenase	-	-	-	-	-	-	-	-	-	-
1.1.1.44	phosphogluconate dehydrogenase (decarb.)	x	-	-	-	x	x	x	-	x	x
1.1.1.47	glucose 1-dehydrogenase	-	-	-	-	-	-	-	-	-	-
1.1.1.49	glucose-6-phosphate dehydrogenase	x	-	-	-	x	x	x	x	x	x
1.1.3.4	glucose oxidase	-	-	-	-	-	-	-	-	-	-
1.1.3.5	hexose oxidase	-	-	-	-	-	-	-	-	-	-
1.1.5.2	quinoprotein glucose dehydrogenase	-	-	-	-	-	-	-	-	-	-
1.1.99.10	glucose dehydrogenase (acceptor)	-	-	-	-	-	-	-	-	-	-
1.1.99.3	gluconate 2-dehydrogenase (acceptor)	-	-	-	-	-	-	-	-	-	-
1.2.7.5	aldehyde ferredoxin oxidoreductase	-	-	-	-	-	-	-	-	-	-
2.2.1.1	transketolase	x	x	x	x	x	x	x	x	x	x
2.2.1.2	transaldolase	x	-	-	x	x	x	x	-	x	x
2.7.1.11	6-phosphofructokinase	x	x	x	x	x	x	x	x	-	-
2.7.1.12	gluconokinase	-	-	-	-	x	-	-	-	x	-
2.7.1.13	dehydrogluconokinase	-	-	-	-	-	-	-	-	-	-
2.7.1.146	ADP-specific phosphofructokinase	-	-	-	-	-	-	-	-	-	-
2.7.1.15	ribokinase	x	x	-	x	x	x	x	-	x	x
2.7.1.165	glycerate 2-kinase	-	-	-	-	-	-	-	-	-	-
2.7.1.45	2-dehydro-3-deoxygluconokinase	-	-	-	-	-	-	-	-	-	-
2.7.4.23	ribose 1,5-bisphosphate phosphokinase	-	-	-	-	-	-	-	-	-	-
2.7.6.1	ribose-phosphate diphosphokinase	x	x	x	x	x	x	x	-	x	x
3.1.1.17	gluconolactonase	-	-	-	x	x	-	x	-	x	-
3.1.1.31	6-phosphogluconolactonase	x	-	-	-	x	x	x	-	x	-
3.1.3.11	fructose-bisphosphatase	x	x	x	x	x	x	x	x	x	x
4.1.2.-		-	-	-	-	x	x	-	-	x	x
4.1.2.13	fructose-bisphosphate aldolase	x	x	x	x	x	x	x	x	x	x
4.1.2.14	2-dehydro-3-deoxy-phosphogluconate aldolase	-	-	-	-	x	-	-	-	-	-
4.1.2.4	deoxyribose-phosphate aldolase	-	-	x	x	-	-	-	-	x	-
4.1.2.43	3-hexulose-6-phosphate synthase	-	-	-	-	-	-	-	-	-	-
4.1.2.9	phosphoketolase	-	-	-	x	-	-	-	-	-	-
4.2.1.12	phosphogluconate dehydratase	-	-	-	-	x	-	-	-	-	-
4.2.1.39	gluconate dehydratase	-	-	-	-	-	-	-	-	-	-
4.3.1.9	glucosaminate ammonia-lyase	-	-	-	-	-	-	-	-	-	-
5.1.3.1	ribulose-phosphate 3-epimerase	x	x	x	x	x	x	x	x	x	x
5.3.1.27	6-phospho-3-hexuloisomerase	-	-	-	-	-	-	-	-	-	-
5.3.1.6	ribose-5-phosphate isomerase	x	x	x	x	x	x	x	-	x	x
5.3.1.9	glucose-6-phosphate isomerase	x	x	x	x	x	x	x	x	x	x
5.4.2.2	phosphoglucomutase	x	x	x	x	x	x	x	-	x	x
5.4.2.7	phosphopentomutase	-	-	-	-	-	-	-	-	-	-
		auto	mixo	mixo	hetero						
		Chrysophytes				Diatoms		Brown algae		Oomycetes	Pelagophytes

Table 5.4C: Presence of enzymes putatively involved in carbon fixation for different stramenopiles. EC numbers are listed according to KEGG pathway map 00710 “Carbon fixation in photosynthetic organisms”. “x” marks that a putative enzyme was found, “-“ marks that no putative enzyme was found. Data was retrieved from KEGG pathway mapping performed in this study for the Chrysophytes and from the JGI database for all other stramenopiles except for *Ectocarpus siliculosus* for which data originates from Cock et al. (2010) and BLAST (blastx) search against the NCBI database with query sequences from the Chrysophytes (see also Supplementary Table S 5.3). Ma: *Mallomonas annulata*; Dd: *Dinobryon divergens*; Pm: *Poterioochromonas malhamensis*; Pl: *Poteriospumella lacustris*; Pt: *Phaeodactylum tricornutum*; Tp: *Thalassiosira pseudonana*; Es: *Ectocarpus siliculosus*; Sl: *Saccharina latissima*; Ps: *Phytophthora* spp.; Aa: *Aureococcus anophagefferens*.

EC number	Name	Ma	Dd	Pm	Pl	Pt	Tp	Sl	Es	Ps	Aa
1.1.1.37	malate dehydrogenase	x	x	x	x	x	x	-	x	x	x
1.1.1.39	malate dehydrogenase (decarb.)	-	-	-	-	x	x	-	x	x	x
1.1.1.40	malate dehydrogenase (oxaloacetate-decarb.)	x	-	x	-	x	-	-	x	x	x
1.1.1.82	malate dehydrogenase (NADP+)	-	-	-	-	-	-	-	-	-	-
1.2.1.13	glyceraldehyde-3-phosphate dehydrogenase (NADP+)	-	-	-	x	x	-	-	-	x	-
1.2.1.59	glyceraldehyde-3-phosphate dehydrogenase (NAD(P)+)	-	-	x	x	-	-	x	x	-	-
2.2.1.1	transketolase	x	x	x	x	x	x	x	x	x	x
2.6.1.1	aspartate transaminase	x	-	x	-	x	x	x	x	x	x
2.6.1.2	alanine transaminase	x	x	x	x	x	x	x	x	x	x
2.7.1.14	sedoheptulokinase	-	-	-	-	-	-	-	-	-	-
2.7.1.19	phosphoribulokinase	x	x	x	-	x	x	x	x	-	-
2.7.1.40	pyruvate kinase; phosphoenolpyruvate kinase	x	x	x	x	x	x	x	x	x	x
2.7.2.3	phosphoglycerate kinase	x	x	x	x	x	x	x	x	x	x
2.7.9.1	pyruvate, phosphate dikinase	-	-	-	-	x	x	-	-	x	-
3.1.3.11	fructose-bisphosphatase	x	x	x	x	x	x	x	x	x	x
3.1.3.37	sedoheptulose-bisphosphatase	x	x	x	-	x	x	x	-	-	-
4.1.1.31	phosphoenolpyruvate carboxylase	x	x	x	x	x	x	-	x	-	x
4.1.1.39	ribulose-bisphosphate carboxylase	x	x	x	-	-	-	x	x	-	-
4.1.1.49	phosphoenolpyruvate carboxykinase (ATP)	-	x	x	x	x	x	x	x	x	x
4.1.2.13	fructose-bisphosphate aldolase	x	x	x	x	x	x	x	x	x	x
4.1.2.22	fructose-6-phosphate phosphoketolase	-	-	-	x	-	-	-	-	-	-
4.1.2.9	phosphoketolase	-	-	-	x	-	-	-	-	-	-
5.1.3.1	ribulose-phosphate 3-epimerase	x	x	x	x	x	x	x	x	x	x
5.3.1.1	triose-phosphate isomerase	x	x	x	-	x	x	x	x	x	x
5.3.1.6	ribose-5-phosphate isomerase	x	x	x	x	x	x	-	x	x	x
		auto	mixo		hetero						
		Chrysophytes				Diatoms		Brown algae		Oomycetes	Pelagophytes

5.8. Supplementary

Table S 5.1: Most common transcripts found in the datasets of the chrysophytes. Grey shaded contigs met annotation requirements.

Most common transcripts *Mallomonas annulata*

total reads	contig	sequence describtion
605	M_ann_c27	no hit
420	M_ann_c699	abc transporter family
276	M_ann_c3013	ribosomal protein l2
274	M_ann_c325	hypothetical protein
267	M_ann_c333	elongation factor
261	M_ann_c1328	no hit
260	M_ann_c200	no hit
255	M_ann_c299	bnr asp box repeat protein
244	M_ann_c808	no hit
283	M_ann_c283	cation proton exchanger
231	M_ann_c531	no hit
225	M_ann_c577	hypothetical protein
224	M_ann_c444	glycosyl transferase
220	M_ann_c537	zinc finger protein
217	M_ann_c287	zinc finger protein
206	M_ann_c231	no hit
202	M_ann_c37	vacular atp synthase subunit
202	M_ann_c1513	ferredoxin dependent bilin reductase
198	M_ann_c295	glycosyl hydrolase
198	M_ann_c443	phosphoglycolate phosphatase (a?)

Most common transcripts *Dinobryon divergens*

total reads	contig	sequence describtion
584	D_div_c2607	no hit
488	D_div_c1646	no hit
429	D_div_c1991	possible vacuolar protein
426	D_div_c362	no hit
425	D_div_c1256	ribosomal protein S1
405	D_div_c162	hypothetical protein
398	D_div_c3871	no hit
394	D_div_c570	rna-intron encoded homing endonuclease
317	D_div_c1358	no hit
310	D_div_c702	SyrP-like protein
300	D_div_c644	protein kinase
287	D_div_c7814	hypothetical protein
282	D_div_c544	serine threonine protein kinase
280	D_div_c3241	no hit
280	D_div_c1533	no hit
278	D_div_c5772	no hit
277	D_div_c2024	hypothetical ctc00065-like protein
266	D_div_c1245	no hit
258	D_div_c11735	no hit
254	D_div_c799	hypothetical protein

Most common transcripts *Poterioochromonas malhamensis*

total reads	contig	sequence describtion
366	P_mal_c2189	phospholipase b like protein
316	P_mal_c4051	3-hydoxyisobutyryl-coenzyme a hydrolase
309	P_mal_c2350	probable rubisco-expression enzyme
298	P_mal_c269	hypothetical protein
287	P_mal_c3553	hsp88-like protein
273	P_mal_c583	rrna-intron encoded homing nuclease
260	P_mal_c7757	hypothetical protein
249	P_mal_c2813	pg1 homology to homo sapiens
239	P_mal_c5523	fatty acid elongase
233	P_mal_c7297	trehalose-6-phosphate-synthase
228	P_mal_lrc29612	no hit
227	P_mal_c3235	s-adenosyl homocysteine hydrolase
222	P_mal_c21133	hypothetical protein
216	P_mal_c14360	dna-heat shock n-terminal domain-containing protein
211	P_mal_c1555	conserved domain protein
208	P_mal_c1737	calreticulin
200	P_mal_c3111	no hit
199	P_mal_c3954	hypothetical protein
198	P_mal_c281	peptidase s1 and chymotrypsin hap
197	P_mal_c6832	hypothetical protein

Most common transcripts *Poteriospumella lacustris*

total reads	contig	sequence describtion
2360	S_JBM_c50	calmodulin
2282	S_JBM_c48	40s ribosomal protein s10
2047	S_JBM_c114	60s ribosomal protein l10
2008	S_JBM_c37	60s ribosomal protein l26
1903	S_JBM_c35	ribosomal protein s20
1827	S_JBM_c80	40s ribosomal protein s15
1793	S_JBM_lrc513	ribosomal/ubiquitin fusion protein
1641	S_JBM_c94	40s ribosomal protein s7
1617	S_JBM_c22	hypothetical, ribosome
1453	S_JBM_c44	60s ribosomal protein l11
1317	S_JBM_c126	ribosomal protein l27
1279	S_JBM_lrc570	60s ribosomal l14
1273	S_JBM_lrc518	ribosome
1268	S_JBM_lrc516	40s ribosomal protein s19
1243	S_JBM_c27	protein, ribosome
1187	S_JBM_c32	ribosomal protein s28
1163	S_JBM_lrc517	ribosome
1146	S_JBM_c177	60s ribosomal protein l10-3
1094	S_JBM_c79	40s ribosomal proetin s16
1070	S_JBM_lrc514	ribosomal ubiquitin fusion protein

Table S 5.2: Number of putative enzyme categories assigned to the different KEGG pathways. Coloring applies to the amount of putative enzymes within one pathway. Dark green: most entries; light green: 2nd most entries; yellow: 3rd most entries; red: least entries. First the chrysophyte with the most and the least number of enzymes within a pathway were determined, followed by 2nd and 3rd place ranking. Coloring of *P. tricornutum* entries was performed last, classifying the range compared to the chrysophytes. Mal: *Mallomonas annulata*, Din: *Dinobryon divergens*, Pot: *Poterioochromonas malhamensis*, Spu: *Poteriospumella lacustris*, Pha: *Phaeodactylum tricornutum*. KEGG-annotations for *P. tricornutum* were retrieved from the JGI database.

Pathway	Mal	Din	Pot	Spu	Pha
Carbohydrate metabolism	**161**	**140**	**152**	**169**	**205**
Amino sugar and nucleotide sugar metabolism	18	19	16	18	25
Ascorbate and aldarate metabolism	3	5	6	4	10
Butanoate metabolism	11	8	8	11	16
C5-Branched dibasic acid metabolism	2	1	1	1	2
Citrate cycle (TCA cycle)	17	14	15	17	16
Fructose and mannose metabolism	10	11	11	12	16
Galactose metabolism	7	7	8	6	6
Glycolysis / Gluconeogenesis	18	19	20	23	20
Glyoxylate and dicarboxylate metabolism	10	7	10	11	12
Inositol phosphate metabolism	12	5	6	8	13
Pentose and glucuronate interconversions	5	5	5	4	7
Pentose phosphate pathway	14	11	12	15	17
Propanoate metabolism	12	9	10	15	15
Pyruvate metabolism	15	12	16	15	21
Starch and sucrose metabolism	7	7	8	9	9
Energy metabolism	**81**	**69**	**71**	**78**	**71**
Carbon fixation in photosynthetic organisms	16	15	18	16	19
Carbon fixation pathways in prokaryotes	18	12	15	18	8
Methane metabolism	19	18	16	21	5
Nitrogen metabolism	11	9	8	10	18
Oxidative phosphorylation	8	8	7	8	8
Photosynthesis	2	2	2	1	3
Sulfur metabolism	7	5	5	4	9
Photosynthesis -antenna proteins					1
Lipid metabolism	**65**	**66**	**56**	**68**	**127**
alpha-Linolenic acid metabolism	3	3	1	3	7
Arachidonic acid metabolism	4	4	3	3	7
Biosynthesis of unsaturated fatty acids	4	5	3	4	11
Cutin, suberine and wax biosynthesis	1	1	1	1	
Fatty acid biosynthesis	7	7	6	6	7
Fatty acid elongation	3	5	4	4	5
Fatty acid metabolism	5	5	6	8	12
Glycerolipid metabolism	7	9	8	10	15
Glycerophospholipid metabolism	9	5	7	8	18
Primary bile acid biosynthesis		1	1	1	2
Sphingolipid metabolism	8	6	7	6	12
Steroid biosynthesis	5	4	5	4	13
Steroid hormone biosynthesis	3	5	2	3	1
Synthesis and degradation of ketone bodies	4	3	2	5	4
Ether lipid metabolism	1	2		1	9
Linoleic acid metabolism	1	1		1	2
Secondary bile acid biosynthesis					2
Nucleotide metabolism	**63**	**55**	**52**	**60**	**82**
Purine metabolism	40	36	33	38	40
Pyrimidine metabolism	23	19	19	22	42
Amino acid metabolism	**155**	**127**	**141**	**135**	**220**
Alanine, aspartate and glutamate metabolism	17	11	12	13	22
Arginine and proline metabolism	22	20	21	20	30
Cysteine and methionine metabolism	20	16	17	18	21
Glycine, serine and threonine metabolism	21	15	15	17	25
Histidine metabolism	7	8	7	8	11
Lysine biosynthesis	7	5	7	4	10
Lysine degradation	5	6	7	8	13
Phenylalanine metabolism	5	4	7	6	9
Phenylalanine, tyrosine and tryptophan biosynthesis	16	10	13	7	17
Tryptophan metabolism	8	5	7	9	16
Tyrosine metabolism	6	5	9	6	16
Valine, leucine and isoleucine biosynthesis	9	7	7	2	12
Valine, leucine and isoleucine degradation	12	15	12	17	18

Pathway	Mal	Din	Pot	Spu		Pha
Other biosynthetic pathways	**336**	**286**	**298**	**280**		**340**
Biosynthesis of alkaloids derived from histidine and purine	49	41	42	42		46
Biosynthesis of alkaloids derived from ornithine, lysine and nicotinic acid	39	35	39	37		44
Biosynthesis of alkaloids derived from shikimate pathway	42	34	37	36		41
Biosynthesis of alkaloids derived from terpenoid and polyketide	40	37	37	34		40
Biosynthesis of phenylpropanoids	46	36	39	39		48
Biosynthesis of plant hormones	76	64	64	58		74
Biosynthesis of terpenoids and steroids	44	39	40	34		47
Metabolism of other aminoacids	**30**	**30**	**33**	**39**		**50**
beta-Alanine metabolism	6	9	8	9		10
Cyanoamino acid metabolism	3	2	2	4		6
Glutathione metabolism	9	9	11	15		17
Selenocompound metabolism	6	6	7	7		9
Taurine and hypotaurine metabolism	3	4	3	2		3
D-Arginine and D-ornithine metabolism	1			1		1
D-Glutamine and D-glutamate metabolism	2		1	1		
Phosphonate and phosphinate metabolism			1			3
D-Alanine metabolism						1
Glycan biosynthesis and metabolism	**18**	**23**	**23**	**25**		**52**
Glycosaminoglycan degradation	1	2	2	2		3
Glycosphingolipid biosynthesis - ganglio series	1	2	2	2		3
Glycosphingolipid biosynthesis - globo series	1	3	2	2		2
N-Glycan biosynthesis	6	5	5	5		12
Other glycan degradation	3	4	5	6		5
Other types of O-glycan biosynthesis	1	1	1	1		1
Peptidoglycan biosynthesis	1	1	1	1		2
Various types of N-glycan biosynthesis	3	3	3	3		1
Glycosaminoglycan biosynthesis - keratan sulfate			1	1		3
Glycosylphosphatidylinositol(GPI)-anchor biosynthesis	1	1		1		5
Glycosphingolipid biosynthesis - lacto and neolacto series		1		1		3
Lipopolysaccharide biosynthesis			1			7
Glycosaminoglycan biosynthesis-chondroitin sulfate biosynthesis						1
Glycosaminoglycan biosynthesis-heparan sulfate biosynthesis						2
Mucin type O-Glycan biosynthesis						2
Metabolism of cofactors and vitamins	**71**	**58**	**53**	**62**		**103**
Folate biosynthesis	6	5	6	7		9
Lipoic acid metabolism	1	1	1	1		
Nicotinate and nicotinamide metabolism	6	5	5	7		12
One carbon pool by folate	11	9	11	13		11
Pantothenate and CoA biosynthesis	10	9	7	6		11
Porphyrin and chlorophyll metabolism	18	17	12	10		24
Riboflavin metabolism	7	5	5	6		8
Thiamine metabolism	4	3	3	4		4
Ubiquinone and other terpenoid-quinone biosynthesis	2	1	1	2		7
Vitamin B6 metabolism	4	2	1	3		6
Biotin metabolism	1	1		2		5
Retinol metabolism	1		1	1		6
Metabolism of terpenoids and polyketids	**25**	**26**	**23**	**20**		**52**
Biosynthesis of ansamycins	1	1	1	1		1
Biosynthesis of vancomycin group antibiotics	1	1	1	1		1
Geraniol degradation	2	4	2	4		4
Limonene and pinene degradation	1	2	2	2		7
Polyketide sugar unit biosynthesis	3	3	3	3		1
Terpenoid backbone biosynthesis	14	13	12	8		13
Tetracycline biosynthesis	1	1	1	1		
Carotenoid biosynthesis	2	1	1			8
Biosynthesis of siderophore group nonribosomal proteins						3
Biosynthesis of type II polyketide backbone						3
Biosynthesis of type II polyketide products						1
Brassinosteroid biosynthesis						2
Diterpenoid biosynthesis						4
Insect hormone biosynthesis						3
Zeatin biosynthesis						1

Pathway	Mal	Din	Pot	Spu		Pha
Biosynthesis of other secondary metabolites	**22**	**14**	**18**	**21**		**50**
beta-Lactam resistance	1	1	1	1		
Butirosin and neomycin biosynthesis	1	1	1	1		
Glucosinolate biosynthesis	1	1	1	1		4
Isoquinoline alkaloid biosynthesis	2	1	2	2		6
Penicillin and cephalosporin biosynthesis	1	1	1	2		1
Phenylpropanoid biosynthesis	1	1	1	3		4
Streptomycin biosynthesis	7	5	6	6		5
Tropane, piperidine and pyridine alkaloid biosynthesis	3	2	3	3		3
Caffeine metabolism	1					1
Flavonoid biosynthesis	1					6
Novobiocin biosynthesis	1		1	1		3
Betalain biosynthesis	1	1				3
Indole alkaloid biosynthesis	1		1	1		
Anthocyanin biosynthesis						3
Benzoxazinoid biosynthesis						3
Flavone and flavonol biosynthesis						1
Isoflavonoid biosynthesis						1
Puromycin biosynthesis						2
Stilbenoid, diarylheptanoid and gingerol synthesis						4
Xenobiotics biodegradation and metabolism	**23**	**26**	**35**	**34**		**64**
Aminobenzoate degradation	5	3	5	4		2
Benzoate degradation	3	2	3	5		3
Caprolactam degradation	1	2	3	2		6
Drug metabolism - cytochrome P450	2	2	4	4		3
Drug metabolism - other enzymes	7	7	7	8		9
Metabolism of xenobiotics by cytochrome P450	2	2	4	3		4
Toluene degradation	1	2	3	2		1
Chloroalkane and chloroalkene degradation		2	2	3		2
Chlorocyclohexane and chlorobenzene degradation		1	1			6
Styrene degradation		1	1	1		2
Naphthalene degradation			1	1		6
Ethylbenzene degradation	1	1		1		3
Atrazine degradation	1	1	1			2
Bisphenol degradation						3
Fluorobenzoate degradation						1
DDT degradation						3
Polycyclic Aromatic Hydrocarbon degradation						7
Nitrotoluene degradation						1
Translation	**19**	**19**	**16**	**20**		**22**
Aminoacyl-tRNA biosynthesis	19	19	16	20		22
Signal transduction	**12**	**4**	**5**	**6**		**0**
mTOR signaling pathway	2	2	2	2		
Phosphatidylinositol signaling system	10	2	3	4		
Other	**1**	**1**	**2**	**2**		**0**
T cell receptor signaling pathway	1	1	1	2		

Table S 5.3: Protein sequence identification numbers and EC numbers of *Ectocarpus siliculosus*. The sequences were retrieved from blastx search (NCBI database) with chrysophyte queries assigned to the KEGG pathway maps of glycolysis/gluconeogenesis (map: 00010), pentose phosphate pathway (map: 00030) and carbon fixation in photosynthetic organisms (map: 00710). Data is, if available, compared to results of Cock et al. (2010).

Map: 00010 Glycolysis / Gluconeogenesis

EC number	Name	Protein sequence GI numbers (found by blastx; NCBI database)	Cock et al.
1.1.1.1	alcohol dehydrogenase	not found	not listed
1.1.1.2	alcohol dehydrogenase (NADP+)	298708975	not listed
1.1.1.27	L-lactate dehydrogenase	not found	not listed
1.1.2.7	methanol dehydrogenase (cytochrome c)	not analyzed	not listed
1.1.2.8	alcohol dehydrogenase	not analyzed	not listed
1.2.1.12	glyceraldehyde-3-phosphate dehydrogenase	298709303	not listed
1.2.1.3	aldehyde dehydrogenase (NAD+)	299469994	not listed
1.2.1.5	aldehyde dehydrogenase (NAD(P)+)	298710684	not listed
1.2.1.59	glyceraldehyde-3-phosphate dehydrogenase (NAD(P)+)	not found	not listed
1.2.1.9	glyceraldehyde-3-phosphate dehydrogenase (NADP+)	298709303	not listed
1.2.4.1	pyruvate dehydrogenase (acetyl-transferring)	299471547; 298705611	not listed
1.2.7.1	pyruvate synthase	not analyzed	not listed
1.2.7.5	aldehyde ferredoxin oxidoreductase	not analyzed	not listed
1.2.7.6	glyceraldehyde-3-phosphate dehydrogenase	not analyzed	not listed
1.8.1.4	dihydrolipoyl dehydrogenase	299472082; 299469809	not listed
2.3.1.12	dihydrolipoyllysine-residue acetyltransferase	298707059	not listed
2.7.1.1	hexokinase	not analyzed	not listed
2.7.1.11	6-phosphofructokinase	298708853; 298710116; 298712394; 298712393	not listed
2.7.1.146	ADP-specific phosphofructokinase	not analyzed	not listed
2.7.1.147	ADP-specific glucokinase	not analyzed	not listed
2.7.1.2	glucokinase	299469720	not listed
2.7.1.40	pyruvate kinase	298711450; 299117170; 298708122; 299472727	not listed
2.7.1.41	glucose-1-phosphate phosphodismutase	not analyzed	not listed
2.7.1.63	polyphosphate-glucose phosphotransferase	not analyzed	not listed
2.7.1.69	protein-Npi-phosphohistidine-sugar phosphotransferase	not analyzed	not listed
2.7.2.3	phosphoglycerate kinase	299115459; 299117084; 298710726; 299470729	5
3.1.3.10	glucose-1-phosphatase	not analyzed	not listed
3.1.3.11	fructose-bisphosphatase	298706472; 299116438	not listed
3.1.3.13	bisphosphoglycerate phosphatase	not analyzed	not listed
3.1.3.9	glucose-6-phosphatase	not analyzed	not listed
3.2.1.86	6-phospho-beta-glucosidase	not analyzed	not listed
4.1.1.1	pyruvate decarboxylase	not analyzed	not listed
4.1.1.32	phosphoenolpyruvate carboxykinase (GTP)	not analyzed	not listed
4.1.1.49	phosphoenolpyruvate carboxykinase (ATP)	298711537	1
4.1.2.13	fructose-bisphosphate aldolase	298707862; 298714707	3
4.2.1.11	phosphopyruvate hydratase	299470119; 298711447	not listed
5.1.3.15	glucose-6-phosphate 1-epimerase	not analyzed	not listed
5.1.3.3	aldose 1-epimerase	not analyzed	not listed
5.3.1.1	triose-phosphate isomerase	298712036; 298707924	3
5.3.1.9	glucose-6-phosphate isomerase	299116873	not listed
5.4.2.1	phosphoglycerate mutase	299471829	not listed
5.4.2.2	phosphoglucomutase	299472461	not listed
5.4.2.4	bisphosphoglycerate mutase	not analyzed	not listed
6.2.1.1	acetate-CoA ligase	299470777	not listed
6.2.1.13	acetate-CoA ligase (ADP-forming)	not analyzed	not listed

Map: 00030 Pentose phosphate pathway

EC number	Name	Protein sequence GI numbers (found by blastx; NCBI database)	Cock et al
1.1.1.215	gluconate 2-dehydrogenase	not analyzed	not listed
1.1.1.43	phosphogluconate 2-dehydrogenase	not analyzed	not listed
1.1.1.44	phosphogluconate dehydrogenase (decarboxylating)	298707464; 298708231; 299471868; 298706774	not listed
1.1.1.47	glucose 1-dehydrogenase	not analyzed	not listed
1.1.1.49	glucose-6-phosphate dehydrogenase	298706775	not listed
1.1.3.4	glucose oxidase	not analyzed	not listed
1.1.3.5	hexose oxidase	not analyzed	not listed
1.1.5.2	quinoprotein glucose dehydrogenase	not analyzed	not listed
1.1.99.10	glucose dehydrogenase (acceptor)	not analyzed	not listed
1.1.99.3	gluconate 2-dehydrogenase (acceptor)	not analyzed	not listed
1.2.7.5	aldehyde ferredoxin oxidoreductase	not analyzed	not listed
2.2.1.1	transketolase	298708424; 299471379	2
2.2.1.2	transaldolase	298710454	not listed
2.7.1.11	6-phosphofructokinase	not found	not listed
2.7.1.12	gluconokinase	not analyzed	not listed
2.7.1.13	dehydrogluconokinase	not analyzed	not listed
2.7.1.146	ADP-specific phosphofructokinase	not analyzed	not listed
2.7.1.15	ribokinase	298707688	not listed
2.7.1.165	glycerate 2-kinase	not analyzed	not listed
2.7.1.45	2-dehydro-3-deoxygluconokinase	not analyzed	not listed
2.7.4.23	ribose 1,5-bisphosphate phosphokinase	not analyzed	not listed
2.7.6.1	ribose-phosphate diphosphokinase	298709576; 298712313	not listed
3.1.1.17	gluconolactonase	299472163	not listed
3.1.1.31	6-phosphogluconolactonase	299471731	not listed
3.1.3.11	fructose-bisphosphatase	see Glycolysis	see Glycolysis
4.1.2.-		not analyzed	not listed
4.1.2.13	fructose-bisphosphate aldolase	see Glycolysis	see Glycolysis
4.1.2.14	2-dehydro-3-deoxy-phosphogluconate aldolase	not analyzed	not listed
4.1.2.4	deoxyribose-phosphate aldolase	299469818	not listed
4.1.2.43	3-hexulose-6-phosphate synthase	not analyzed	not listed
4.1.2.9	phosphoketolase	not found	not listed
4.2.1.12	phosphogluconate dehydratase	not analyzed	not listed
4.2.1.39	gluconate dehydratase	not analyzed	not listed
4.3.1.9	glucosaminate ammonia-lyase	not analyzed	not listed
5.1.3.1	ribulose-phosphate 3-epimerase	299469833; 299473285	2
5.3.1.27	6-phospho-3-hexuloisomerase	not analyzed	not listed
5.3.1.6	ribose-5-phosphate isomerase	299470524	1
5.3.1.9	glucose-6-phosphate isomerase	see Glycolysis	see Glycolysis
5.4.2.2	phosphoglucomutase	299472461	not listed
5.4.2.7	phosphopentomutase	not analyzed	not listed

Map: 00710 Carbon fixation in photosynthetic organisms

EC number	Name	Protein sequence GI numbers (found by blastx; NCBI database)	Cock et al
1.1.1.37	malate dehydrogenase	299473211; 298708587	not listed
1.1.1.39	malate dehydrogenase (decarboxylating)	not analyzed	2
1.1.1.40	malate dehydrogenase (oxaloacetate-decarboxylating)	298710532	1
1.1.1.82	malate dehydrogenase (NADP+)	not analyzed	not listed
1.1.1.82/37			3
1.2.1.13	glyceraldehyde-3-phosphate dehydrogenase (NADP+)	not found	5
1.2.1.59	glyceraldehyde-3-phosphate dehydrogenase (NAD(P)+)	298709303	not listed
2.2.1.1	transketolase	see Pentose	see Pentose
2.6.1.1	aspartate transaminase	298705899	2
2.6.1.2	alanine transaminase	298714844; 298710373	2
2.7.1.14	sedoheptulokinase	not analyzed	not listed
2.7.1.19	phosphoribulokinase	299469835	1
2.7.1.40	pyruvate kinase; phosphoenolpyruvate kinase	see Glycolysis	see Glycolysis
2.7.2.3	phosphoglycerate kinase	see Glycolysis	see Glycolysis
2.7.9.1	pyruvate, phosphate dikinase	299115879	1
3.1.3.11	fructose-bisphosphatase	298706472	5
3.1.3.37	sedoheptulose-bisphosphatase	not found	2
4.1.1.31	phosphoenolpyruvate carboxylase	299117425	1
4.1.1.39	ribulose-bisphosphate carboxylase	269101142; 266631650; 270118780	no details
4.1.1.49	phosphoenolpyruvate carboxykinase (ATP)	see Glycolysis	1
4.1.2.13	fructose-bisphosphate aldolase	see Glycolysis	see Glycolysis
4.1.2.22	fructose-6-phosphate phosphoketolase	not found	not listed
4.1.2.9	phosphoketolase	not found	not listed
5.1.3.1	ribulose-phosphate 3-epimerase	see Pentose	see Pentose
5.3.1.1	triose-phosphate isomerase	see Glycolysis	see Glycolysis
5.3.1.6	ribose-5-phosphate isomerase	see Pentose	see Pentose

Table S 5.4: Putative glyceraldehydes-3-phosphate dehydrogenase (GAPDH) sequences from the chrysophyte EST-dataset which were utilized for phylogenetic analyses (Figure 5.7). Poterioochromonas malhamensis 21 was removed from the phylogenetic analyses as it formed a long separate branch.

Name in phylogenetic tree	Contig name	Enzyme codes	Seq. length	Best Hit species by blastx (NCBI, nr)	NCBI Hit ACC	E-Value	Similarity [%]	Alignment length	Posi-tives	5' end?
Mallomonas annulata1	M_ann_c30942	EC:1.2.1.12	440	Siniperca chuatsi	ADH43627	7,5E-30	87	79	69	5' truncated
Mallomonas annulata 2	M_ann_c88	EC:1.2.1.12	1190	Mallomonas rasilis	AAQ63754	1,9E-168	96	318	308	start
Mallomonas annulata 3	M_ann_c7243	EC:1.2.1.9; EC:1.2.1.12	1387	Mallomonas rasilis	AAQ63755	3,1E-168	96	315	304	start
Dinobryon divergens 1	D_div_c695	EC:1.2.1.12	817	Yersinia enterocolitica	ADZ42800	4,7E-47	86	144	125	5' truncated
Dinobryon divergens 2	D_div_c24840	EC:1.2.1.12	478	Mallomonas rasilis	AAQ63754	6,0E-54	88	137	121	start
Dinobryon divergens 3	D_div_c44032	EC:1.2.1.12; EC:1.2.1.9	446	Stanieria cyanosphaera	CAC81002	9,1E-42	79	148	117	5' truncated
Dinobryon divergens 4	D_div_c17646	EC:1.2.1.9; EC:1.2.1.12	892	Stanieria cyanosphaera	CAC81002	3,3E-100	88	245	217	start
Poterioochromonas malhamensis 1	P_mal_c59246	EC:1.1.1.8	532	Mallomonas rasilis	AAQ63754	4,4E-64	81	171	140	5' truncated
Poterioochromonas malhamensis 2	P_mal_lrc59165	EC:1.2.1.12	408	Siniperca chuatsi	ADH43627	1,9E-33	82	105	87	5' truncated
Poterioochromonas malhamensis 3	P_mal_lrc51328	EC:1.2.1.12	399	Guillardia theta	O09452	4,7E-19	88	75	66	5' truncated
Poterioochromonas malhamensis 4	P_mal_lrc50542	EC:1.2.1.12	583	Guillardia theta	O09452	5,1E-37	91	74	68	5' truncated
Poterioochromonas malhamensis 5	P_mal_lrc48927	EC:1.2.1.12	477	Guillardia theta	O09452	7,8E-27	87	93	81	5' truncated
Poterioochromonas malhamensis 6	P_mal_lrc46380	EC:1.2.1.12	516	Guillardia theta	O09452	1,5E-26	86	93	80	5' truncated
Poterioochromonas malhamensis 7	P_mal_lrc45658	EC:1.2.1.12	344	Guillardia theta	O09452	2,1E-11	87	58	51	5' truncated
Poterioochromonas malhamensis 8	P_mal_lrc43690	EC:1.2.1.12	473	Guillardia theta	O09452	5,5E-28	86	96	83	5' truncated
Poterioochromonas malhamensis 9	P_mal_lrc41006	EC:1.2.1.12	430	Stanieria cyanosphaera	CAC81002	5,3E-23	96	77	74	5' truncated
Poterioochromonas malhamensis 10	P_mal_lrc40939	EC:1.2.1.12	435	Rhizomucor miehei	Q8NK47	6,4E-13	90	42	38	5' truncated
Poterioochromonas malhamensis 11	P_mal_lrc36841	EC:1.2.1.12	443	Guillardia theta	O09452	4,7E-27	86	94	81	5' truncated
Poterioochromonas malhamensis 12	P_mal_lrc35526	EC:1.2.1.12	563	Guillardia theta	O09452	3,3E-41	91	72	66	5' truncated
Poterioochromonas malhamensis 13	P_mal_lrc30353	EC:1.2.1.12	505	Guillardia theta	O09452	5,5E-28	86	96	83	5' truncated
Poterioochromonas malhamensis 14	P_mal_lrc29850	EC:1.2.1.12	545	Guillardia theta	O09452	5,7E-38	88	115	102	5' truncated
Poterioochromonas malhamensis 15	P_mal_c6033	EC:1.2.1.12	534	Siniperca chuatsi	ADH43627	1,8E-41	87	107	94	5' truncated
Poterioochromonas malhamensis 16	P_mal_c5574	EC:1.2.1.12	1176	Mallomonas rasilis	AAQ63754	1,9E-128	89	297	266	5' truncated
Poterioochromonas malhamensis 17	P_mal_c3162	EC:1.2.1.12	1340	Ochromonas danica	CAD54626	1,4E-136	89	315	283	5' truncated
Poterioochromonas malhamensis 18	P_mal_c26403	EC:1.2.1.12	439	Ochromonas danica	CAD54626	3,7E-53	85	143	122	5' truncated
Poterioochromonas malhamensis 19	P_mal_c25284	EC:1.2.1.12	449	Guillardia theta	O09452	5,7E-25	85	90	77	5' truncated
Poterioochromonas malhamensis 20	P_mal_c25178	EC:1.2.1.12	383	Achlya bisexualis	AAF44720	7,4E-17	95	48	46	5' truncated
Poterioochromonas malhamensis 21	P_mal_c24616	EC:1.2.1.12	547	Siniperca chuatsi	ADH43627	1,7E-32	83	87	73	5' truncated
Poterioochromonas malhamensis 22	P_mal_c19774	EC:1.2.1.12	583	Guillardia theta	O09452	8,6E-28	86	96	83	5' truncated
Poterioochromonas malhamensis 23	P_mal_c18973	EC:1.2.1.12	468	Rhizomucor miehei	Q8NK47	6,5E-13	90	42	38	5' truncated
Poterioochromonas malhamensis 24	P_mal_lrc36803	EC:1.2.1.12	421	Gonyaulax polyedra	AAD01871	4,1E-23	84	85	72	5' truncated
Poterioochromonas malhamensis 25	P_mal_c9831	EC:1.2.1.9; EC:1.2.1.12	640	Guillardia theta	O09452	6,5E-57	90	152	137	5' truncated
Poterioochromonas malhamensis 26	P_mal_c2133	EC:1.2.1.9; EC:1.2.1.59; EC:1.2.1.12	954	Stanieria cyanosphaera	CAC81002	3,6E-129	92	272	252	start
Poteriospumella lacustris 1	S_JBM_c24045	EC:1.2.1.12	482	Stanieria cyanosphaera	CAC81002	7,6E-30	95	70	67	5' truncated
Poteriospumella lacustris 2	S_JBM_lrc12769	EC:1.2.1.12	528	Pinus sylvestris	P34924	1,3E-36	89	97	87	5' truncated
Poteriospumella lacustris 3	S_JBM_c5657	EC:1.2.1.12	1315	Ochromonas danica	CAD54626	1,3E-136	89	315	282	start
Poteriospumella lacustris 4	S_JBM_c852	EC:1.2.1.12	1324	Ochromonas danica	CAD54626	1,3E-136	89	315	282	start
Poteriospumella lacustris 5	S_JBM_c3828	EC:1.2.1.9; EC:1.2.1.12	656	Stanieria cyanosphaera	CAC81002	1,1E-73	89	167	150	start
Poteriospumella lacustris 6	S_JBM_c1395	EC:1.2.1.9; EC:1.2.1.59; EC:1.2.1.12; EC:1.2.1.13	2466	Stanieria cyanosphaera	CAC81002	1,3E-149	93	312	293	start

Table S 5.5: List of key enzymes evaluated to prepare Figure 5.5

Enzyme code	Description
<u>Glycolysis</u>	
2.7.1.11	6-phosphofructokinase
2.7.1.2	glucokinase
2.7.1.40	pyruvate kinase
<u>Gluconeogenesis</u>	
2.7.9.1	pyruvate, phosphate dikinase
2.7.9.2	pyruvate, water dikinase
3.1.3.11	fructose-bisphosphatase
4.1.1.32/49	phosphoenolpyruvate carboxykinase
6.4.1.1	pyruvate carboxylase
<u>Oxidative pentose phosphate pathway</u>	
1.1.1.44	phosphogluconate dehydrogenase
1.1.1.49	glucose-6-phosphate dehydrogenase
3.1.1.31	6-phosphogluconolactonase
<u>Reductive pentose phosphate pathway</u>	
2.7.1.19	phosphoribulokinase
4.1.1.39	ribulose-bisphosphate carboxylase
<u>Additional enzymes involved in carbon fixation and decarboxylation</u>	
1.1.1.40/39/37	malate dehydrogenase
4.1.1.31	phosphoenolpyruvate carboxylase
4.2.1.1	carbonic anhydrase

Chapter 6

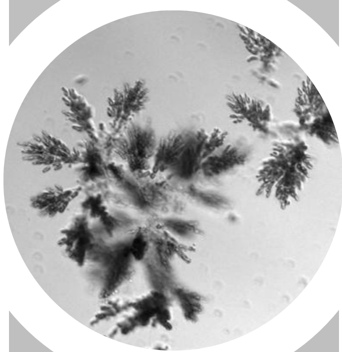

General Discussion

by Julia Rottberger

6. General discussion

Mixotrophic algae may act as primary producers at times when they perform photosynthesis and may also act as consumers while they ingest bacteria or organic compounds. The competitive advantage is obvious: if light is limited mixotrophs may switch to heterotrophic nutrition and if organic carbon sources are limited they may strive by performing photosynthesis. In fact, mixotrophs are able to compete successfully with exclusive phagotrophs or exclusive heterotrophs under laboratory conditions (Rothhaupt, 1996b). Mixotrophic algae also are of ecological relevance as they are abundant in all freshwater habitats and contribute significantly to phytoplankton biomass especially in oligotrophic lakes like Lake Constance. Based on its broad phylogenetic distribution (Figure 1.1) mixotrophy may appear to be a successful nutritional concept. Yet, mixotrophs overall are not the most competitive and abundant algae in aquatic environments. In the following benefits and limitations of mixotrophy in chrysophytes based on the physiological and molecular investigations in this thesis are discussed.

6.1. The ecological relevance of strains investigated in this thesis

In the beginning of this work, mixotrophic strains suitable for physiological and molecular investigations were chosen and their cultures were newly established in the laboratory. Regarding the broader context of this thesis, the strains needed to be of ecological relevance in Lake Constance. Based on literature records, chrysophytes were promising candidates regarding their abundances in the mixotrophic phytoplankton population of Lake Constance (Gaedke, 1998; Brachvogel et al., 2001; Kamjunke et al., 2007) and the amount of physiological data already available.

Initially, the mixotrophic *Ochromonas danica* strain 933-7 purchased from the Culture Collection of Algae at Göttingen University was utilized to establish experimental procedures in the laboratory (Chapter 2). This chrysophyte was originally isolated from a bog pool in Denmark (Pringsheim, 1955). The strain has been cultivated under laboratory conditions since 1954. No records of more recently isolated *Ochromonas danica* strains exist. Thus, the ecological relevance of conclusions drawn from investigations of only this alga for Lake Constance would have been doubtful. Therefore, additional strains were investigated (Chapters 3-5). To be able to relate strains with different manifestations of mixotrophic nutrition to each other, *Poterioochromonas malhamensis* and *Dinobryon divergens* were selected (Figure 6.1). The *P. malhamensis* strain investigated in this thesis was originally isolated from Lake Constance. *D. divergens*, together with *D. sociale,* is the dominating *Dinobryon* species in Lake Constance (Kamjunke et al., 2007). Additionally, a purely photoautotrophic and a purely heterotrophic chrysophyte, *Mallomonas annulata* and *Poteriospumella lacustris*, were chosen as references. *D. divergens* and the reference strains *M. annulata* and *P. lacustris* were both isolated from oligotrophic lakes in Austria (for references see Chapter 4).

The diatom *Phaeodactylum tricornutum* served as a photoautotrophic reference organism for this thesis. *P. tricornutum* was originally isolated from brackish water but may survive in freshwater as well as in seawater under laboratory conditions. This is different to the investigated chrysophytes which are freshwater algae (Chapter 2, 3, 4). Although, *P. tricornutum* might not be ideally suited as a reference organism to demonstrate ecological relevant similarities to chrysophytes, a number of other features made it a convenient reference.

P. tricornutum is a well-studied model organism regarding its physiology, metabolism and molecular biology. Thus, *P. tricornutum* served as a standard to compare findings regarding the chrysophytes to other algal groups. *P. tricornutum* is a heterokont alga as well as chrysophytes are. It is very interesting to see whether or not chrysophytes and diatoms differ substantially in their genetic and molecular features.

And, as chrysophytes are discussed to have certain disadvantages regarding their photosynthetic competitiveness compared to other algae (Maberly et al., 2009), it was of major importance to include a reference organism like *P. tricornutum* which is known to perform well under photolithoautotrophic conditions.

Though *P. tricornutum* is accepted and promoted as photoautotrophic alga there is little but nevertheless conclusive evidence for mixotrophic features. It is proposed that *P. tricornutum* is able to exploit organic carbon sources osmotrophically because the diatom performs better when grown in the presence of organic substrates like glycerol, acetate and glucose (Garcia et al., 2000; Garcia et al., 2005; Liu et al., 2009). Though these findings surely need further research, they make *P. tricornutum* even more interesting as a reference organism for this thesis. In contrast to *D. divergens* and *P. malhamensis*, there is no literature evidence for phagotrophic uptake of particles or organisms. Also, *P. tricornutum*, like *D. divergens*, is not capable of growing in complete darkness in organic media whereas *P. malhamensis* can (Chapter 2 and 3). Thus, finally it depends on the definition applied whether *P. tricornutum* may be regarded as organism with mixotrophic features or not.

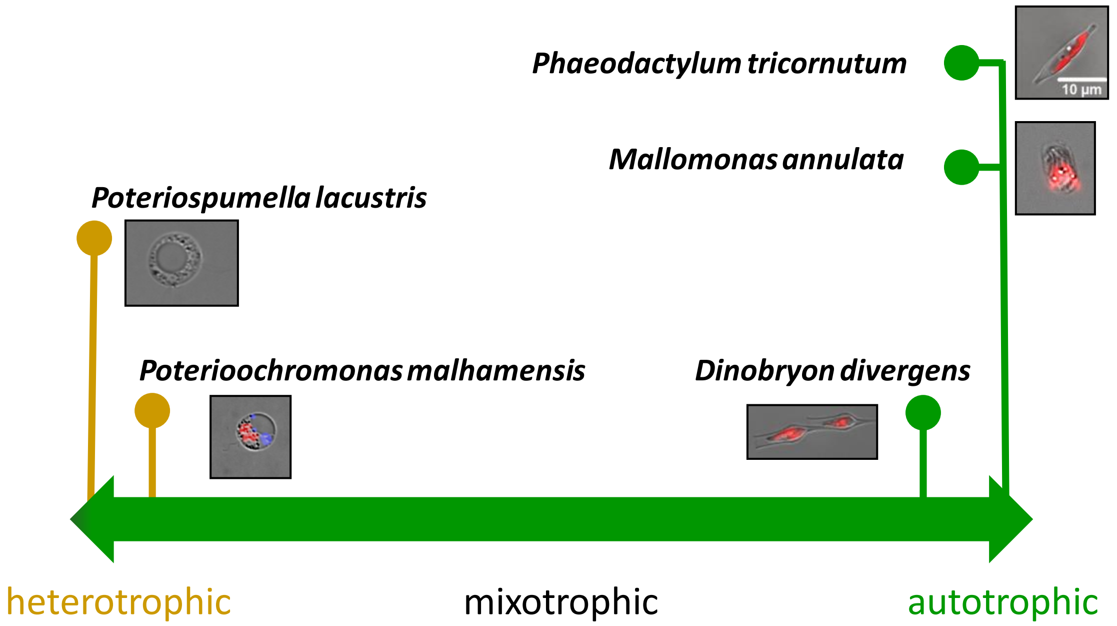

Figure 6.1: Nutritional classification of the different protists investigated in this thesis on a scale between purely heterotrophic and purely autotrophic nutrition according to the physiological investigations performed.

6.2. Mixotrophic chrysophytes in relation to other chrysophytes

Chrysophytes are of special importance for this thesis because they are dominating mixotrophic protists in Lake Constance. Apart from that, they have been found in freshwater environments all over the world (Kristiansen, 2008) including extreme habitats like glaciers (Tanabe et al., 2011). Chrysophytes are also found in the water column and ice of the oceans (Ikävalko and Thomsen, 1997; Stöcker et al., 1997). There are considerable more studies addressing mixotrophic freshwater chrysophytes than marine strains. Yet, there are marine mixotrophic chrysophytes known like *Dinobryon faculiferum* (Unrein et al., 2010), *Dinobryon balticum* (Mckenzie et al., 1995) or *Ochromonas minima* (Flöder et al., 2006). Physiological studies on mixotrophic chrysophytes from marine and freshwater environments agree upon the finding that mixotrophic chrysophytes may thrive under nutrient conditions which are limiting for photoautotrophic algae (Flöder et al., 2006; Kamjunke et al., 2007; Unrein et al., 2010). Mixotrophic chrysophytes can live on the surface of sea-ice (Ikävalko and Thomsen, 1997) and snow patches (Tanabe et al., 2011) which are extreme habitats regarding temperature fluctuations, solar irradiance levels and, in case of sea-ice, salinity. This is of special interest when considering that chrysophytes in general are regarded as rather sensitive to environmental changes (e.g. this study chapter 4, Herth and Zugenmaier, 1979; Veen, 1991) and therefore are utilized as indicator organisms (Dixit et al., 1999; Pla and Anderson, 2005; Ginn et al., 2010). So far, it remains unanswered how the sensitivity of mixotrophic chrysophytes living in the water column correlates with the adaptation to the highly variable conditions on ice surfaces.

6.3. Mixotrophic chrysophytes in relation to other mixotrophic algae

Currently, there are few mixotrophic eukaryotes which have been investigated on the genetic, physiologic and molecular level. Prokaryotes lack organelles and therefore are simpler model organisms to study intracellular distribution and regulation of carbon metabolism compared to chrysophytes and other eukaryotic algae. Apparently all photosynthetic life derived from a cyanobacteria-like cell (Keeling, 2004; Figure 1.1). Thus, looking at regulation of carbon metabolism in cyanobacteria may reveal the basic mechanisms operating in the diverse endocytobiotic lineages of photosynthetic organisms. In the cyanobacterium *Synechocystis* sp. carbon flux has been analyzed under autotrophic, mixotrophic and heterotrophic conditions. *Synechocystis* sp. is obligatory light-dependent. Even under otherwise heterotrophic conditions cultures need to receive at least 5 min of blue light a day to prosper (Anderson and Mcintosh, 1991). Here, mRNA levels of most key enzymes of central metabolic pathways are roughly unchanged comparing mixotrophic, autotrophic and heterotrophic conditions (Yang et al., 2002a). Instead post-transcriptional regulatory mechanisms are common. The flux of CO_2 fixation in *Synechocystis* sp. is directed through the Calvin cycle under mixotrophic and photoautotrophic conditions. Under heterotrophic conditions not glycolysis but the oxidative pentose phosphate pathway is the major pathway of glucose metabolism (Yang et al., 2002b; Yoshikawa et al., 2013). Thus, cyanobacteria show different metabolic phenotypes though they basically operate with the same set of expressed genes.

Cell organization of the eukaryotic chrysophytes naturally is more complex compared to cyanobacteria. During re-organization of the cell in the cause of endocytobiosis there probably was an increase in metabolic control because both the host and the endosymbiont brought along a complete metabolic apparatus. In the beginning, some pathways probably were present in duplicates or even more often and there were no mechanisms to control whether the endosymbiont immediately consumed intermediates produced by the host or *vice versa*. Somehow insurance of the metabolic balance and inhibition of the exploitation of either symbiotic partner by the other was established during evolution. Nuclear genes have been found to regulate plastid development and chloroplast signals were shown to affect nuclear gene expression in plants and algae (Taylor, 1989) which both hints at complex control mechanisms.

Green algae derived from a primary endocytobiotic event and therefore have an intermediary complexity of intracellular organization between cyanobacteria and chrysophytes which derived by secondary endocytobiosis. A well-investigated mixotrophic green alga is *Chlamydomonas reinhardtii*. Yet, in contrast to *Synechocystis* spp. comprehensive datasets comparing gene expression of carbohydrate metabolism in *Chlamydomonas reinhardtii* under autotrophic, mixotrophic and heterotrophic conditions were not found in the literature (an actual review describes the central carbon metabolism in *Chlamydomonas reinhardtii* (Johnson and Alric, 2013). Yet, mRNA levels have been shown to vary during anaerobic acclimatization. Also, quantitative control of gene expression under photoautotrophic conditions in dependency of the CO_2 concentration was found to involve a zinc-finger type transcription regulator called *CIA5* or *CCM1* (Yamano et al., 2008; Fang et al., 2012). A massive impact of *CIA5* and CO_2 one gene expression levels was observed affecting almost 25 % of the transcriptome. In *Chlamydomonas reinhardtii*, glycolysis and the oxidative pentose phosphate pathways are not duplicated in the cytosol and the chloroplast like in higher plants but instead are highly compartmentalized (Johnson and Alric, 2013). Compared to the prokaryote *Synechocystis* sp. these findings imply a more complex regulatory control on the transcript level, also implying that in unicellular endocytobiotically derived algae compartmentalization is utilized to control biochemical pathways by spatial separation.

Compartmentalization of carbohydrate pathways is not restricted to mixotrophic algae but is also found in purely photoautotrophic algae like the diatom *P. tricornutum* (Kroth et al., 2008; Gruber et al., 2009). However, even in diatoms the full impact of the differential distributions of metabolic pathways is still under investigation.

Interestingly, qualitative expression of pathways is not very different between autotrophic, mixotrophic and heterotrophic chrysophytes apart from the lack of major photosynthetic enzymes and components in the heterotrophic *P. lacustris* (Chapter 5). Similar to *Synechocystis* sp. mixotrophic and photoautotrophic chrysophytes showed distinct physiological phenotypes (Figure 6.1) though they operate with a similar set of expressed pathways. Due to normalization of the EST-libraries quantitative transcript expression analysis is not applicable for the datasets. However, given that biosynthetic reactions may be controlled on the transcriptional level, it is anticipated that the number of enzymes found within a metabolic pathway will be higher if a pathway is active than if the pathway was down-regulated or inactive. Therefore, a qualitative expression analysis might yet hint at the relevance of certain metabolic reactions for an organism. The number of enzymes assigned to certain pathways was found to correspond to the nutritional behavior of the chrysophytes. For example the highest number of glycolytic enzymes was found in the heterotrophic and the lowest in the photoautotrophic chrysophyte (Chapter 5). Thus, there may be transcriptional regulators operating on the qualitative expression level in chrysophytes. The presence of expression regulation mechanisms operating on the quantitative level seem likely as this was discovered in primary endocytobionts like *Chlamydomonas reinhardtii* which presumably are even less complex than chrysophytes.

Future analyses of the subcellular distribution of pathways may reveal additional differences between the four chrysophytes. So far, mixotrophic chrysophytes were shown to differ from photoautotrophs by the lack of key enzymes of the oxidative pentose phosphate pathway (Figure 6.2). Additionally, only few decarboxylating and CO_2 fixing enzymes have been intracellularly located for the mixotrophs. These may be decisive features explaining the physiological differences between the mixotrophic and the photoautotrophic strains. Yet, the oxidative pentose phosphate pathway in the mixotrophic strains may have been inactive under the conditions applied and, thus, further quantitative transcriptomic analysis under various conditions is necessary to proof these findings.

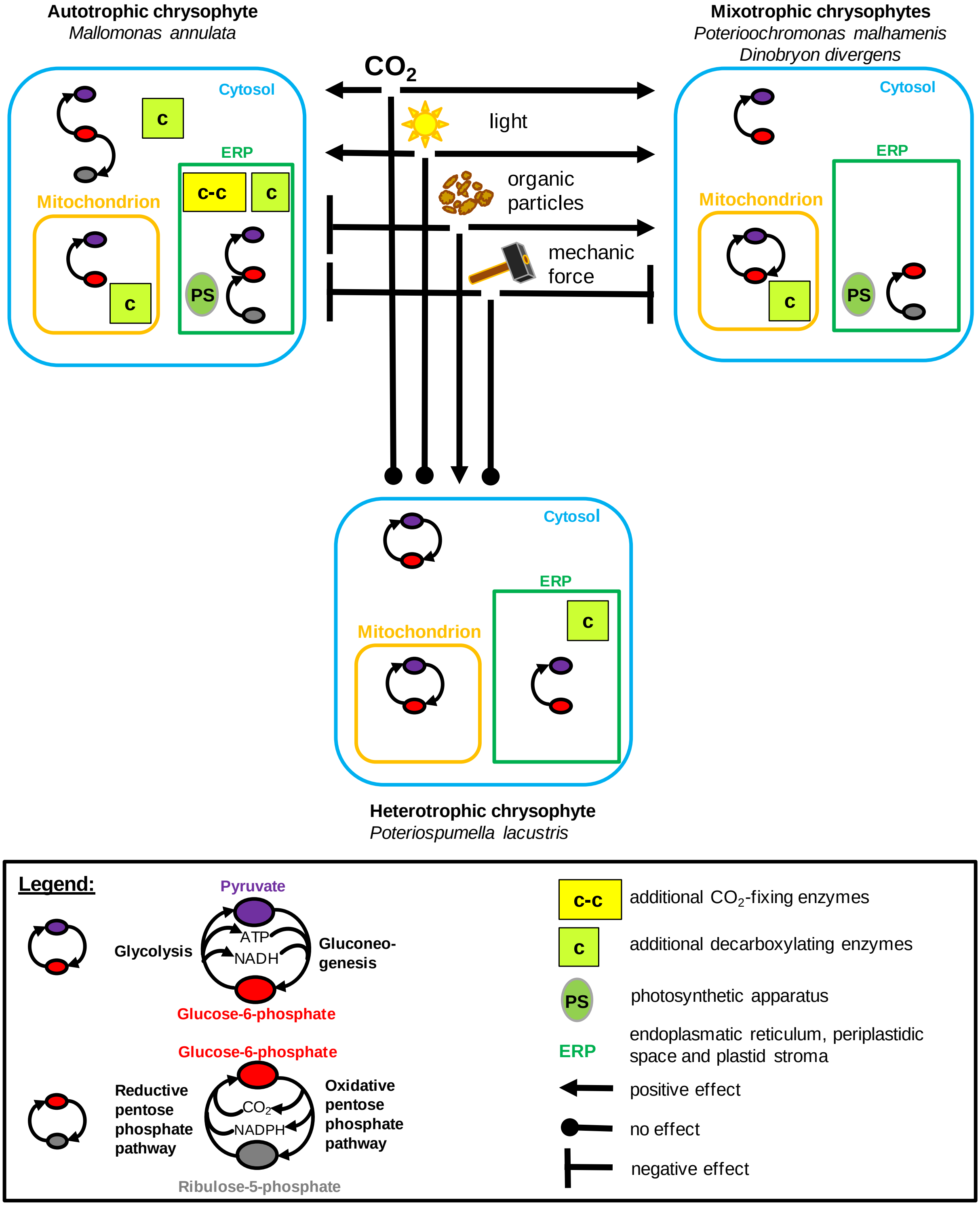

Figure 6.2: Comparative model of findings regarding important molecular and physiological features of the carbon metabolism in autotrophic, mixotrophic and heterotrophic chrysophytes. Simplified cells of the nutritionally differing protists are illustrated. The intracellular distribution of important carbon pathways in the cytosol, the mitochondria and the ERP are schematically shown. This data is based on the *de novo* annotations and localization predictions of mRNA sequences performed in this thesis. The effect of improved CO_2 supply, light, addition of organic particles (bacteria) or mechanical stress on growth rates of the protists is indicated by different arrows. This data is based on the growth experiments performed in this thesis.

Localization predictions based on the cDNA sequences are a powerful tool to provide first insight into metabolism which was demonstrated in this thesis by *P. lacustris* as an example. First proof of the presence of a partial plastidic glycolysis was shown in the heterotrophic chrysophyte (Chapter 5). Until now, the function of the non-photosynthetic plastid in *P. lacustris* and other *Spumella*-like flagellates is unknown. In this thesis a first hint for metabolic activity in the plastid of *P. lacustris* is presented (Figure 6.2). The question when and why this glycolytic pathway is actually active will need to be answered by further investigations and may possibly illuminate why the plastid as a metabolic compartment is still important for this protist though photosynthetic activity has been lost secondarily.

6.4. The disadvantages in photosynthetic performance of chrysophytes

It has been proposed, that one major drawback of mixotrophic and photoautotrophic chrysophytes compared to other algae might be the lack of carbon concentrating mechanisms or the inability to use bicarbonate as a carbon source besides of CO_2 (Maberly et al., 2009). One way of CO_2 concentration is the fusion and reduction of CO_2 to an organic intermediate in any cell compartment other than the plastid, followed by transport of the synthesized compound into the plastid where CO_2 then is released by decarboxylating enzymes. These processes ensure that the ribulose-1,5-bisphosphate carboxylase/oxygenase (RuBisCO) which cannot utilize any other low-molecular carbon compounds fixes CO_2 at maximum rates. This of course only works if the CO_2 fixing enzymes outside of the plastid have higher affinities to CO_2 or if they are more abundant than RuBisCO.

A number of putative carbon fixing and releasing enzymes were found in the transcriptomic dataset of the mixotrophic and the autotrophic chrysophytes (Chapter 5). Putative carbonic anhydrases were found. These enzymes reversibly catalyze the transformation of CO_2 to bicarbonate in the cell. The presence of a membrane-bound carbonic anhydrase would present one possible mechanism to ensure carbon concentration outside of the plastid but also bicarbonate transporters or semi-permeable ion channels are imaginable. Once CO_2 is transported and transformed to bicarbonate in the cytoplasm, it is basically trapped inside the cell because diffusion of CO_2 but not of bicarbonate is possible across the cell membranes. It is not possible to conclude whether these putative enzymes are functional based on automatically annotated transcripts alone. Here, analyzing whether there are sequence homologies to catalytic domains of functional enzymes from other organisms would be a first next step. Next, additional experiments under different pH conditions and CO_2/bicarbonate levels clarifying the transcript and the protein expression levels as well as enzyme activity tests are needed to make further conclusions as well as localization studies. Nevertheless, based on the transcriptomic data there are putative enzymes involved in bicarbonate interconversion, carboxylating and decarboxylating reactions in chrysophytes (Figure 6.2). Therefore, it is probably not the absence of enzymes but the subcellular localization or post-transcriptional regulation of the respective gene products causing the postulated drawback in photosynthetic performance of chrysophytes compared to other photoautotrophs.

6.5. Energy and biomass in mixotrophic chrysophytes

Organisms use ATP as an energy equivalent to grow and multiply. ATP may be generated by substrate-level phosphorylation in the cytoplasm or by electron transport chains across membranes.

In the studied chrysophytes only a few soluble components of the photosynthetic and the respiratory electron transport chains were identified from the transcriptomic datasets via automatic KEGG-annotation. This is not only the case for chrysophytes but is also true for other protists like for example *P. tricornutum* (http://genome.jgi.doe.gov/Phatr2_bd/Phatr2_bd.home.html). One possible explanation is that sequences of membrane proteins are difficult to identify by automatic similarity search, because they generally contain low complexity regions i.e. regions with a large number of homopolymers. Another reason may be that several components, like e.g. subunits of the photosystems and ATP-synthase, are encoded on the plastidic and not the nuclear genome in a very conservative manner among photosynthetic eukaryotes (Oudot-Le Secq et al., 2007; Green, 2011). Thus, it is unlikely that these components are nuclear encoded in chrysophytes.

The physiological experiments performed in this thesis delivered new insights regarding photosynthetic oxygen evolution of chrysophytes which is the initial step of the photosynthetic electron transport chain (Chapter 4). The photosynthetic oxygen evolution rates of the mixotrophic chrysophytes were similar. Thus, the capacities to oxidize water to oxygen at corresponding light intensities are similar in both organisms. Yet, *P. malhamensis* usually showed higher growth rates than *D. divergens*. Until electrons from the water splitting reaction finally reduce CO_2 to organic carbon intermediates many reactions and steps are required and on the way there are various other sinks for electrons than carbon fixation. Thus, under identical conditions even two purely photoautotrophic algae with similar oxygen evolution rates do not necessarily need to have the same capacities to generate biomass.
Regarding mixotrophic organisms, the situation is even more complex because biomass may be produced from external organic carbon sources as well as from inorganic carbon. Moreover, the organic carbon sources may serve as energy and electron source. A good example demonstrating this complexity is that under light limiting conditions in the presence of organic carbon *P. malhamensis* showed the same growth performance as before whereas growth rates of *D. divergens* were reduced. There is no evidence from the transcriptomic dataset for completely different heterotrophic or autotrophic pathways between *P. malhamensis* and *D. divergens* (Chapter 5). Thus, the most likely explanation for the different effects of light limitation is that carbon pathways are regulated differently. *D. divergens* might predominantly perform photosynthesis and generate only little energy and biomass by heterotrophic pathways. *P. malhamensis* on the other hand may predominantly utilize heterotrophic pathways. Accordingly, light limitation affects growth of *D. divergens* stronger than *P. malhamensis* (Chapter 4).
Both mixotrophs are able to perform photosynthesis and utilize organic carbon sources in parallel (Chapter 4). Yet, *P. malhamensis* can grow in complete darkness on organic substrates but does not grow in the light if CO_2 is the only carbon source available. *D. divergens* does not grow in the dark even when organic carbon sources are provided. In accordance with the classifications proposed by (Jones, 2000), this demonstrates that mixotrophs have sophisticated nutritional capacities and, thus, are not able to switch between a purely heterotrophic and a purely autotrophic mode of life without restrictions. The differences in their nutritional mode may possibly lead to the occupation of different natural habitats by the two mixotrophic chrysophytes in oligotrophic lakes (discussed in detail in Chapter 4).

6.6. There is more to mixotrophy than inorganic and organic carbon sources

Despite of their flexibility regarding the exploitable carbon sources, mixotrophs might be very sensitive towards changes regarding other growth-determining factors (Figure 6.1). As demonstrated in this thesis (Chapter 3 and 4) mixotrophic chrysophytes respond very differentially towards changes in light- and prey- availability. Such differential feedbacks made paleontologists discover chrysophytes as reliable and sensitive indicator organisms for environmental changes because e.g. pH changes or eutrophication result in the extinction of certain species (Dixit et al., 1999). However, this is only true for silica-scaled chrysophytes and therefore manly applies to photoautotrophic genera. Their inorganic scales may outlast a century in the sediments of lakes whereas cell fragments and organic cell walls of mixotrophic chrysophytes are decomposed more quickly. Though growth of mixotrophic chrysophytes has been shown to be influenced by temperature fluctuations, light-, carbon-, nitrogen-, phosphorous-, iron- and vitamin-availability and other factors, extinction of mixotrophs in their natural habitats caused by distinct changes in conditions has not yet been reported.

Lake Constance is one of the few existing long-term freshwater sampling sites. Here, changes in the natural conditions in deed had an effect on mixotrophic chrysophytes which has been linked to the competitive advantage of phagotrophic representatives which successfully exploit bacteria as a phosphorus source (Kamjunke et al., 2007). Other multiannual studies indicate that phosphorus is a nutrient capable of increasing the biomass of mixotrophic chrysophytes (Pålsson and Daniel, 2004), yet, at the same time the authors state that patterns are not very predictable because there also is an influence of light availability and probably even other factors. Thus, complexity of natural systems and the amount of traceable regulatory factors make it an on-going challenge to investigate mixotrophic chrysophytes in their ever changing natural environments.

Here, it seems more promising to develop a holistic understanding of mixotrophic chrysophytes by going from the particular to the general. In this thesis two fundamental steps have been performed towards this direction (Figure 6.2). First, two mixotrophic strains with differing nutritional characteristics have been compared to each other and autotrophic or heterotrophic representatives under identical conditions (Chapter 2-4). It is only by comparison that characteristics, such as that *Dinobryon divergens* is rather prey-selective and performing primarily photoautotrophic, may be related to other algae. And it was only by performing experiments under controlled conditions that small differences became obvious. Nonetheless, even little differences may be decisive to explain colonization of different vertical layers or different temporal distributions (Chapter 4). Second, transcriptomic datasets of all four organisms were produced, analyzed and compared to each other (Chapter 5). Currently, it probably even represents the largest transcriptomic dataset of phagotrophic mixotrophs available. In this thesis, the focus was on the analysis of carbon pathways; however, many other features affecting growth performance may be investigated and compared on the base of these data.

Bibliography

Allen, A.E., Dupont, C.L., Obornik, M., Horak, A., Nunes-Nesi, A., McCrow, J.P., Zheng, H., Johnson, D.A., Hu, H., Fernie, A.R., and Bowler, C. (2011). Evolution and metabolic significance of the urea cycle in photosynthetic diatoms. Nature **473,** 203-207.

Andersen, R.A., Van de Peer, Y., Potter, D., Sexton, J.P., Kawachi, M., and LaJeunesse, T. (1999). Phylogenetic analysis of the SSU rRNA from members of the Chrysophyceae. Protist **150,** 71-84.

Anderson, S.L., and Mcintosh, L. (1991). Light-activated heterotrophic growth of the cyanobacterium *Synechocystis* sp strain Pcc-6803 - a blue-light-requiring process. J Bacteriol **173,** 2761-2767.

Anneville, O., and Pelletier, J.P. (2000). Recovery of Lake Geneva from eutrophication: quantitative response of phytoplankton. Fundam Appl Limnol **148,** 607-624.

Apt, K.E., Kroth-Pancic, P.G., and Grossman, A.R. (1996). Stable nuclear transformation of the diatom *Phaeodactylum tricornutum*. Mol Gen Genet **252,** 572-579.

Apt, K.E., Clendennen, S.K., Powers, D.A., and Grossman, A.R. (1995). The gene family encoding the fucoxanthin chlorophyll proteins from the brown alga *Macrocystis pyrifera*. Mol Gen Genet **246,** 455-464.

Archibald, J.M. (2009). The puzzle of plastid evolution. Curr Biol **19,** R81-R88.

Badger, M.R., and Price, G.D. (1994). The role of carbonic-anhydrase in photosynthesis. Annu Rev Plant Phys **45,** 369-392.

Bartual, A., Galvez, J.A., and Ojeda, F. (2008). Phenotypic response of the diatom *Phaeodactylum tricornutum* Bohlin to experimental changes in the inorganic carbon system. Bot Mar **51,** 350-359.

Bauwe, H., Hagemann, M., and Fernie, A.R. (2010). Photorespiration: players, partners and origin. Trends Plant Sci **15,** 330-336.

Bayer, T., Aranda, M., Sunagawa, S., Yum, L.K., Desalvo, M.K., Lindquist, E., Coffroth, M.A., Voolstra, C.R., and Medina, M. (2012). *Symbiodinium* transcriptomes: genome insights into the dinoflagellate symbionts of reef-building corals. PloS one **7,** e35269.

Beattie, A., Percival, E., and Hirst, E.L. (1961). Studies on metabolism of Chrysophyceae - comparative structural investigations on leucosin (chrysolaminarin) separated from diatoms and laminarin from brown algae. Biochem J **79,** 531-&.

Bender, S.J., Parker, M.S., and Armbrust, E.V. (2012). Coupled effects of light and nitrogen source on the urea cycle and nitrogen metabolism over a diel cycle in the marine diatom *Thalassiosira pseudonana*. Protist **163,** 232-251.

Bhatti, S., and Colman, B. (2008). Inorganic carbon acquisition in some synurophyte algae. Physiol Plantarum **133,** 33-40.

Bhatti, S., and Colman, B. (2011). Evidence for the occurrence of photorespiration in synurophyte algae. Photosynth Res **109,** 251-256.

Bhaya, D., and Grossman, A. (1991). Targeting proteins to diatom plastids involves transport through an endoplasmic reticulum. Mol Gen Genet **229,** 400–4.

Bird, D.F., and Kalff, J. (1987). Algal phagotrophy - regulating factors and importance relative to photosynthesis in *Dinobryo*n (Chrysophyceae). Limnol Oceanogr **32,** 277-284.

Bird, D.F., and Kalff, J. (1989). Phagotrophic sustenance of a metalimnetic phytoplankton peak. Limnol Oceanogr **34,** 155-162.

Boenigk, J., and Arndt, H. (2002). Bacterivory by heterotrophic flagellates: community structure and feeding strategies. Antonie Leeuwenhoek Int J G M **81,** 465-480.

Boenigk, J., Pfandl, K., and Hansen, P.J. (2006). Exploring strategies for nanoflagellates living in a 'wet desert'. Aquat Microb Ecol **44,** 71-83.

Boenigk, J., Pfandl, K., Stadler, P., and Chatzinotas, A. (2005). High diversity of the '*Spumella*-like' flagellates: an investigation based on the SSU rRNA gene sequences of isolates from habitats located in six different geographic regions. Environ Microbiol **7,** 685-697.

Bowler, C., Allen, A.E., Badger, J.H., Grimwood, J., Jabbari, K., Kuo, A., Maheswari, U., Martens, C., Maumus, F., Otillar, R.P., Rayko, E., Salamov, A., Vandepoele, K., Beszteri, B., Gruber, A., Heijde, M., Katinka, M., Mock, T., Valentin, K., Verret, F., Berges, J.A., Brownlee, C., Cadoret, J.P., Chiovitti, A., Choi, C.J., Coesel, S., De Martino, A., Detter, J.C., Durkin, C., Falciatore, A., Fournet, J., Haruta, M., Huysman, M.J., Jenkins, B.D., Jiroutova, K., Jorgensen, R.E., Joubert, Y., Kaplan, A., Kroger, N., Kroth, P.G., La Roche, J., Lindquist, E., Lommer, M., Martin-Jezequel, V., Lopez, P.J., Lucas, S., Mangogna, M., McGinnis, K., Medlin, L.K., Montsant, A., Oudot-Le Secq, M.P., Napoli, C., Obornik, M., Parker, M.S., Petit, J.L., Porcel, B.M., Poulsen, N., Robison, M., Rychlewski, L., Rynearson, T.A., Schmutz, J., Shapiro, H., Siaut, M., Stanley, M., Sussman, M.R., Taylor, A.R., Vardi, A., von Dassow, P., Vyverman, W., Willis, A., Wyrwicz, L.S., Rokhsar, D.S., Weissenbach, J., Armbrust, E.V., Green, B.R., Van de Peer, Y., and Grigoriev, I.V. (2008). The *Phaeodactylum* genome reveals the evolutionary history of diatom genomes. Nature **456,** 239-244.

Brachvogel, T., Schweitzer, B., and Simon, M. (2001). Dynamics and bacterial colonization of microaggregates in a large mesotrophic lake. Aquat Microb Ecol **26,** 23-35.

Bucka, H. (2005). Ecological aspects of selected principal phytoplankton taxa in lake Piaseczno. Oceanol Hydrobiol Stud **34,** 79-94.

Butterwick, C., Heaney, S.I., and Talling, J.F. (2005). Diversity in the influence of temperature on the growth rates of freshwater algae, and its ecological relevance. Freshwater Biol **50,** 291-300.

Caron, D.A., Porter, K.G., and Sanders, R.W. (1990). Carbon, nitrogen, and phosphorus budgets for the mixotrophic phytoflagellate *Poterioochromonas malhamensis* (Chrysophyceae) during bacterial ingestion. Limnol Oceanogr **35,** 433-443.

Caron, D.A., Sanders, R.W., Lim, E.L., Marrase, C., Amaral, L.A., Whitney, S., Aoki, R.B., and Porter, K.G. (1993). Light-dependent phagotrophy in the fresh-water mixotrophic chrysophyte *Dinobryon cylindricum*. Microbial Ecol **25,** 93-111.

Cavalier-Smith, T. (2002). The phagotrophic origin of eukaryotes and phylogenetic classification of Protozoa. International Journal of Systematic and Evolutionary Microbiology **52**, 297–354

Cavalier-Smith, T., and Chao, E.E.Y. (2006). Phylogeny and megasystematics of phagotrophic heterokonts (kingdom Chromista). J Mol Evol **62,** 388-420.

Chauton, M.S., Winge, P., Brembu, T., Vadstein, O., and Bones, A.M. (2013). Gene regulation of carbon fixation, storage, and utilization in the diatom *Phaeodactylum tricornutum* acclimated to light/dark cycles. Plant Physiol **161,** 1034-1048.

Chrzanowski, T.H., and Simek, K. (1990). Prey size selection by fresh-water flagellated Protozoa. Limnol Oceanogr **35,** 1429-1436.

Cock, J.M., Sterck, L., Rouze, P., Scornet, D., Allen, A.E., Amoutzias, G., Anthouard, V., Artiguenave, F., Aury, J.M., Badger, J.H., Beszteri, B., Billiau, K., Bonnet, E., Bothwell, J.H., Bowler, C., Boyen, C., Brownlee, C., Carrano, C.J., Charrier, B., Cho, G.Y., Coelho, S.M., Collen, J., Corre, E., Da Silva, C., Delage, L., Delaroque, N., Dittami, S.M., Doulbeau, S., Elias, M., Farnham, G., Gachon, C.M.M., Gschloessl, B., Heesch, S., Jabbari, K., Jubin, C., Kawai, H., Kimura, K., Kloareg, B., Küpper, F.C., Lang, D., Le Bail, A., Leblanc, C., Lerouge, P., Lohr, M., Lopez, P.J., Martens, C., Maumus, F., Michel, G., Miranda-Saavedra, D., Morales, J., Moreau, H., Motomura, T., Nagasato, C., Napoli, C.A., Nelson, D.R., Nyvall-Collen, P., Peters, A.F., Pommier, C., Potin, P., Poulain, J., Quesneville, H., Read, B., Rensing, S.A., Ritter, A., Rousvoal, S., Samanta, M., Samson, G., Schroeder, D.C., Segurens, B., Strittmatter, M., Tonon, T., Tregear, J.W., Valentin, K., von Dassow, P., Yamagishi, T., Van de Peer, Y., and Wincker, P. (2010). The *Ectocarpus* genome and the independent evolution of multicellularity in brown algae. Nature **465,** 617-621.

Coleman, A.W., Thompson, W.F., and Goff, L.J. (1991). Identification of the mitochondrial genome in the chrysophyte alga *Ochromonas danica*. J Protozool **38,** 129-135.

Conesa, A., Götz, S., Garcia-Gomez, J.M., Terol, J., Talon, M., and Robles, M. (2005). Blast2GO: a universal tool for annotation, visualization and analysis in functional genomics research. Bioinformatics **21,** 3674-3676.

de Castro, F., Gaedke, U., and Boenigk, J. (2009). Reverse evolution: Driving forces behind the loss of acquired photosynthetic traits. PloS one. DOI:10.1371/journal.pone.0008465.

De Hoyos, C., Aldasoro, J.J., Toro, M., and Comin, F.A. (1998). Specific composition and ecology of chrysophyte flagellates in Lake Sanabria (NW Spain). Hydrobiologia **370,** 287-295.

Dixit, S.S., Dixit, A.S., and Smol, J.P. (1999). Lake sediment chrysophyte scales from the northeastern USA and their relationship to environmental variables. J Phycol **35,** 903-918.

Dokulil, M.T., and Teubner, K. (2005). Do phytoplankton communities correctly track trophic changes? An assessment using directly measured and palaeolimnological data. Freshwater Biol **50,** 1594-1604.

Dorrell, R.G., and Smith, A.G. (2011). Do red and green make brown?: Perspectives on plastid acquisitions within Chromalveolates. Eukaryot Cell **10,** 856-868.

Douglas, S.E., and Turner, S. (1991). Molecular evidence for the origin of plastids from a cyanobacterium-like ancestor. J Mol Evol **33,** 267-273.

Elbein, A.D., Pan, Y.T., Pastuszak, I., and Carroll, D. (2003). New insights on trehalose: a multifunctional molecule. Glycobiology **13,** 17R-27R.

Elnabarawy, M.T., and Welter, A.N. (1984). A technique for the enumeration of unicellular algae. Bul Environ Contam Toxicol **32,** 333-338.

Emanuelsson, O., Brunak, S., von Heijne, G., and Nielsen, H. (2007). Locating proteins in the cell using TargetP, SignalP and related tools. Nat Prot **2,** 953-971.

Fabris, M., Matthijs, M., Rombauts, S., Vyverman, W., Goossens, A., and Baart, G.J.E. (2012). The metabolic blueprint of *Phaeodactylum tricornutum* reveals a eukaryotic Entner-Doudoroff glycolytic pathway. Plant J **70,** 1004-1014.

Fang, W., Si, Y.Q., Douglass, S., Casero, D., Merchant, S.S., Pellegrini, M., Ladunga, I., Liu, P., and Spalding, M.H. (2012). Transcriptome-wide changes in *Chlamydomonas reinhardtii* gene expression regulated by carbon dioxide and the CO_2-concentrating mechanism regulator CIA5/CCM1. Plant Cell **24,** 1876-1893.

Fast, A.G., and Papoutsakis, E.T. (2012). Stoichiometric and energetic analyses of non-photosynthetic CO_2-fixation pathways to support synthetic biology strategies for production of fuels and chemicals. Curr Opin Chem Eng **1,** 380-395.

Fernandez, E., Schnell, R., Ranum, L.P.W., Hussey, S.C., Silflow, C.D., and Lefebvre, P.A. (1989). Isolation and characterization of the nitrate reductase structural gene of *Chlamydomonas reinhardtii*. PNAS **86,** 6449-6453.

Finlay, B.J., and Clarke, K.J. (1999). Ubiquitous dispersal of microbial species. Nature **400,** 828-828.

Fleige, T., Fischer, K., Ferguson, D.J.P., Gross, U., and Bohne, W. (2007). Carbohydrate metabolism in the *Toxoplasma gondii* apicoplast: Localization of three glycolytic isoenzymes, the single pyruvate dehydrogenase complex, and a plastid phosphate translocator. Eukaryot Cell **6,** 984-996.

Flöder, S., Hansen, T., and Ptacnik, R. (2006). Energy-dependent bacterivory in *Ochromonas minima* - A strategy promoting the use of substitutable resources and survival at insufficient light supply. Protist **157,** 291-302.

Frommolt, R., Werner, S., Paulsen, H., Goss, R., Wilhelm, C., Zauner, S., Maier, U.G., Grossman, A.R., Bhattacharya, D., and Lohr, M. (2008). Ancient recruitment by chromists of green algal genes encoding enzymes for carotenoid biosynthesis. Molecular Biol Evo **25,** 2653-2667.

Fuchs, G., and Schlegel, H.G. (2007). Allgemeine Mikrobiologie. eds (Stuttgart, Germany: Thieme).

Gaedke, U. (1998). Functional and taxonomic properties of the phytoplankton community of large and deep lake Constance: Interannual variability and response to re-oligotrophication (1979-1993). Fundam Appl Limnol Spec Issues Adv Limnol. **53,** 119-141.

Gaju, N., Guerrero, R., and Pedrosalio, C. (1989). Measurement of cell-volume of phototrophic bacteria in pure cultures and natural samples - phase-contrast, epifluorescence and particle sizing. Fems Microbiol Ecol **62,** 295-302.

Garcia, M.C.C., Sevilla, J.M.F., Fernandez, F.G.A., Grima, E.M., and Camacho, F.G. (2000). Mixotrophic growth of *Phaeodactylum tricornutum* on glycerol: growth rate and fatty acid profile. J Appl Phycol **12,** 239-248.

Garcia, M.C.C., Miron, A.S., Sevilla, J.M.F., Grima, E.M., and Camacho, F.G. (2005). Mixotrophic growth of the microalga *Phaeodactylum tricornutum* - Influence of different nitrogen and organic carbon sources on productivity and biomass composition. Process Biochem **40,** 297-305.

Ginn, B.K., Rate, M., Cumming, B.F., and Smol, J.P. (2010). Ecological distribution of scaled-chrysophyte assemblages from the sediments of 54 lakes in Nova Scotia and southern New Brunswick, Canada. Journal Paleolimnol **43,** 293-308.

Glibert, P.M., Burkholder, J.M., Kana, T.M., Alexander, J., Skelton, H., and Shilling, C. (2009). Grazing by *Karenia brevis* on *Synechococcus* enhances its growth rate and may help to sustain blooms. Aquat Microb Ecol **55,** 17-30.

Gobler, C.J., Berry, D.L., Dyhrman, S.T., Wilhelm, S.W., Salamov, A., Lobanov, A.V., Zhang, Y., Collier, J.L., Wurch, L.L., Kustka, A.B., Dill, B.D., Shah, M., VerBerkmoes, N.C., Kuo, A., Terry, A., Pangilinan, J., Lindquist, E.A., Lucas, S., Paulsen, I.T., Hattenrath-Lehmann, T.K., Talmage, S.C., Walker, E.A., Koch, F., Burson, A.M., Marcoval, M.A., Tang, Y.Z., Lecleir, G.R., Coyne, K.J., Berg, G.M., Bertrand, E.M., Saito, M.A., Gladyshev, V.N., and Grigoriev, I.V. (2011). Niche of harmful alga *Aureococcus anophagefferens* revealed through ecogenomics. PNAS **108,** 4352-4357.

Goddijn, O.J.M., and van Dun, K. (1999). Trehalose metabolism in plants. Trends Plant Sci **4,** 315-319.

Gould, S.B., Waller, R.R., and McFadden, G.I. (2008). Plastid evolution. Annu Rev Plant Biol **59,** 491-517.

Grauvogel, C., and Petersen, J. (2007). Isoprenoid biosynthesis authenticates the classification of the green alga *Mesostigma viride* as an ancient streptophyte. Gene **396,** 125-133.

Green, B.R. (2011). Chloroplast genomes of photosynthetic eukaryotes. Plant J **66,** 34-44.

Gruber, A., Weber, T., Bartulos, C.R., Vugrinec, S., and Kroth, P.G. (2009). Intracellular distribution of the reductive and oxidative pentose phosphate pathways in two diatoms. J Basic Microb **49,** 58-72.

Gruber, A., Vugrinec, S., Hempel, F., Gould, S.B., Maier, U.G., and Kroth, P.G. (2007). Protein targeting into complex diatom plastids: functional characterisation of a specific targeting motif. Plant Mol Biol **64,** 519-530.

Gschloessl, B., Guermeur, Y., and Cock, J.M. (2008). HECTAR: A method to predict subcellular targeting in heterokonts. Bmc Bioinformatics **9**, 393.

Guillard, R.R., and Ryther, J.H. (1962). Studies of marine planktonic diatoms .1. *Cyclotella nana hustedt*, and *Detonula confervacea (Cleve) gran*. Can J Microbiol **8,** 229-239.

Guillard, R.R., and Lorenzen, C.J. (1972). Yellow-green algae with chlorophyllide C. J Phycol **8,** 10-14.

Guillard, R.R.L. (1975). Culture of phytoplankton for feeding marine invertebrates. In: Culture of marine invertebrate animals, W.L. Smith and M.H. Chanley, eds (New York, USA: Plenum Press).

Guindon, S., Dufayard, J.F., Lefort, V., Anisimova, M., Hordijk, W., and Gascuel, O. (2010). New algorithms and methods to estimate maximum-likelihood phylogenies: assessing the performance of PhyML 3.0. Syst Biol **59,** 307-321.

Hackett, J.D., Scheetz, T.E., Yoon, H.S., Soares, M.B., Bonaldo, M.F., Casavant, T.L., and Bhattacharya, D. (2005). Insights into a dinoflagellate genome through expressed sequence tag analysis. BMC Genomics **6**.

Hahn, M.W. (2003). Isolation of strains belonging to the cosmopolitan *Polynucleobacter necessarius* cluster from freshwater habitats located in three climatic zones. AEM **69,** 5248-5254.

Hahn, M.W., and Höfle, M.G. (1998). Grazing pressure by a bacterivorous flagellate reverses the relative abundance of *Comamonas acidovorans* PX54 and *Vibrio* strain CB5 in chemostat cocultures. AEM **64,** 1910-1918.

Harper, J.T., and Keeling, P.J. (2003). Nucleus-encoded, plastid-targeted glyceraldehyde-3-phosphate dehydrogenase (GAPDH) indicates a single origin for chromalveolate plastids. Mol Biol Evol **20,** 1730-1735.

Heinrich, H.C. (1955). Der B-vitamin-Bedarf der Chrysophyceen „*Ochromonas danica* nom. provis.Pringsheim" und „*Ochromonas malhamensis* Pringsheim". Naturwissenschaften **42,** 418-418.

Heinrich, S., Frickenhaus, S., Glockner, G., and Valentin, K. (2012). A comprehensive cDNA library of light- and temperature-stressed *Saccharina latissima* (Phaeophyceae). Eur J Phycol **47,** 83-94.

Herth, W., and Zugenmaier, P. (1979). Lorica of *Dinobryon*. J Ultrastruc Research **69,** 262-272.

Herth, W., Kuppel, A., and Schnepf, E. (1977). Chitinous fibrils in lorica of flagellate chrysophyte *Poteriochromonas stipitata* (syn. *Ochromonas malhamensis*). J Cell Biol **73,** 311-321.

Holen, D.A. (1999). Effects of prey abundance and light intensity on the mixotrophic chrysophyte *Poterioochromonas malhamensis* from a mesotrophic lake. Freshwater Biol **42,** 445-455.

Hutner, S.H., Provasoli, L., and Filfus, J. (1953). Nutrition of some phagotrophic fresh-water chrysomonads. Ann N Y Acad Sci **56,** 852-862.

Huysman, M.J.J., Martens, C., Vandepoele, K., Gillard, J., Rayko, E., Heijde, M., Bowler, C., Inze, D., Van de Peer, Y., De Veylder, L., and Vyverman, W. (2010). Genome-wide analysis of the diatom cell cycle unveils a novel type of cyclins involved in environmental signaling. Genome Biol **11,** R17.

Ikävalko, J., and Thomsen, H.A. (1997). The Baltic Sea ice biota (March 1994): A study of the Protistan community. Eur J Protistol **33,** 229-243.

Jarvis, P. (2008). Targeting of nucleus-encoded proteins to chloroplasts in plants. New Phytol **179,** 257–285.

Jarvis, P., Dormann, P., Peto, C.A., Lutes, J., Benning, C., and Chory, J. (2000). Galactolipid deficiency and abnormal chloroplast development in the *Arabidopsis* MGD synthase 1 mutant. PNAS **97,** 8175-8179.

Jeppesen, E., Søndergaard, M., Jensen, J.P., Havens, K.E., Anneville, O., Carvalho, L., Coveney, M.F., Deneke, R., Dokulil, M.T., Foy, B.O.B., Gerdeaux, D., Hampton, S.E., Hilt, S., Kangur, K., Köhler, J.A.N., Lammens, E.H.H.R., Lauridsen, T.L., Manca, M., Miracle, M.R., Moss, B., Nöges, P., Persson, G., Phillips, G., Portielje, R.O.B., Romo, S., Schelske, C.L., Straile, D., Tatrai, I., Willén, E.V.A., and Winder, M. (2005). Lake responses to reduced nutrient loading – an analysis of contemporary long-term data from 35 case studies. Freshwater Biol **50,** 1747-1771.

Johnson, X., and Alric, J. (2013). Central carbon metabolism and electron transport in *Chlamydomonas reinhardtii*: Metabolic Constraints for Carbon Partitioning between Oil and Starch. Eukaryot Cell **12,** 776-793.

Johnston, A.M., and Raven, J.A. (1996). Inorganic carbon accumulation by the marine diatom *Phaeodactylum tricornutum*. Eur J Phycol **31,** 285-290.

Jomaa, H., Wiesner, J., Sanderbrand, S., Altincicek, B., Weidemeyer, C., Hintz, M., Turbachova, I., Eberl, M., Zeidler, J., Lichtenthaler, H.K., Soldati, D., and Beck, E. (1999). Inhibitors of the nonmevalonate pathway of isoprenoid biosynthesis as antimalarial drugs. Science **285,** 1573-1576.

Jones, R.I. (2000). Mixotrophy in planktonic protists: an overview. Freshwater Biol **45,** 219-226.

Jones, R.I., and Rees, S. (1994). Influence of temperature and light on particle ingestion by the freshwater phytoflagellate *Dinobryon*. Fundam Appl Limnol **132,** 203-211.

Jordan, R.W., and Iwataki, M. (2012). Chrysophyceae and Synurophyceae. In: eLS (John Wiley & Sons, Ltd, DOI:10.1002/9780470015902.a0023690.

Kamjunke, N., Henrichs, T., and Gaedke, U. (2007). Phosphorus gain by bacterivory promotes the mixotrophic flagellate *Dinobryon* spp. during re-oligotrophication. J Plankton Res **29,** 39-46.

Kamp, A., de Beer, D., Nitsch, J.L., Lavik, G., and Stief, P. (2011). Diatoms respire nitrate to survive dark and anoxic conditions. PNAS **108,** 5649-5654.

Kang, R.J., Wang, J., Shi, D.J., Cong, W., Cai, Z.L., and Fan, O.Y. (2004). Interactions between organic and inorganic carbon sources during mixotrophic cultivation of *Synechococcus* sp. Biotechnol Lett **26,** 1429-1432.

Keeling, P.J. (2004). Diversity and evolutionary history of plastids and their hosts. Am J Bot **91,** 1481-1493.

Kerimoglu, O., Straile, D., and Peeters, F. (2013). Seasonal, inter-annual and long term variation in top-down versus bottom-up regulation of primary production. Oikos **122,** 223-234.

Kilian, O., and Kroth, P.G. (2005). Identification and characterization of a new conserved motif within the presequence of proteins targeted into complex diatom plastids. Plant J **41,** 175-183.

Kim, J.H., Lee, K.L., and Kim, H.S. (2009). Effect of nutrients and light intensity on growth of *Mallomonas caudata* (Synurophyceae). Nord J Bot **27,** 516-522.

Kim, Y.C., Yakunin, A.F., Kuznetsova, E., Xu, X.H., Pennycooke, M., Gu, J., Cheung, F., Proudfoot, M., Arrowsmith, C.H., Joachimiak, A., Edwards, A.M., and Christendat, D. (2004). Structure- and function-based characterization of a new phosphoglycolate phosphatase from *Thermoplasma acidophilum*. J Biol Chem **279,** 517-526.

Kristiansen, J. (2008). Dispersal and biogeography of silica-scaled chrysophytes. Biodivers Conserv **17,** 419-426.

Kristiansen, J., and Preisig, H.R. (2007). Süßwasserflora von Mitteleuropa Vol1/2. In: Chrysophyte and haptophyte algae, H.R. Preisig, eds (Berlin, Heidelberg; Germany: Spektrum Akad. Verl).

Kroth, P.G., Chiovitti, A., Gruber, A., Martin-Jezequel, V., Mock, T., Parker, M.S., Stanley, M.S., Kaplan, A., Caron, L., Weber, T., Maheswari, U., Armbrust, E.V., and Bowler, C. (2008). A model for carbohydrate metabolism in the diatom *Phaeodactylum tricornutum* deduced from comparative whole genome analysis. PloS one **3**.

Lacoste-Royal, G., and Gibbs, S.P. (1985). *Ochromonas* mitochondria contain a specific chloroplast protein. PNAS **82,** 1456-1459.

Laliberte, G., and Delanoue, J. (1993). Autotrophic, heterotrophic, and mixotrophic growth of *Chlamydomonas humicola* (Chlorophyceae) on acetate. J Phycol **29,** 612-620.

Lang, M., Apt K.E., and Kroth, P.G (1998). Protein transport into “complex” diatom plastids utilizes two different targeting signals. J Biol Chem **273**, 30973–8.

Lange, B.M., Rujan, T., Martin, W., and Croteau, R. (2000). Isoprenoid biosynthesis: The evolution of two ancient and distinct pathways across genomes. PNAS **97,** 13172-13177.

Le, S.Q., and Gascuel, O. (2008). An improved general amino acid replacement matrix. Mol Biol Evol **25,** 1307-1320.

Lee, K.L., Kim, J.H., Yoon, H.-S., and Kim, H.S. (2012). Growth characteristics of two bloom-forming synurophytes (*Mallomonas elongata* and *Synura petersenii*) at different nitrate and phosphate concentrations. Nord J Bot **30,** 104-108.

Lehman, J.T. (1976). Ecological and nutritional studies on *Dinobryon* Ehrenb - seasonal periodicity and phosphate toxicity problem. Limnol Oceanogr **21,** 646-658.

Liaud, M.F., Lichtle, C., Apt, K., Martin, W., and Cerff, R. (2000). Compartment-specific isoforms of TPI and GAPDH are imported into diatom mitochondria as a fusion protein: evidence in favor of a mitochondrial origin of the eukaryotic glycolytic pathway. Mol Biol Evol **17,** 213-223.

Lim, L., and McFadden, G.I. (2010). The evolution, metabolism and functions of the apicoplast. Philos T R Soc B **365,** 749-763.

Liu, X.J., Duan, S.S., Li, A.F., Xu, N., Cai, Z.P., and Hu, Z.X. (2009). Effects of organic carbon sources on growth, photosynthesis, and respiration of *Phaeodactylum tricornutum*. J Appl Phycol **21,** 239-246.

Lohr, M., and Wilhelm, C. (2001). Xanthophyll synthesis in diatoms: quantification of putative intermediates and comparison of pigment conversion kinetics with rate constants derived from a model. Planta **212,** 382-391.

Maberly, S.C., Ball, L.A., Raven, J.A., and Sultemeyer, D. (2009). Inorganic carbon acquisition by chrysophytes. J Phycol **45,** 1052-1061.

Maguire, M.J., Goff, L.J., and Coleman, A.W. (1995). *In situ* plastid and mitochondrial DNA determination: Implication of the observed minimal plastid genome number. Am J Bot **82,** 1496-1506.

Massana, R. (2011). Eukaryotic picoplankton in surface oceans. Annu Rev Microbiol, Vol 65 **65,** 91-110.

Matsuda, Y., Nakajima, K., and Tachibana, M. (2011). Recent progresses on the genetic basis of the regulation of $CO_{(2)}$ acquisition systems in response to $CO_{(2)}$ concentration. Photosynth Res **109,** 191-203.

Mckenzie, C.H., Deibel, D., Paranjape, M.A., and Thompson, R.J. (1995). The marine mixotroph *Dinobryon balticum* (Chrysophyceae) - phagotrophy and survival in a cold ocean. J Phycol **31,** 19-24.

Meyer, O. (1993). Functional groups of microorganisms. In: Biodiversity and ecosystem function, E.-D. Schulze and H. Mooney, eds (Berlin, Heidelberg; Germany: Springer), pp. 67-96.

Moreira, D., Le Guyader, H., and Philippe, H. (2000). The origin of red algae and the evolution of chloroplasts. Nature **405,** 69-72.

Moser, M., and Weisse, T. (2011a). The outcome of competition between the two chrysomonads *Ochromonas* sp. and *Poterioochromonas malhamensis* depends on pH. Eur J Protistol **47,** 79-85.

Moser, M., and Weisse, T. (2011b). Combined stress effect of pH and temperature narrows the niche width of flagellates in acid mining lakes. J Plankton Res **33,** 1023-1032.

Müller, A.-M., and Wilhelm, C. (1997). Light adaptation of the phytoplankton diatom *Phaeodactylum tricornutum* under conditions of natural light climate. Inter Rev Hydrobiol **82,** 315-328.

Mulligan, H.F., and Kingsbury, J.M. (1968). Application of an electronic particle counter in analyzing natural populations of phytoplankton. Limnol Oceanogr **13,** 499-506.

Myers, J., and Graham, J.R. (1956). The role of photosynthesis in the physiology of *Ochromonas*. J Cell Physiol **47,** 397-414.

Oesterhelt, C., Schnarrenberger, C., and Gross, W. (1999). Characterization of a sugar/polyol uptake system in the red alga *Galdieria sulphuraria*. Eur J Phycol **34,** 271-277.

Olrik, K. (1998). Ecology of mixotrophic flagellates with special reference to *Chrysophyceae* in Danish lakes. Hydrobiologia **370,** 329-338.

Oudot-Le Secq, M.P., Grimwood, J., Shapiro, H., Armbrust, E.V., Bowler, C., and Green, B.R. (2007). Chloroplast genomes of the diatoms *Phaeodactylum tricornutum* and *Thalassiosira pseudonana*: comparison with other plastid genomes of the red lineage. Mol Genet Genomics **277,** 427-439.

Pålsson, C., and Graneli, W. (2003). Diurnal and seasonal variations in grazing by bacterivorous mixotrophs in an oligotrophic clearwater lake. Fundam Appl Limnol **157,** 289-307.

Pålsson, C., and Daniel, C. (2004). Effects of prey abundance and light intensity on nutrition of a mixotrophic flagellate and its competitive relationship with an obligate heterotroph. Aquat Microb Ecol **36,** 247-256.

Pancic, P.G., and Strotmann, H. (1993). Structure of the nuclear encoded gamma-subunit of Cf_0cf_1 of the diatom *Odontella sinensis* including its presequence. Febs Letters **320,** 61-66.

Patel, B.N., and Merrett, M.J. (1986). Inorganic-carbon uptake by the marine diatom *Phaeodactylum-tricornutum*. Planta **169,** 222-227.

Peck, R.K. (2010). Structure of loricae and stalks of several bacterivorous chrysomonads (Chrysophyceae): Taxonomical Importance and Possible Ecological Significance. Protist **161,** 148-159.

Pellicer, M.T., Nunez, M.F., Aguilar, J., Badia, J., and Baldoma, L. (2003). Role of 2-phosphoglycolate phosphatase of *Escherichia coli* in metabolism of the 2-phosphoglycolate formed in DNA repair. J Bacteriol **185,** 5815-5821.

Pla, S., and Anderson, N.J. (2005). Environmental factors correlated with chrysophyte cyst assemblages in low arctic lakes of southwest Greenland. J Phycol **41,** 957-974.

Porter, K.G. (1988). Phagotrophic phytoflagellates in microbial food webs. Hydrobiologia **159,** 89-97.

Pringsheim, E.G. (1952). On the nutrition of *Ochromonas*. Q J Microsc Sci **93,** 71-96.

Pringsheim, E.G. (1955). Uber *Ochromonas danica* n. sp. und andere Arten der Gattung. Arch Mikrobiol **23,** 181-192.

Raven, J.A. (1997). Phagotrophy in phototrophs. Limnol Oceanogr **42,** 198-205.

Raven, J.A., Holen, D.A., and Boraas, M.E. (1995). Development, physiology and nutrition. In: Chrysophyte algae: Ecology, phylogeny, and development, C.D. Sandgren, J.P. Smol, and J. Kristiansen, eds (Cambridge, England: Cambridge University Press), pp. 93-119.

Raven, J.A., Giordano, M., Beardall, J., and Maberly, S.C. (2012). Algal evolution in relation to atmospheric CO_2: carboxylases, carbon-concentrating mechanisms and carbon oxidation cycles. Philos T R Soc B **367,** 493-507.

Ravi, V., Khurana, J.P., Tyagi, A.K., and Khurana, P. (2008). An update on chloroplast genomes. Plant Syst Evol **271,** 101-122.

Reazin, G.H. (1956). The metabolism of glucose by the alga *Ochromonas malhamensis*. Plant Physiol **31,** 299-303.

Rothhaupt, K.O. (1996a). Utilization of substitutable carbon and phosphorus sources by the mixotrophic chrysophyte *Ochromonas* sp. Ecology **77,** 706-715.

Rothhaupt, K.O. (1996b). Laboratory experiments with a mixotrophic chrysophyte and obligately phagotrophic and phototrophic competitors. Ecology **77,** 716-724.

Rottberger, J., Gruber, A., and Kroth, P.G. (2013). Analysing size variation during light-starvation response of nutritionally diverse chrysophytes with a Coulter counter. Algological Studies **141(1),** 37-51.

Sanchez, B., Zuniga, M., Gonzalez-Candelas, F., de los Reyes-Gavilan, C.G., and Margolles, A. (2010). Bacterial and eukaryoticpPhosphoketolases: Phylogeny, distribution and evolution. J Mol Microb Biotech **18,** 37-51.

Sanders, R.W. (2011). Alternative nutritional strategies in Protists: Symposium introduction and a review of freshwater protists that combine photosynthesis and heterotrophy. J Eukaryot Microbiol **58,** 181-184.

Sanders, R.W., and Porter, K.G. (1988). Phagotrophic phytoflagellates. Advan Microbial Ecol **10,** 167-192.

Sanders, R.W., Porter, K.G., and Caron, D.A. (1990). Relationship between phototrophy and phagotrophy in the mixotrophic chrysophyte *Poterioochromonas malhamensis*. Microbial Ecol **19,** 97-109.

Sanders, R.W., Caron, D.A., Davidson, J.M., Dennett, M.R., and Moran, D.M. (2001). Nutrient acquisition and population growth of a mixotrophic alga in axenic and bacterized cultures. Microbial Ecol **42,** 513-523.

Sandgren, C.D. (1988). The ecology of chrysophyte flagellates: their growth and perennation strategies as freshwater phytoplankton. In: Growth and reproductive strategies of freshwater phytoplankton, C.D. Sandgren, eds (Cambridge, England: Cambridge University Press), pp. 9-104.

Schlösser, U.G. (1994). SAG – Sammlung von Algenkulturen at the University of Gottingen - catalog of strains 1994. Botanica Acta **107,** 113-186.

Scholz, K. (2011). Physiologische, molekularbiologische und bioinformatische Charakterisierung von Dinobryon-Arten. Bachelor thesis, Biology, Universität Konstanz.

Scott, C.E., Saros, J.E., Williamson, C.E., Salm, C.R., Peters, S.C., and Mitchell, D.L. (2009). Effects of nutrients and dissolved organic matter on the response of phytoplankton to ultraviolet radiation: experimental comparison in spring versus summer. Hydrobiologia **619,** 155-166.

Selosse, M.A., and Roy, M. (2009). Green plants that feed on fungi: facts and questions about mixotrophy. Trends Plant Sci **14,** 64-70.

Sherr, B.F., Sherr, E.B., and Fallon, R.D. (1987). Use of monodispersed, fluorescently labeled bacteria to estimate in situ protozoan bacterivory. Appl Environ Microbiol **53,** 958-965.

Soll, J. and Schleiff, E. (2004). Protein import into chloroplasts. Nat Rev Mol Cell Biol **5,** 198–208.

Stanley, M.S., Perry, R.M., and Callow, J.A. (2005). Analysis of expressed sequence tags from the green alga *Ulva linza* (Chlorophyta). J Phycol **41,** 1219-1226.

Stöcker, D., Tillmann, U., and Granéli, E. (2006). Phagotrophy in harmful algae. In: Ecology of harmful algae, E. Granéli and J. Turner, eds (Berlin, Heidelberg; Germany: Springer), pp. 177-187.

Stöcker, D.K., Gustafson, D.E., Merrell, J.R., Black, M.M.D., and Baier, C.T. (1997). Excystment and growth of chrysophytes and dinoflagellates at low temperatures and high salinities in Antarctic sea-ice. J Phycol **33,** 585-595.

Takaichi, S. (2011). Carotenoids in algae: Distributions, biosyntheses and functions. Mar Drugs **9,** 1101-1118.

Tanabe, Y., Shitara, T., Kashino, Y., Hara, Y., and Kudoh, S. (2011). Utilizing the effective xanthophyll cycle for blooming of *Ochromonas smithii* and *O. itoi* (Chrysophyceae) on the snow surface. PloS one **6**.

Taylor, W.C. (1989). Regulatory Interactions between nuclear and plastid genomes. Annu Rev Plant Phys **40,** 211-233.

Terauchi, M., Kato, A., Nagasato, C., and Motomura, T. (2010). Research note: Analysis of expressed sequence tags from the chrysophycean alga *Ochromonas danica* (Heterokontophyta). Phycol Res **58,** 217-221.

Thingstad, T.F., Havskum, H., Garde, K., and Riemann, B. (1996). On the strategy of "eating your competitor": A mathematical analysis of algal mixotrophy. Ecology **77,** 2108-2118.

Timmis, J.N., Ayliffe, M.A., Huang, C.Y., and Martin, W. (2004). Endosymbiotic gene transfer: organelle genomes forge eukaryotic chromosomes. Nat Rev Genet **5,** 123-U116.

Unrein, F., Gasol, J.M., and Massana, R. (2010). *Dinobryon faculiferum* (Chrysophyta) in coastal Mediterranean seawater: presence and grazing impact on bacteria. J Plankton Res **32,** 559-564.

Unrein, F., Massana, R., Alonso-Saez, L., and Gasol, J.M. (2007). Significant year-round effect of small mixotrophic flagellates on bacterioplankton in an oligotrophic coastal system. Limnol Oceanogr **52,** 456-469.

Van Donk, E., Veen, A., and Ringelberg, J. (1988). Natural community bioassays to determine the abiotic factors that control phytoplankton growth and succession. Freshwater Biol **20,** 199-210.

Van Donk, E., Cerbin, S., Wilken, S., Helmsing, N.R., Ptacnik, R., and Verschoor, A.M. (2009). The effect of a mixotrophic chrysophyte on toxic and colony-forming cyanobacteria. Freshwater Biol **54,** 1843-1855.

Veen, A. (1991). Ecophysiological studies on the phagotrophic phytoflagellate *Dinobryon divergens* Imhof. In: Fundamental and Applied Ecology (Amsterdam, Netherlands: University of Amsterdam), pp. 128.

Vigna, M.S., and Siver, P.A. (2003). Biodiversity and biogeographical implications of silica-scaled chrysophytes (Chrysophyceae and Synurophyceae) of the northeast wetlands of Argentina. Fundam Appl Limnol **158,** 359-372.

Waller, R.F., Keeling, P.J., Donald, R.G.K., Striepen, B., Handman, E., Lang-Unnasch, N., Cowman, A.F., Besra, G.S., Roos, D.S., and McFadden, G.I. (1998). Nuclear-encoded proteins target to the plastid in *Toxoplasma gondii* and *Plasmodium falciparum*. PNAS **95,** 12352-12357.

Wan, L.L., Han, J., Sang, M., Li, A.F., Wu, H., Yin, S.J., and Zhang, C.W. (2012). *De novo* transcriptomic analysis of an oleaginous microalga: Pathway description and gene discovery for production of next-generation biofuels. PloS one **7**.

Watson, S.B., and McCauley, E. (2010). Light and bacteria: substitutable energy sources for chrysophyte blooms? Nova Hedwigia**,** 213-230.

Watson, S.B., Satchwill, T., Dixon, E., and McCauley, E. (2001). Under-ice blooms and source-water odour in a nutrient-poor reservoir: biological, ecological and applied perspectives. Freshwater Biol **46,** 1553-1567.

Wilken, S., Huisman, J., Naus-Wiezer, S., and Van Donk, E. (2013). Mixotrophic organisms become more heterotrophic with rising temperature. Ecol Lett **16,** 225-233.

Yamano, T., Miura, K., and Fukuzawa, H. (2008). Expression analysis of genes associated with the induction of the carbon-concentrating mechanism in *Chlamydomonas reinhardtii*. Plant Physiol **147,** 340-354.

Yang, C., Hua, Q., and Shimizu, K. (2002a). Integration of the information from gene expression and metabolic fluxes for the analysis of the regulatory mechanisms in *Synechocystis*. Appl Microbiol Biot **58,** 813-822.

Yang, C., Hua, Q., and Shimizu, K. (2002b). Metabolic flux analysis in *Synechocystis* using isotope distribution from C-13-labeled glucose. Metab Eng **4,** 202-216.

Yoshikawa, K., Hirasawa, T., Ogawa, K., Hidaka, Y., Nakajima, T., Furusawa, C., and Shimizu, H. (2013). Integrated transcriptomic and metabolomic analysis of the central metabolism of *Synechocystis* sp PCC 6803 under different trophic conditions. Biotechnol J **8,** 571-580.

Zhang, X.M., and Watanabe, M.M. (2001). Grazing and growth of the mixotrophic chrysomonad *Poterioochromonas malhamensis* (Chrysophyceae) feeding on algae. J Phycol **37,** 738-743.

Zimmermann, U., Pilwat, G., Beckers, F., and Riemann, F. (1976). Effects of external electrical fields on cell membranes. Bioelectrochem Bioenerg **3,** 58-83.

Zwart, K.B., and Darbyshire, J.F. (1992). Growth and nitrogenous excretion of a common soil flagellate *Spumella* sp - a laboratory experiment. J Soil Sci **43,** 145-157.

List of side projects

Physiology and Ecology

1.) Enrichment of *Ochromonas* sp. from Lake Constance

Ochromonas strains were enriched from water samples of Lake Constance (September 2009) by two approaches. Aliquots of unified lake water samples from 0-20 m depth were kept in darkness (dark cultures) or in a 12:12 dark:light rhythm at 30 µE (light cultures). Dark cultures were transferred to lowlight conditions every 3-4 days for a maximum of 10 hours. Partial medium exchange was performed every 1-3 weeks. Light cultures were supplied with sterile lake water and dark cultures were subsequently adapted to 50 % BM with 0.1 % Glucose. After 4 months the *Ochromonas* strains were maintained in liquid culture by transferring 1 ml of a culture to 50 ml of fresh BM with 0.1 % Glucose every 2 months. The cultures are neither unialgal nor axenic. The *Ochromonas* strains were identified as *Ochromonas* sp. by Pia Mahler, Limnological Institut, Konstanz. Her identification was confirmed by observing blue autofluorescence of vesicles using fluorescence microscopy, which is a characteristic feature of *Ochromonas*-like strains.

2.) Isolation of *Dinobryon* sp. from Lake Constance

Dinobryon colonies from Lake Constance water samples (0-20 m, June 2010) were cleaned five times in drops of 50 % WC medium on an object slide by gently pipetting them up and down using a confocal microscope. Five of the cleaned colonies were transferred into 10 ml of 50 % WC medium. Washing and transfer of colonies was performed weekly over two months. Afterwards unialgal Dinobryon cultures were successfully maintained by transferring 1 ml of a culture to 50 ml of 100 % WC medium every 2 months. The isolate probably is *Dinobryon divergens* as determined by sequencing and analyzing of the 18S-rRNA gene by the student Katharina Scholz (Scholz, 2011).

3.) Chlorophyll concentration determination during growth experiments with *Ochromonas danica* and *Poterioochromonas malhamensis* DS

Ochromonas danica and *Poterioochromonas malhamensis* were grown in their standard medium in darkness and under lowlight (300 µE) and highlight (100 µE) conditions applying a 16:8 h light:dark rhythm. Cell densities per ml were determined using an automatic particle counter. Cells were harvested from 1 ml culture samples by centrifugation. The cell pellet was re-suspended thoroughly in 90 % acetone. Cell-fragments were removed by centrifugation. Chlorophyll a (Chla) concentrations per ml were determined spectrophotometrically and calculated to µg Chla per cell. The Chla concentrations per cell increased under all conditions and for both strains during exponential phase and in the beginning of stationary phase. Chlorophyll contents were lowest under dark conditions. In stationary phase the chlorophyll content in cells of both strains decreased substantially under high-light conditions but continued to slightly increase under low-light conditions. In darkness, chlorophyll contents stagnated in stationary phase. However, absolute numbers of chlorophyll concentrations differed substantially between the cultures within one treatment and therefore standard deviations of values were high. The significance of results is therefore questionable. This experiment could probably be improved by applying a more quantitative method of cell disruptor during acetone extraction like e.g. grinding of cells with glass beads.

4.) Growth of *Ochromonas danica* and *Poterioochromonas malhamensis* with different amino acids

Ochromonas danica and *Poterioochromonas malhamensis* were grown under standard conditions replacing the DOM in the standard media with the amino acids arginine, glycine, histidine, glutamate, methionine or combinations of these amino acids at pH 7 in the presence of 1 % glucose. In some treatments growth was visible by eye after several weeks or months but these results were not reproducible. As *P. malhamensis* grows rather weakly with glucose other factors promoted growth in the experiments with amino acids. Further experiments are necessary.

5.) Effects of diverse compounds on oxygen production of *Poterioochromonas malhamensis*

Oxygen production of *P. malhamensis* cells was monitored using a Clark electrode (for details see chapter 4). The effect of DCMU (inhibitor of photosystem II), TMPD (electron donor), coenzyme A and of the substrates pyruvate and succinate on whole cells were tested. Oxygen production was shown to decrease after addition of DCMU. The effect could partially be reversed by addition of TMPD. Addition of coenzyme A had no effect on oxygen evolution rates. After the addition of succinate or pyruvate oxygen evolution rates decreased suggesting either the inhibition of photosynthesis or enhanced oxygen consumption in relation to oxygen evolution. Repetition of these experiments is necessary as the amount of replicates was low.

Molecular biology and transcriptomics

1.) Verification of the identity of chrysophyte strains used for transcriptomic approaches

The identity of *Poterioochromonas malhamensis* DS, *Poteriospumella lacustris* JBM10, *Dinobryon divergens* and *Mallomonas annulata* used for transcriptomic analysis was verified on the species level through sequencing and analyses of the 18S-rRNA genes by the students Katharina Scholz and Julia Thielicke under my supervision.

7.) Isolation of total RNA from *Dinobryon divergens* using a citric acid method

A protocol was established to isolate high quantities of RNA from *D. divergens* cell material using a cell-lysis puffer with SDS, citric acid, citrate and EDTA and a protein extraction buffer containing sodium chloride, citrate and citric acid. Nucleic acids were precipitated with isopropanol. Contaminations by DNA were high; therefore a DNA digestion was performed to increase purity of RNA. The advantage of the protocol is that the application of toxic phenol or TRIzol@ reagent is not necessary.

8.) Transcriptomic analysis of the freshwater diatom *Achnantidium minutissimum*

Xenic and axenic cultures of *Achnantidium minutissimum* were grown at 20 °C with 35 µE light and a light:dark rhythm of 16:8 h in AM medium (BM medium without soil extract) at 100 rpm on a horizontal shaker. Cells from 600 ml of each axenic and xenic culture were harvested by centrifugation in exponential phase at cell densities between 300,000 and 2,700,000 cells ml^{-1}. Total RNA preparation was performed from the nitrogen-frozen cell pellets using TRIzol@ agent as described for chrysophytes in chapter 5. DNA digestion was performed for all samples using the Ambion-Turbo DNAse Kit. RNA-samples were pooled (1 µg RNA from the xenic cultures and 34 µg from axenic cultures). Poly(A)+ -RNA isolation, cDNA library preparation, 454-sequencing and clustering and assembly of sequences were performed by the company Eurofins MWG Operon, Ebersberg, Germany. Sequencing resulted in 619,553 reads which were assembled into 34.721 contigs leaving 59.560 singletons. Automatic annotation was performed using BLAST2GO (for annotation parameters see chapter 5). EC annotations assigned by BLAST- and InterPro search were functionally sorted into KEGG pathway maps. Evaluation of annotation results and functional sorting has been performed partially. Dariia Bova assisted during computational annotation and by numeric listing of KEGG pathway map entries.

9.) <u>Design of degenerated primer oligomeres for housekeeping genes of chrysophytes as controls for real-time PCR approaches</u>

When transcript expression levels are compared between different conditions by real-time PCR approaches it is necessary to include control transcripts for quantification. So called internal controls are transcripts ideally having the same expression profile under all conditions applied. Transcripts of the ribosomal protein RP-S1, the transcription factor TATA-box binding protein (TBP) and hypoxanthine phosphoribosyltransferase (Hprt) which is involved in purine metabolism were shown to be suitable as internal qRT-PCR controls for transcripts of enzymes involved in carbohydrate metabolism of *Phaeodactylum tricornutum* by Matthias Sachse et al., Universität Konstanz.

Contigs encoding TBP were found for all four investigated chrysophytes in the EST-datasets (Chapter 5). Thus, TBP specific primer oligomers for real-time PCR approaches may be designed directly for each of the four protists. Regarding the remaining two controls only three of four chrysophytes had contigs encoding the respective gene products. Contigs encoding the RP-S1 gene were found for *Mallomonas annulata*, *Poterioochromonas malhamensis* and *Dinobryon divergens*. Degenerated primer oligomers were designed based on an assembly of all RPS-1 encoding contigs to be able to amplify a region of the RPS-1 gene from *Poteriospumella lacustris*. Contigs encoding Hprt were found for *Poteriospumella lacustris*, *Poterioochromonas malhamensis* and *Dinobryon divergens*. Degenerated primer oligomers were designed based on an assembly of all Hprt encoding contigs to be able to amplify a region of the Hprt gene from *Mallomonas annulata*.

List of contributions

I wrote and designed this thesis and performed the experiments by myself; other persons contributed as listed in the following:

Chapter 2: Detection of bacterial contaminants in algal cultures using the Multisizer III, Beckman Coulter

- Dr. Ansgar Gruber and Prof. Peter G. Kroth helped with advice regarding the experimental design and contributed by proof-reading of the manuscript.

Chapter 3: Analysing size variation during light-starvation response of nutritionally diverse chrysophytes with a Coulter counter

- Two anonymous reviewers contributed by comments during the publishing process with Algological Studies.
- Katharina Scholz performed preliminary growth experiments under my supervision and according to my instructions during her bachelor thesis.
- Dr. Ansgar Gruber and Prof. Peter G. Kroth helped with advice regarding the experimental design and contributed by proof-reading of the manuscript.

Chapter 4: Influence of nutrients and light on autotrophic, mixotrophic and heterotrophic freshwater chrysophytes

- Three anonymous reviewers contributed by their comments during the review process at Aquatic Microbial Ecology.
- Prof. Peter G. Kroth and Prof. Karl-Otto Rothhaupt helped with advice regarding the experimental design.
- The students Katharina Scholz, Julia Thielicke, Karin Ojamäe, Sandra Braçun and Alexander Förderer performed preliminary growth experiments under my supervision and according to my instructions.
- Dr. Ansgar Gruber helped with laser scanning microscopy of *Dinobryon divergens*
- Dr. Ansgar Gruber, Prof. Jens Boenigk and Prof. Peter G. Kroth contributed by proof-reading of the manuscript.

Chapter 5: Primary metabolism of autotrophic, mixotrophic and heterotrophic chrysophytes according to *de novo* transcriptomic analysis

- Prof. Peter G. Kroth and Prof. Jens Boenigk helped with advice regarding the choice of the sequencing approach.
- Poly(A)+ -RNA isolation, cDNA library preparation, 454-sequencing and clustering and assembly of sequences were performed by the company Eurofins MWG Operon, Ebersberg, Germany.
- The students Katharina Scholz and Dariia Bova performed parts of the statistical analyses of annotated sequences under my supervision and according to my instructions.
- Dr. Carolina Rio Bartulos performed the phylogenetic analyses of putative GAPDH sequences and helped with advice regarding RNA extraction methods, TargetP analyses and the interpretation of phylogenetic analysis.
- Dr. Sabina Wodniok, Prof. Peter G. Kroth, Dr. Bernard Lepetit and Dr. Ansgar Gruber helped with discussions regarding evaluation and sorting of the sequencing data.
- Prof. Peter G.Kroth and Dr. Carolina Rio Bartulos contributed by proof-reading of the manuscript.

List of publications

Publications

11/2011 (accepted)	**Application note** Rottberger J, Kroth PG, Gruber A (2011) “Detection of bacterial contaminations in algal cultures from the size distribution.” *Beckmann Coulter*
01/2013 (published)	**Research article** Rottberger J, Gruber A, Kroth PG (2013) „Analysing size variation during light-starvation response of nutritionally diverse Chrysophytes with a Coulter counter.” *Algological Studies 141(1):37-51*
06/2013 (submitted)	**Research article** Rottberger J, Gruber A, Boenigk J, Kroth PG “Influence of nutrients and light on autotrophic, mixotrophic and heterotrophic freshwater chrysophytes." *Aquatic Microbial Ecology*
in preparation	**Research article** Rottberger J, Rio Bartulos C, Wodniok S, Boenigk J, Kroth PG “Primary metabolism of mixotrophic, autotrophic and heterotrophic chrysophytes according to *de novo* transcriptomic analysis.”

Presentations

28/02/2012	„Nutritional requirements and metabolic characteristics of heterotrophic, mixotrophic and autotrophic freshwater chrysophytes“ *14. Wissenschaftliche Tagung der Sektion Phykologie 2012, Wuppertal, Germany*

Poster

18/09/2011 - 23/09/2011	„Ecophysiology of mixotrophic flagellates“ *Botanikertagung 2011, Berlin, Germany*
14/03/2010 - 17/03/2010	„Ecophysiology of mixotrophic flagellates“ *13. Wissenschaftliche Tagung der Sektion Phykologie 2010, Reichenau Island, Germany*
6/09/2009 - 11/09/2009	„Ecophysiology of mixotrophic Chrysophyceans“ *Botanikertagung 2009, Leipzig, Germany*

Acknowledgements

I deeply want to thank Prof. Peter Kroth for inviting me in his group, trusting me with this project and for the naturalness of supporting me in any and every possible way. Peter, it is under your guidance over the past few years that I grew a self-organized, constructive and open-minded, but yet questioning scientist. I am quite confident time will prove that these are exactly the features necessary to successfully guide me through (scientific) life.

I am very thankful to Prof. Karl-Otto Rothhaupt for agreeing on co-supervision of this project, for his review of the thesis and for helpful discussions regarding initial steps.

I am very grateful to Prof. Jens Boenigk for financing the next generation sequencing approaches, the quick and thorough proof-reading of manuscripts, helpful discussions and comments and his trust and honesty which significantly contributed to a fruitful and pleasant cooperation.

I am thankful to the University of Konstanz for financial support and to AG Diederichs, AG Schink, AG Adamska and the bioimaging centre for providing facilities.

Caro and Ansgar, thank you, for sharing your profound knowledge with me and for providing advice at any time and in any situation. Ansgar, I am especially thankful for the thoroughness and soundness with which you reviewed any kind of paperwork; it was always worth it waiting on your comments a bit longer than anticipated. Caro, it is hard to shortly summarize all the support you provided regarding carbohydrate metabolism in algae, “lab stuff” (two words but in fact a never-ending story) and maintenance of the atmosphere – if I needed to express my thanks in Gin Tonic units, you would be drunk the rest of your life.

I thank Sandra Heinrich for convincing me to apply BLAST2GO.

Bernard, Jens L. and Dirk, I thank you, for proof-reading, helpful discussions and advice regarding literature.

I am grateful to all the graduate and undergraduate students who at times assisted me with experiments in the lab, especially Katharina Scholz, Dariia Bova, Julia Thielicke and Alexander Förderer.

I thank Doris and Annette for adopting the chrysophyte strains now that my experimental work is done.

I want to thank all the rest of AG Kroth for help and the pleasant time inside and outside of the lab – MS for making me an underwear-selling dwarf, MB for the possibility to translate a wedding ceremony, Anna for good food in “essbar”, Miriam for the nice time at “Schurahüsli”, Dani for sharing my repulsion towards the Cell Lab Quanta software, Birgit for good talk on the sofa, Martin for oregano and the possibility to tease someone, Manuel for taking over my place in teasing Martin, Angelika for advice regarding herbs and gardening, Chao for Chinese dumplings, LiLi for small talk in M936 and Kathrin for small talk in M907.

I want to thank my parents for supporting every single step and decision of my scientific career and for providing a recreative environment far from the scientific world.

Patrick, thank you for sharing my life and for all the compromises you unhesitatingly and selflessly made over the last years to cover my back while completing this thesis.